Published for SISSA by Springer

Received: *July 29, 2016*
Revised: *September 9, 2016*
Accepted: *September 11, 2016*
Published: *September 19, 2016*

Gauge-independent $\overline{\text{MS}}$ renormalization in the 2HDM

Ansgar Denner, Laura Jenniches, Jean-Nicolas Lang and Christian Sturm

Institut für Theoretische Physik und Astrophysik, Julius-Maximilians-Universität Würzburg, Emil-Hilb Weg 22, 97074 Würzburg, Germany

E-mail: Ansgar.Denner@physik.uni-wuerzburg.de, Laura.Jenniches@physik.uni-wuerzburg.de, Jean-Nicolas.Lang@physik.uni-wuerzburg.de, Christian.Sturm@physik.uni-wuerzburg.de

Abstract: We present a consistent renormalization scheme for the CP-conserving Two-Higgs-Doublet Model based on $\overline{\text{MS}}$ renormalization of the mixing angles and the soft-Z_2-symmetry-breaking scale M_{sb} in the Higgs sector. This scheme requires to treat tadpoles fully consistently in all steps of the calculation in order to provide gauge-independent S-matrix elements. We show how bare physical parameters have to be defined and verify the gauge independence of physical quantities by explicit calculations in a general R_ξ-gauge. The procedure is straightforward and applicable to other models with extended Higgs sectors. In contrast to the proposed scheme, the $\overline{\text{MS}}$ renormalization of the mixing angles combined with popular on-shell renormalization schemes gives rise to gauge-dependent results already at the one-loop level. We present explicit results for electroweak NLO corrections to selected processes in the appropriately renormalized Two-Higgs-Doublet Model and in particular discuss their scale dependence.

Keywords: NLO Computations

ArXiv ePrint: 1607.07352

doi:10.1007/JHEP09(2016)115

JHEP09(2016)115

Contents

JHEP09(2016)115

1 Introduction

The discovery of a Higgs boson at the Large Hadron Collider (LHC) [1, 2] was a tremendous success for elementary particle physics. The Higgs boson is now a central object of intense research in both experiment and theory in order to determine its properties precisely. In particular, it is interesting to investigate whether the Higgs boson belongs to the Standard Model (SM) or whether it is part of a more general theory. In this context, models with additional Higgs bosons are of special interest. An extended Higgs sector can contribute to solve open problems in particle physics, like for example the question of the origin of the matter-antimatter asymmetry in the universe or the nature of dark matter.

At the LHC, detectable differences between the SM and a theory with an extended Higgs sector can be small. Therefore, accurate theory predictions are strongly desirable and in turn require the knowledge of higher-order corrections. QCD corrections essentially dress the basic electroweak (EW) interactions of the Higgs boson and do not fundamentally change by adding additional Higgs bosons to the theory. Electroweak corrections, on the other hand, can significantly modify the predictions for physical observables, like cross sections and partial decay widths, through an extended Higgs sector. For this reason, we dedicate special attention to the calculation of next-to-leading order (NLO) EW corrections to Higgs production. This requires a renormalization of the new physical parameters and fields of the extended Higgs sector.

Within this work, we consider in particular the CP-conserving 2HDM of type II with a softly broken Z_2 symmetry [3, 4]. The Higgs sector of this model depends on four physical mass parameters, the masses M_{H_l} and M_{H_h} of the light and heavy, neutral, scalar Higgs bosons, the mass M_{H_a} of the pseudo-scalar Higgs boson, and the mass $M_{H^\pm}$ of the charged Higgs boson. In addition, there are two mixing angles, α and β, as well as the soft-Z_2-breaking scale M_sb. The renormalization of the 2HDM of type II has been discussed in the context of supersymmetry (see e.g. refs. [5–7]) and also in the general case [8–11]. A reasonable renormalization scheme should fulfil the following three conditions [6]: it should lead to gauge-independent physical counterterms, it should be numerically stable, i.e. the size of the higher-order corrections should be moderate, and it should preferably be defined in a process-independent way.

The masses of the Higgs bosons, vector bosons and fermions are naturally renormalized in the classical on-shell scheme, which is straightforward to apply. In contrast, for the

JHEP09(2016)115

parameters α, β, and $M_{\rm sb}$ there is no natural renormalization scheme. As long as these parameters are unknown, it is difficult to identify processes that can be measured precisely and that would allow to extract the values of these parameters accurately and in a stable way. Moreover, process-dependent renormalization can lead to unnaturally large corrections for the predictions of other processes (see e.g. ref. [11]) or require to artificially split off IR singularities [6]. Motivated by studies on the renormalization of the quark-mixing matrix in the SM [12], process-independent renormalization of the mixing angles α and β based on the field renormalization constants of the Higgs fields have been proposed [9, 10, 13]. Taking these recipes naively leads, however, to gauge-dependent renormalization of the mixing angles [14]. Therefore, it has been suggested [11, 15] to render these methods gauge independent by applying the pinch technique [16, 17]. This, however, merely trades the gauge dependence for a dependence on the prescription intrinsic in the pinch technique.

We consider it favourable to stick to a renormalization scheme that does not depend on particular conventions and propose to use the $\overline{\rm MS}$ renormalization scheme which is by default used in perturbative QCD. $\overline{\rm MS}$ renormalization is simple to apply and to implement. In addition, it leads to a residual scale dependence that helps to estimate the uncertainty caused by unknown higher-order corrections via a suitable scale variation. If the perturbative corrections become large along with the scale dependence, this signals the onset of the non-perturbative regime where the Higgs sector becomes strongly coupled. This will be illustrated in this work.

The use of an $\overline{\rm MS}$ renormalization scheme, however, requires particular attention in the proper treatment of the Higgs tadpoles. Tadpoles have no physical meaning and drop out in properly calculated S-matrix elements. If all parameters of the theory can be renormalized on-shell, as in the SM, (some) tadpoles can be consistently omitted to simplify practical calculations. However, if parameters are renormalized in the $\overline{\rm MS}$ scheme, it becomes crucial to define all bare physical parameters and counterterms, like for instance the mass counterterms of the EW gauge bosons or Higgs bosons, in a gauge-independent way. This in turn requires a consistent treatment of tadpoles. Within the 2HDM, we show that a careless treatment of tadpoles, as often used in the literature, in combination with $\overline{\rm MS}$ renormalization of the mixing angles α and β yields gauge-dependent results already at the one-loop level.

A consistent treatment of tadpoles has been formulated for the SM by Fleischer and Jegerlehner in ref. [18]. In this paper, we generalize this scheme, which we dub *FJ Tadpole Scheme*, and apply it to the 2HDM in order to allow for a consistent gauge-independent $\overline{\rm MS}$ renormalization of the mixing angles α and β as well as the soft-breaking scale $M_{\rm sb}$. We stress that the *FJ Tadpole Scheme* as introduced here provides a consistent universal description of tadpoles in arbitrary theories with spontaneous symmetry breaking (SSB), such as general multi-Higgs models.

The outline of this paper is as follows. In section 2 we discuss the role of the Higgs tadpoles for the proper definition of gauge-independent, physical parameters and counterterms for a general Higgs sector and recapitulate the use of the *FJ Tadpole Scheme* within the SM. Our notation and conventions for the 2HDM are introduced in section 3. Section 4 is devoted to the extension of the *FJ Tadpole Scheme* to the 2HDM and the formulation of the renormalization conditions. In section 5 we discuss the gauge dependence of popular

JHEP09(2016)115

schemes and relate these schemes to the *FJ Tadpole Scheme*. In section 6 we demonstrate the applicability of the *FJ Tadpole Scheme* by employing it in NLO calculations of Higgs-boson production processes in the 2HDM. In particular, we discuss Higgs-boson production in gluon fusion as well as Higgs-boson production through Higgs strahlung. Finally, in section 7 we close with our conclusions. In the appendices we present results for the Higgs-tadpole counterterms in the 2HDM, proof the gauge dependence of the $\overline{\text{MS}}$ renormalization of β in popular tadpole schemes, and illustrate the tadpole contributions to the two-loop Higgs-boson self-energy.

2 The role of tadpoles and gauge dependence

Before discussing the renormalization of the 2HDM, we examine the tadpole renormalization in theories with an extended Higgs sector in general, and we revisit the treatment of tadpoles in the SM. As tadpole contributions are gauge dependent (see e.g. refs. [19, 20] or appendix A), their gauge-dependent parts have to cancel in any physical quantity. This cancellation is always given when a physical renormalization scheme such as the on-shell scheme is applied, which is usually the case in the EW SM. For Beyond-Standard-Model (BSM) theories, on the other hand, on-shell renormalization of parameters may introduce a process dependence and/or lead to unnaturally large NLO corrections. Hence, it is preferable to renormalize new parameters in the $\overline{\text{MS}}$ scheme, at least until first evidence of the BSM theory allows for a meaningful definition of a process-dependent renormalization scheme. In this case, the treatment of tadpole counterterms requires some care to warrant the gauge independence of S-matrix elements: if $\overline{\text{MS}}$ counterterms are used, it is essential to ensure that all counterterms of physical parameters are gauge independent. This requires a gauge-independent definition of bare physical parameters which, in particular, must not employ shifted vacuum expectation values (vevs) in the presence of SSB. We show how this can be achieved in general and in a systematic way. In section 2.1, we discuss a proper definition of the vevs for a general Higgs sector. The treatment of tadpoles closely follows the arguments which have been presented by Fleischer and Jegerlehner in appendix A of ref. [18] for the SM. We refer to this scheme as the *FJ Tadpole Scheme* in the following.

The tadpole counterterms are absent at tree level. At higher orders in perturbation theory, they can be used to remove explicit tadpole contributions, which simplifies practical calculations. We show that the *FJ Tadpole Scheme* is gauge independent regardless of whether tadpoles are removed by a consistent renormalization or taken into account explicitly. This implies that any physical quantity is independent of the (consistent) renormalization of tadpoles.

2.1 The FJ Tadpole Scheme for a general Higgs sector

The bare Higgs Lagrangian is defined in terms of bare fields $\Phi_{i,\text{B}}$ and bare parameters $c_{j,\text{B}}$,

$$\mathcal{L}_{\text{H,B}}\left(\Phi_{1,\text{B}},\ldots,\Phi_{l,\text{B}};c_{1,\text{B}},\ldots,c_{k,\text{B}};\ldots\right), \tag{2.1}$$

with $i=1,\ldots,l$ and $j=1,\ldots,k$. We stress that $c_{j,\text{B}}$ are the theory-defining parameters, i.e. the bare parameters of the original Lagrangian with unbroken gauge symmetry. After

JHEP09(2016)115

spontaneous symmetry breaking, the neutral scalar components $\varphi_{i,\mathrm{B}}$ of the Higgs multiplets obtain vevs $v_{i,\mathrm{B}} + \Delta v_i$, and the Lagrangian can be written as

$$\mathcal{L}_{\mathrm{H,B}}\left(\varphi_{1,\mathrm{B}} + v_{1,\mathrm{B}} + \Delta v_1, \ldots, \varphi_{l,\mathrm{B}} + v_{l,\mathrm{B}} + \Delta v_l; \ldots; c_{1,\mathrm{B}}, \ldots, c_{k,\mathrm{B}}; \ldots\right), \tag{2.2}$$

where the shifts of the vevs Δv_i are introduced for later convenience. The $v_{i,\mathrm{B}}$ are chosen in such a way that the vevs of the shifted fields $\varphi_{i,\mathrm{B}}$

$$\langle \varphi_{i,\mathrm{B}} \rangle = 0 + t_i\left(\Delta v_1, \ldots, \Delta v_l\right) + \text{higher-order corrections}, \tag{2.3}$$

vanish at tree level, where $\Delta v = 0$. Here $\Delta v = 0$ is short for $\Delta v_1 = 0, \ldots, \Delta v_l = 0$. Since the $v_{i,\mathrm{B}}$ are thus defined to minimize the bare scalar potential, they are directly given in terms of the bare (theory-defining) parameters of the Lagrangian [see (2.32) for the SM].

The tadpole counterterm t_i is defined by the expression obtained by taking the derivative of the Lagrangian with respect to the field φ_i, setting all fields to zero and keeping only the linear and higher-order terms in Δv_i. This can be generalized to tadpole counterterms of n-point functions. To this end, we define the tadpole Lagrangian $\Delta\mathcal{L}$ in the *FJ Tadpole Scheme*, which gives rise to all the tadpoles in the theory, as

$$\Delta\mathcal{L} := \mathcal{L} - \mathcal{L}|_{\Delta v = 0}\,. \tag{2.4}$$

Then, the tadpole counterterm is defined by the expression

$$t_i\left(\Delta v_1, \ldots, \Delta v_l\right) \equiv \Delta\mathcal{L}_i\left(\Delta v_1, \ldots, \Delta v_l; \ldots\right) \quad \text{with} \quad \Delta\mathcal{L}_i := \left.\frac{\partial \Delta\mathcal{L}}{\partial \varphi_i}\right|_{\varphi=0}, \tag{2.5}$$

where the field φ_i can be any scalar in the theory. The tadpole counterterms to two-point functions are given by derivatives of the Lagrangian with respect to φ_i and φ_j, i.e.

$$t_{ij}\left(\Delta v_1, \ldots, \Delta v_l\right) \equiv \Delta\mathcal{L}_{ij}\left(\Delta v_1, \ldots, \Delta v_l; \ldots\right) \quad \text{with} \quad \Delta\mathcal{L}_{ij} := \left.\frac{\partial^2 \Delta\mathcal{L}}{\partial \varphi_i \partial \varphi_j}\right|_{\varphi=0}, \tag{2.6}$$

where the fields φ_i and φ_j can be scalars, vector bosons or fermions. Analogously, we obtain the tadpole counterterm to the interaction of three fields

$$t_{ijk}\left(\Delta v_1, \ldots, \Delta v_l\right) \equiv \Delta\mathcal{L}_{ijk}\left(\Delta v_1, \ldots, \Delta v_l; \ldots\right) \quad \text{with} \quad \Delta\mathcal{L}_{ijk} := \left.\frac{\partial^3 \Delta\mathcal{L}}{\partial \varphi_i \partial \varphi_j \partial \varphi_k}\right|_{\varphi=0}, \tag{2.7}$$

where the fields φ_i, φ_j and φ_k can only be scalars or vector bosons in renormalizable quantum field theories. Tadpole counterterms to scalars arise from the Higgs potential, while the tadpole counterterms involving vector bosons and fermions originate from the kinetic terms and the Yukawa terms, respectively, of the Lagrangian of the theory. The one-particle irreducible (1PI) tadpole loop corrections are given by

$T_i = 0 +$ 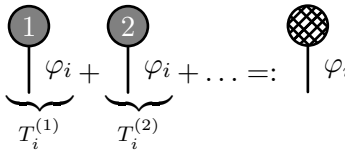 $+ \ldots =:$ φ_i, (2.8)

with the contributions[1] at tree level (0), one loop ($T_i^{(1)}$), two loops ($T_i^{(2)}$), and the hatched graph denoting the sum of all 1PI tadpole graphs. Note that $T_i^{(N)}$ contains $(N-1)$-loop counterterm contributions.

Choosing the shifts of the vevs as $\Delta v = 0$ implies that all tadpole counterterms t_i vanish, and $\langle \varphi_{i,\mathrm{B}} \rangle = 0$ holds at tree level. Already at one-loop order, the bare fields receive a non-vanishing vev due to the tadpole loop corrections in eq. (2.8). In the following, we illustrate the tadpole renormalization for general two-point functions. We define the self-energy $\Sigma_{ii}(q^2)$ of a field i as the higher-order (beyond tree-level) contributions to the inverse connected 2-point function and denote the corresponding 1PI contributions by $\Sigma_{ii}^{1\mathrm{PI}}$. We indicate renormalized functions by a hat. The renormalized self-energy at one-loop order can be written in terms of 1PI graphs as follows

$\hat{\Sigma}_{ii}^{(1)}(q^2) =$ 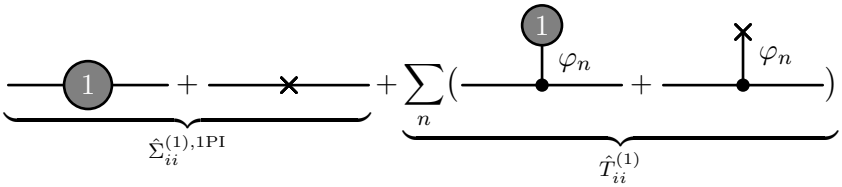

(2.9)

$=$ 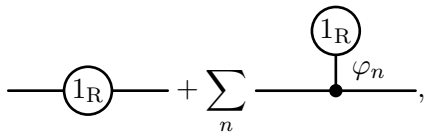

, (2.10)

where the subscript R indicates renormalized 1PI graphs. For the two-loop contributions we obtain

$\hat{\Sigma}_{ii}^{(2)}(q^2) =$ 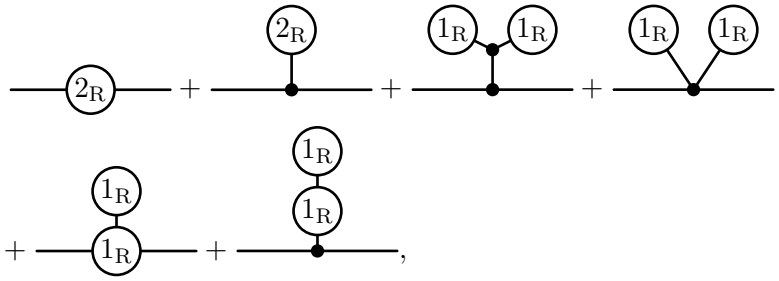

, (2.11)

where we suppressed the summation over tadpoles of different fields for simplicity. In the *FJ Tadpole Scheme* the counterterm corresponding to the two-point irreducible part reads

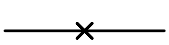 $= t_{ii}(\Delta v_1, \ldots, \Delta v_l) - \delta m_i^2 + (p^2 - m_i^2)\,\delta Z_i,$ (2.12)

where the tadpole counterterm t_{ii} is defined in eq. (2.6), δm_i^2 is the mass counterterm, and δZ_i is the field-renormalization counterterm. In addition, the renormalized tadpole contribution $\hat{T}_{ii}$ with the sum over all scalar fields has to be taken into account. The physical mass is defined as the zero of the full 2-point function.[2] Accordingly in the on-shell scheme the mass counterterm δm_i^2 is obtained by requiring the renormalized on-shell self-energy $\hat{\Sigma}_{ii}(m_i^2)$, as defined in eq. (2.9), to vanish. One can show that the resulting

[1] The tadpole loop contributions T_i should not be confused with the tadpole counterterms t_i.

[2] In the presence of mixing this requires an appropriate renormalization of the mixing energies Σ_{ij}, $i \neq j$.

JHEP09(2016)115

counterterm is gauge independent, for example, by means of extended BRST symmetry (following the proof for W bosons in ref. [19] in the R_ξ-gauge). We have verified that the gauge parameters ξ_Z and ξ_W [see eq. (5.2)] cancel for mass counterterms in the SM and the 2HDM by explicit calculations in the R_ξ gauge.

As stated above, both t_{ii} and t_i vanish for $\Delta v = 0$. Therefore, the non-renormalized sum of the tadpole diagrams T_{ii}, i.e. the third contribution in eq. (2.9), has to be taken into account. To avoid calculating these contributions, we can allow $\Delta v \neq 0$ in eq. (2.2) and relate Δv to the loop tadpole corrections. More precisely, we choose the shift in the vev Δv such that the fields φ do not develop a vev to any order in perturbation theory, which is equivalent to setting all renormalized tadpole contributions $\hat{T}_i$ of the theory to zero. The shifts Δv are determined by solving the non-linear equations

$$-T_i = t_i\left(\Delta v_1, \ldots, \Delta v_l\right), \tag{2.13}$$

with t_i defined in eq. (2.5). This equation is solved order by order in perturbation theory upon using the perturbative expansion of Δv,

$$\Delta v_i = \Delta v_i^{(1)} + \Delta v_i^{(2)} + \ldots, \tag{2.14}$$

and the perturbative expansion of the tadpole contributions (2.8).

As an important consequence of the consistent inclusion of tadpole contributions, as in eqs. (2.10) and (2.11), connected Green's functions do not depend on a particular choice of Δv. To proof this, we consider the generating functional of Green's functions $Z[j]$ defined using the Lagrangian (2.2) with $\Delta v = 0$ and the generating functional $Z'[j]$ based on eq. (2.2) with an arbitrary $\Delta v \neq 0$. Restricting ourselves for simplicity to the case with only one Higgs field φ, the two functionals can be related by a field redefinition $\varphi \to \varphi - \Delta v$ in $Z'[j]$ using the invariance of the path integral measure under a constant shift. The corresponding generating functionals of connected Green's functions $W[j] = \log Z[j]$ and $W'[j] = \log Z'[j]$ are related by

$$W'[j] = W[j] - \mathrm{i}\Delta v \int \mathrm{d}^4x\, j(x). \tag{2.15}$$

Consequently, it follows for the connected Green's functions

$$\left.\frac{\delta^n W'}{\mathrm{i}\delta j(x_1)\ldots\mathrm{i}\delta j(x_n)}\right|_{j=0} = \left.\frac{\delta^n W}{\mathrm{i}\delta j(x_1)\ldots\mathrm{i}\delta j(x_n)}\right|_{j=0}, \quad \text{for} \quad n > 1, \tag{2.16}$$

$$\left.\frac{\delta W'}{\mathrm{i}\delta j(x_1)}\right|_{j=0} = \left.\frac{\delta W}{\mathrm{i}\delta j(x_1)}\right|_{j=0} - \Delta v. \tag{2.17}$$

Note that this does not imply that the vertex functions are the same. The connection between the vertex functions in both formulations is given by

$$\Gamma'[\bar{\varphi}'(j)] = \Gamma[\bar{\varphi}(j)] \quad \text{with} \quad \bar{\varphi}(j(x)) := \frac{\delta W}{\mathrm{i}\delta j(x)} \quad \text{and} \quad \bar{\varphi}' = \bar{\varphi} - \Delta v. \tag{2.18}$$

Treating Δv perturbatively, the n-point vertex functions are related by

$$\frac{\delta^n\left(\Gamma'[\bar{\varphi}] - \Gamma[\bar{\varphi}]\right)}{\delta\bar{\varphi}(x_1)\ldots\bar{\varphi}(x_n)} = \frac{\delta^n\left(\Gamma[\bar{\varphi}+\Delta v] - \Gamma[\bar{\varphi}]\right)}{\delta\bar{\varphi}(x_1)\ldots\bar{\varphi}(x_n)} =: \frac{\delta^n\Gamma^\Delta[\bar{\varphi}]}{\delta\bar{\varphi}(x_1)\ldots\bar{\varphi}(x_n)} = \mathcal{O}\left(\Delta v\right). \tag{2.19}$$

JHEP09(2016)115

However, eq. (2.16) states that the tadpole counterterm dependence originating from Γ^{Δ} cancels in connected Green's functions with more than one external leg.

According to eq. (2.16) the tadpole renormalization condition $\hat{T}_i = 0$ does not modify connected Green's functions in the *FJ Tadpole Scheme* since Δv can be freely chosen, in particular, such that the tadpole equations (2.13) are fulfilled. This has interesting consequences for the interpretation of the tadpole counterterms. For example, using that the expression (2.9) is independent of Δv, we conclude that the one-loop two-point tadpole counterterm derived from eq. (2.4) obeys

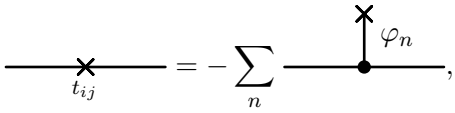

(2.20)

independently of the nature of the external particle(s). This can also be seen directly at one-loop order by computing the two-point tadpole contribution t_{ij} which can be derived from eq. (2.19). To this end, we assume a typical scalar potential V in the Lagrangian (2.1) without derivative interactions. Expanding t_{ij} to first order in Δv and using that Δv acts as a field shift, we obtain

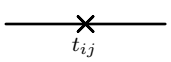

$$
\begin{aligned}
&= \text{F.T.} \sum_n \Delta v_n \left. \frac{\partial \delta^2 S}{\partial \Delta v_n \delta\varphi_i \delta\varphi_j} \right|_{\varphi=0,\Delta v=0} + \mathcal{O}\left((\Delta v)^2\right), \\
&= \text{F.T.} \sum_n \Delta v_n \left. \frac{\delta^3 S}{\delta\varphi_n \delta\varphi_i \delta\varphi_j} \right|_{\varphi=0,\Delta v=0} + \mathcal{O}\left((\Delta v)^2\right),
\end{aligned}
\tag{2.21}
$$

where we use that Γ is given by the action S at tree-level[3] and F.T. denotes the Fourier transform that translates Green's functions from configuration space to momentum space. Defining the mass squared matrix of the scalar fields

$$
(M^2)_{ij} := \left. \frac{\partial^2 V}{\partial\varphi_i \partial\varphi_j} \right|_{\varphi=0,\Delta v=0}, \tag{2.22}
$$

the explicit tadpole counterterm to the two-point function reads

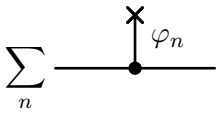

$$
= \sum_{n,k} \left(\text{F.T.} \left. \frac{\delta^3 S}{\delta\varphi_n \delta\varphi_i \delta\varphi_j} \right|_{\varphi=0,\Delta v=0} \right) (M^2)^{-1}_{nk} t_k. \tag{2.23}
$$

For the tadpole counterterm, we find

$$
\begin{aligned}
t_i = \left. \frac{\partial \Delta\mathcal{L}}{\partial\varphi_i} \right|_{\varphi=0} &= \sum_n \left. \frac{\partial^2 \mathcal{L}}{\partial\varphi_i \partial \Delta v_n} \right|_{\varphi=0,\Delta v=0} \Delta v_n + \mathcal{O}\left((\Delta v)^2\right) \\
&= -\sum_n \left. \frac{\partial^2 V}{\partial\varphi_i \partial\varphi_n} \right|_{\varphi=0,\Delta v=0} \Delta v_n + \mathcal{O}\left((\Delta v)^2\right) = -\sum_n \left(M^2\right)_{in} \Delta v_n + \mathcal{O}\left((\Delta v)^2\right).
\end{aligned}
\tag{2.24}
$$

[3]The contribution (2.21) is a higher-order contribution because Δv is identified with a higher-order correction.

JHEP09(2016)115

Inserting this into eq. (2.23), yields

$$\sum_n \; \varphi_n \;= \sum_{n,k,l} \text{F.T.} \left.\frac{\delta^3 S}{\delta\varphi_n \delta\varphi_i \delta\varphi_j}\right|_{\varphi=0,\Delta v=0} \left(M^2\right)^{-1}_{nk} \left[-\left(M^2\right)_{kl} \Delta v_l\right] + \mathcal{O}\left((\Delta v)^2\right)$$
$$= -\text{F.T.} \sum_n \left.\frac{\delta^3 S}{\delta\varphi_n \delta\varphi_i \delta\varphi_j}\right|_{\varphi=0,\Delta v=0} \Delta v_n + \mathcal{O}\left((\Delta v)^2\right). \tag{2.25}$$

Combining this result with eq. (2.21), we have explicitly verified eq. (2.20) at one-loop order.

Using the tadpole renormalization condition (2.13), the one-loop two-point tadpole counterterm can be expressed as

$$\underset{t_{ij}}{\times} = -\sum_n \; \varphi_n \; = \sum_n \; \overset{1}{\bullet}\!\!\varphi_n, \quad \text{if} \quad t_n = -T_n \quad \forall n. \tag{2.26}$$

Therefore, the tadpole counterterms mimic the contribution of tadpole diagrams T_i, once T_i is identified with $-t_i$.

We conclude that the *FJ Tadpole Scheme* is equivalent to a scheme where tadpoles are not renormalized, which corresponds to setting Δv to zero in eq. (2.2) and computing all tadpole diagrams explicitly. The consistent use of the *FJ Tadpole Scheme* defined in eqs. (2.2) and (2.5)–(2.7) guarantees the independence of the chosen tadpole renormalization, meaning that the value for any physical quantity is independent of the value of t_i and thus $\hat{T}_i$.

We stress that the shift Δv_i in the vevs is not a parameter of the theory but can be chosen arbitrarily. By solving the tadpole equation (2.13), which can be done order by order in perturbation theory, the shift can be expressed as a function of tadpole counterterms. After spontaneous symmetry breaking, the bare physical parameters like particle masses can be expressed through the theory defining parameters, i.e. the coupling constants in the Higgs potential before spontaneous symmetry breaking. In the *FJ Tadpole Scheme*, tadpole contributions are never absorbed into the definition of bare physical parameters, which is crucial to assure gauge independence in some renormalization schemes.

Here, we would like to mention a general consequence of BRST invariance [21]: S-matrix elements calculated in terms of the bare theory-defining parameters $c_{j,\text{B}}$ of eq. (2.1) are gauge independent. Thus, renormalization schemes that fix the $c_{j,\text{B}}$ in a gauge-independent way lead to a gauge-independent S-matrix. A possible gauge-dependent definition of Δv does not spoil the gauge independence of the S-matrix, as long as it does not enter the renormalization conditions. However, the latter requirement is violated in popular schemes as detailed below.

In the following, within the *FJ Tadpole Scheme* we always take advantage of the tadpole renormalization condition $\hat{T}_i = 0$, and explicit (counterterm-)tadpoles do not show up. In section 2.2, we describe the *FJ Tadpole Scheme* scheme in the SM, and in section 4.1, it is applied to the 2HDM. For both models, we discuss how the bare physical masses are properly related to the original parameters of the Lagrangian.

JHEP09(2016)115

2.2 The FJ Tadpole Scheme in the SM

In the SM, physical parameters such as the particle masses and the EW couplings are usually renormalized using on-shell and physical renormalization conditions leading to gauge-independent physical observables.[4] Nevertheless, the techniques discussed in the previous section, which result in gauge-independent counterterms to physical parameters in arbitrary renormalization schemes, can already be illustrated in the SM. Following the notation in ref. [22], the bare Lagrangian for the Higgs field Φ_{B} defined in eq. (2.1) can be written as

$$\mathcal{L}_{\mathrm{H,B}} = (D_\mu \Phi_{\mathrm{B}})^\dagger (D^\mu \Phi_{\mathrm{B}}) - V_{\mathrm{B}}(\Phi_{\mathrm{B}}). \tag{2.27}$$

The Higgs field couples to the gauge bosons through the covariant derivative D_μ. The bare Higgs potential is given by

$$V_{\mathrm{B}}(\Phi_{\mathrm{B}}) = \frac{\lambda_{\mathrm{B}}}{4}(\Phi_{\mathrm{B}}^\dagger \Phi_{\mathrm{B}})^2 - \mu_{\mathrm{B}}^2 \Phi_{\mathrm{B}}^\dagger \Phi_{\mathrm{B}} \tag{2.28}$$

with the bare Higgs doublet Φ_{B} defined as

$$\Phi_{\mathrm{B}} = \begin{pmatrix} \phi_{\mathrm{B}}^+(x) \\ \frac{1}{\sqrt{2}}\left[v_{\mathrm{B}} + \Delta v + h_{\mathrm{B}}(x) + \mathrm{i}\chi_{\mathrm{B}}(x)\right] \end{pmatrix}. \tag{2.29}$$

We insert the Higgs doublet into the potential and collect the terms linear, V_{B}^1, and quadratic, V_{B}^2, in the bare, neutral, scalar Higgs field h_{B},

$$\begin{aligned} V_{\mathrm{B}}(\Phi_{\mathrm{B}}) &\supset (v_{\mathrm{B}} + \Delta v)\left(\frac{\lambda_{\mathrm{B}}}{4}(v_{\mathrm{B}} + \Delta v)^2 - \mu_{\mathrm{B}}^2\right) h_{\mathrm{B}}(x) + \left(\frac{3\lambda_{\mathrm{B}}}{8}(v_{\mathrm{B}} + \Delta v)^2 - \frac{1}{2}\mu_{\mathrm{B}}^2\right) h_{\mathrm{B}}^2(x) \\ &\equiv V_{\mathrm{B}}^1(\Delta v, h_{\mathrm{B}}) + V_{\mathrm{B}}^2(\Delta v, h_{\mathrm{B}}). \end{aligned} \tag{2.30}$$

The relation between Δv and the tadpole counterterm t_h is determined according to eq. (2.5),

$$t_h h_{\mathrm{B}}(x) = -V_{\mathrm{B}}^1. \tag{2.31}$$

Using the tree-level condition, $\Delta v = 0 \Leftrightarrow t_h = 0$, gives the relations between the bare parameters

$$\lambda_{\mathrm{B}} = \frac{4\mu_{\mathrm{B}}^2}{v_{\mathrm{B}}^2}, \qquad \mu_{\mathrm{B}}^2 = \frac{M_{\mathrm{h,B}}^2}{2}, \qquad v_{\mathrm{B}} = \frac{2M_{\mathrm{W,B}}}{g_{\mathrm{B}}}, \tag{2.32}$$

where the last relation defines the bare W-boson mass. The exact form of the shift Δv in terms of the tadpole counterterm t_h can be obtained from eq. (2.5), which requires the knowledge of the linear term of the Higgs potential (2.30) for $\Delta v \neq 0$,

$$\begin{aligned} V_{\mathrm{B}}^1(\Delta v, h_{\mathrm{B}}) &= (v_{\mathrm{B}} + \Delta v)\left(\frac{\lambda_{\mathrm{B}}}{4}(v_{\mathrm{B}} + \Delta v)^2 - \mu_{\mathrm{B}}^2\right) h_{\mathrm{B}}(x) \\ &= \frac{M_{\mathrm{h,B}}^2 \Delta v}{8M_{\mathrm{W,B}}^2}(2M_{\mathrm{W,B}} + g_{\mathrm{B}}\Delta v)(4M_{\mathrm{W,B}} + g_{\mathrm{B}}\Delta v)\, h_{\mathrm{B}}(x), \\ &\stackrel{!}{=} -t_h h_{\mathrm{B}}(x). \end{aligned} \tag{2.33}$$

[4] The renormalization of the strong coupling is not influenced by tadpoles at the one-loop level.

JHEP09(2016)115

We can relate Δv to the tadpole counterterms t_h at every order in perturbation theory. For $\Delta v = \Delta v^{(1)} + \Delta v^{(2)} + \ldots$ and $t_h^{(L)}$ being the L-loop tadpole counterterm corresponding to the SM Higgs boson, we obtain

$$\Delta v^{(1)} = -\frac{t_h^{(1)}}{M_{\mathrm{h,B}}^2} \tag{2.34}$$

at one-loop order and

$$\Delta v^{(2)} = -\frac{t_h^{(2)}}{M_{\mathrm{h,B}}^2} - \frac{3 g_{\mathrm{B}} \left(\Delta v^{(1)}\right)^2}{4 M_{\mathrm{W,B}}} \tag{2.35}$$

at two loops. The tadpole counterterm to the two-point function of the SM Higgs boson can be obtained from eq. (2.6)

$$\begin{aligned} V_{\mathrm{B}}^2\left(\Delta v, h_{\mathrm{B}}\right) &= \left(\frac{3\lambda_{\mathrm{B}}}{4}\left(v_{\mathrm{B}} + \Delta v\right)^2 - \mu_{\mathrm{B}}^2\right)\frac{h_{\mathrm{B}}^2(x)}{2} \\ &\stackrel{!}{=} \frac{M_{\mathrm{h,B}}^2 - t_{hh}}{2} h_{\mathrm{B}}^2(x), \end{aligned} \tag{2.36}$$

where λ_{B}, μ_{B}^2, and v_{B} are replaced according to eq. (2.32) as before. This yields

$$t_{hh} h_{\mathrm{B}}^2 = -\left(\frac{3 g_{\mathrm{B}}\, M_{\mathrm{h,B}}^2 \Delta v}{2 M_{\mathrm{W,B}}} + \frac{3 g_{\mathrm{B}}\, M_{\mathrm{h,B}}^2 \left(\Delta v\right)^2}{8 M_{\mathrm{W,B}}^2}\right) h_{\mathrm{B}}^2. \tag{2.37}$$

At one-loop order the bare parameters in eq. (2.37) can be replaced by renormalized ones. Omitting anything beyond one loop, the two-point tadpole counterterm is given by

$$t_{hh}^{(1)} = \frac{3 g t_h^{(1)}}{2 M_{\mathrm{W}}}. \tag{2.38}$$

Using the on-shell condition $q^2 = M_{\mathrm{h,R}}^2$, where $M_{\mathrm{h,R}}$ denotes the renormalized Higgs-boson mass, and the tadpole renormalization condition $\hat{T}_h = 0$, the renormalized on-shell two-point function of the Higgs boson reads

$$\hat{\Sigma}_{hh}^{(1)}(M_{\mathrm{h,R}}^2) = \Sigma_{hh}^{(1),\mathrm{1PI}}(M_{\mathrm{h,R}}^2) - \frac{3 g T_h^{(1)}}{2 M_{\mathrm{W}}} - \left(\delta M_{\mathrm{h}}^2\right)^{(1)}. \tag{2.39}$$

This expression can be used to determine the counterterm of the Higgs-boson mass δM_{h}^2.

We note that at the two-loop order bare parameters need to be expressed in terms of counterterms and renormalized parameters in eqs. (2.34) and (2.37), omitting any terms beyond two loops. The Higgs-boson self-energy at two loops, focussing on the tadpole dependence, is discussed in appendix C.

We note that additional tadpole counterterms are required in the SM for two- and three-point functions of scalars, vector bosons and fermions. Tadpole counterterms for two- and three-point functions involving vector bosons originate from the kinetic terms of the SM Higgs sector, while tadpole counterterms to fermion self-energies result from the Yukawa terms of the SM Lagrangian.

JHEP09(2016)115

2.3 Gauge independence of physical parameters in the SM

As mentioned at the beginning of section 2, the physical parameters of the SM are usually renormalized on shell. In this case, gauge dependencies introduced by careless treatments of tadpoles cancel in all renormalized physical quantities. However, when some parameters are renormalized in the $\overline{\text{MS}}$ scheme this is not generally the case. Such problems can originate from gauge-dependent counterterms resulting from a gauge-dependent definition of bare physical parameters. We use the SM to demonstrate potential problems with gauge dependence in renormalization schemes commonly used in the literature. In order to illustrate the effect of different tadpole renormalization schemes on the gauge dependence of the counterterms of physical parameters, we compare the gauge dependence of the Higgs-boson mass counterterm δM_{h}^2 in the scheme described in ref. [22] and the β_h scheme from ref. [20] to the *FJ Tadpole Scheme*.

The scheme described in ref. [22] requires the vev of the bare Higgs-boson field to vanish at one-loop order

$$\langle h_{\text{B}} \rangle = 0, \tag{2.40}$$

such that t_h is fixed via eq. (2.13) and thus gauge dependent. At the same time, the bare Higgs-boson mass $M_{\text{h,B}}^2$ is defined as the coefficient of the quadratic term in the Higgs field. As a consequence, no tadpole counterterm t_{hh} appears in the two-point function. However, the so-defined bare Higgs-boson mass, e.g. at one loop

$$M_{\text{h,B}}^2 = 2\mu_{\text{B}}^2 - t_{hh} = 2\mu_{\text{B}}^2 - \frac{3g_{\text{B}}t_h}{2M_{\text{W,B}}}, \tag{2.41}$$

depends on the tadpole counterterm t_h and thus becomes gauge dependent as well.

The mass counterterm of the Higgs boson, defined as the difference between the bare mass squared $M_{\text{h,B}}^2$ and the renormalized Higgs-boson mass squared $M_{\text{h,R}}^2$,

$$M_{\text{h,B}}^2 \equiv M_{\text{h,R}}^2 + \delta M_{\text{h}}^2, \tag{2.42}$$

is determined by requiring that the renormalized self-energy (2.9) vanishes on-shell, i.e. for $q^2 = M_{\text{h,R}}^2$. Since the renormalized tadpole contribution $\hat{T}_h^{(1)}$ vanishes [see eq. (2.40)], the Higgs-boson mass counterterm is given by the 1PI contribution

$$\hat{\Sigma}_{hh}^{\text{1PI}}\left(M_{\text{h,R}}^2\right) = \Sigma_{hh}^{\text{1PI}}\left(M_{\text{h,R}}^2\right) - \delta M_{\text{h}}^2 \stackrel{!}{=} 0. \tag{2.43}$$

The gauge dependence of $\Sigma_{hh}^{\text{1PI}}(M_{\text{h,R}}^2)$, which results in a gauge-dependent mass counterterm δM_{h}^2, can be shown by means of an explicit calculation as in ref. [23].

In the scheme of ref. [22] also the bare gauge-boson and fermion masses become gauge dependent, since they are defined using the shifted vev $(v_{\text{B}} + \Delta v)$. For instance, the bare W-boson mass is given by

$$M_{\text{W,B}} = \frac{1}{2}g_{\text{B}}(v_{\text{B}} + \Delta v) = \frac{1}{2}g_{\text{B}}\left(v_{\text{B}} - \frac{t_h}{M_{\text{h,B}}^2}\right) \tag{2.44}$$

at one-loop order.

JHEP09(2016)115

The gauge dependence of the Higgs-boson mass counterterm can also be understood from its definition (2.42). As the renormalized mass parameter is identified with the physical mass in the on-shell scheme, which has to be gauge independent, the gauge dependence of a bare parameter must be compensated by the gauge dependence of the counterterm. Using the short-hand notation ∂_ξ for $\partial/\partial\xi$, (2.42) leads to

$$\partial_\xi M^2_{\mathrm{h,B}} = \partial_\xi M^2_{\mathrm{h,R}} + \partial_\xi \delta M^2_{\mathrm{h}} \tag{2.45}$$

in the R_ξ-gauge with gauge parameter ξ. As $\partial_\xi M^2_{\mathrm{h,R}} = 0$, the gauge dependence of $M^2_{\mathrm{h,B}}$ is directly related to the gauge dependence of δM^2_{h}.

A similar discussion applies to the β_h scheme in ref. [20] which also requires the vev $\langle h_{\mathrm{B}} \rangle$ to vanish at higher orders and defines the bare masses using the shifted vev, e.g.

$$M^2_{\mathrm{h,B}} = \frac{1}{2}\lambda_{\mathrm{B}}(v_{\mathrm{B}} + \Delta v)^2 = \frac{1}{2}\lambda_{\mathrm{B}} v_{\mathrm{B}} \left(v_{\mathrm{B}} - 2\frac{t_h}{M^2_{\mathrm{h,B}}} \right) = \frac{1}{2}\lambda_{\mathrm{B}} v^2_{\mathrm{B}} - \frac{g_{\mathrm{B}} t_h}{M_{\mathrm{W,B}}}, \tag{2.46}$$

$$M_{\mathrm{W,B}} = \frac{1}{2} g_{\mathrm{B}}(v_{\mathrm{B}} + \Delta v) = \frac{1}{2} g_{\mathrm{B}} \left(v_{\mathrm{B}} - \frac{t_h}{M^2_{\mathrm{h,B}}} \right) \tag{2.47}$$

at one-loop order. In this scheme the parameter μ_{B} is eliminated from the bare Lagrangian in favour of t_h and $M^2_{\mathrm{h,B}}$, while λ_{B} is expressed in terms of $M^2_{\mathrm{h,B}}$, $M^2_{\mathrm{W,B}}$ and g_{B}. As a consequence, all tadpoles to 3-point functions are absorbed into the definition of the bare physical parameters. This has the advantage that tadpole counterterms appear exclusively in one- and two-point functions for the Higgs and would-be Goldstone bosons. However, the bare masses become gauge dependent via the dependence on the tadpole t_h. The Higgs-boson mass counterterm reads

$$\delta M^2_{\mathrm{h}} = \Sigma^{\mathrm{1PI}}_{hh}\left(M^2_{\mathrm{h,R}}\right) - \frac{g_{\mathrm{B}} T^{(1)}_h}{2 M_{\mathrm{W,B}}}. \tag{2.48}$$

This definition differs from the one resulting from eq. (2.39) upon imposing the on-shell mass renormalization condition $\hat{\Sigma}_{hh}(M^2_{\mathrm{h,R}}) = 0$ by gauge-dependent tadpole terms. In ref. [20], the β_t scheme has been introduced to cure this problem. There, the bare particle masses are defined in terms of the bare vev and are therefore gauge independent. When tadpoles are renormalized requiring $\hat{T}_h = 0$, the *FJ Tadpole Scheme* in the SM is equivalent to the β_t scheme.

The theory-defining bare parameters of the original Lagrangian, e.g. λ_{B} and μ_{B} are gauge independent by definition. When introducing a new set of bare parameters, these can become gauge dependent if vevs or tadpoles enter their definition. Bare parameters that are defined exclusively by the theory-defining bare parameters remain gauge independent.

In the scheme of ref. [22] and the β_h scheme of ref. [20] discussed above, all bare particle masses are gauge dependent. However, the gauge dependence cancels in physical quantities since all parameters of the theory are defined by on-shell renormalization conditions. This can be seen as follows: the gauge dependence of the counterterms results from the omission of gauge-dependent tadpole contributions. Since these are momentum independent they

JHEP09(2016)115

cancel in renormalized quantities that are defined by subtracting the same quantity at a fixed point in momentum space. This holds for on-shell schemes or momentum-subtraction schemes but not for MS or $\overline{\text{MS}}$ schemes, where only the divergent parts are subtracted. Since in the scheme of ref. [22] as well as in the β_h scheme of ref. [20] all renormalization conditions are based on complete subtraction of the relevant vertex functions, the resulting physical quantities and scattering amplitudes are gauge independent. This changes when some parameters are renormalized in the $\overline{\text{MS}}$ scheme, potentially inducing gauge dependence in the S-matrix if applied to gauge-dependent bare parameters.

For later convenience we describe a simple way to construct the different tadpole schemes from the original bare Lagrangian (2.2) or (2.27) augmented by gauge, fermion and Yukawa terms. The starting point is the bare Lagrangian in terms of the theory-defining parameters, i.e. μ_{B}^2, λ_{B}, g_{B}, ... for the SM, where the bare scalar fields have been shifted by an independent parameter v_{B} (which is not yet fixed by a minimum condition) and vanishing Δv. Then, the tadpole renormalization in the different schemes at one-loop order can be introduced by shifting the bare parameters as follows:

Scheme 1.

The bare Lagrangian in the scheme of ref. [22] is obtained upon performing the shifts

$$\lambda_{\text{B}} \to \lambda_{\text{B}} + \frac{2t_h}{v_{\text{B}}^3}, \qquad \mu_{\text{B}}^2 \to \mu_{\text{B}}^2 + \frac{3}{2}\frac{t_h}{v_{\text{B}}}. \tag{2.49}$$

Scheme 2.

The bare Lagrangian in the β_h scheme of ref. [20] results from the shifts

$$\lambda_{\text{B}} \to \lambda_{\text{B}}, \qquad \mu_{\text{B}}^2 \to \mu_{\text{B}}^2 + \frac{t_h}{v_{\text{B}}}. \tag{2.50}$$

Scheme 3.

Finally, the bare Lagrangian in the *FJ Tadpole Scheme* scheme is obtained via

$$v_{\text{B}} \to v_{\text{B}} - \frac{t_h}{M_{\text{h}}^2}. \tag{2.51}$$

Only after these shifts the vev v_{B} is fixed by minimizing the scalar potential for $t_h = 0$ and thus related to μ_{B}^2 and λ_{B}.

We have shown that the *FJ Tadpole Scheme* is the natural scheme for dealing with the tadpoles, as it prevents that tadpoles are absorbed into the definition of bare parameters. Moreover, the tadpole renormalization condition $\hat{T} = 0$ is very useful since no explicit tadpole loop contributions have to be computed. We stress that the presented tadpole renormalization procedure is general and not restricted to the SM or the 2HDM.

3 Two-Higgs-doublet model — Lagrangian and fields

In this section, we review the definition of the Lagrangian of the 2HDM. We restrict ourselves to the case of a CP-conserving type-II 2HDM with a softly broken Z_2 symmetry. For a comprehensive introduction to the 2HDM we refer to e.g. refs. [3, 4].

JHEP09(2016)115

3.1 Fields and potential in the symmetric basis

Let Φ_i denote the i-th Higgs doublet with $i = 1, 2$ defined by

$$\Phi_i = \begin{pmatrix} \phi_i^+ \\ \frac{1}{\sqrt{2}}\left(v_i + \rho_i + \mathrm{i}\eta_i\right) \end{pmatrix}. \tag{3.1}$$

The most general potential of the 2HDM has 3 quadratic and 7 quartic products of Higgs doublets, each coming with a real or complex coupling constant. Requiring CP conservation and Z_2 symmetry ($\Phi_1 \to -\Phi_1$,$\Phi_2 \to \Phi_2$) simplifies the Lagrangian resulting in five real couplings $\lambda_1 \ldots \lambda_5$ and two real mass parameters m_1^2 and m_2^2. Soft breaking of the Z_2 symmetry allows for the third mass parameter m_{12}^2. Since the theory is spontaneously broken, we assign two vacuum expectation values v_1 and v_2 which, under the same symmetry restriction, can be chosen to be real. The most general potential is then given by

$$\begin{aligned} V = {} & m_1^2 \Phi_1^\dagger \Phi_1 + m_2^2 \Phi_2^\dagger \Phi_2 - m_{12}^2 \left(\Phi_1^\dagger \Phi_2 + \Phi_2^\dagger \Phi_1\right) \\ & + \frac{\lambda_1}{2}\left(\Phi_1^\dagger \Phi_1\right)^2 + \frac{\lambda_2}{2}\left(\Phi_2^\dagger \Phi_2\right)^2 + \lambda_3 \left(\Phi_1^\dagger \Phi_1\right)\left(\Phi_2^\dagger \Phi_2\right) + \lambda_4 \left(\Phi_1^\dagger \Phi_2\right)\left(\Phi_2^\dagger \Phi_1\right) \\ & + \frac{\lambda_5}{2}\left[\left(\Phi_1^\dagger \Phi_2\right)^2 + \left(\Phi_2^\dagger \Phi_1\right)^2\right]. \end{aligned} \tag{3.2}$$

3.2 Fields and potential in the mass eigenbasis

After spontaneous symmetry breaking the eight degrees of freedom in the doublets (3.1) split into three would-be Goldstone bosons G_0 and $G^\pm$ and five physical Higgs bosons $H_\mathrm{l}, H_\mathrm{h}, H_\mathrm{a}, H^\pm$. In order to identify the mass eigenstates, the part of the Lagrangian quadratic in the fields needs to be diagonalized. The mixing angle β is introduced to separate would-be Goldstone bosons from charged and pseudoscalar physical Higgs fields, and the angle α is required to diagonalize the neutral Higgs sector. With the rotation matrices

$$R(\alpha) = \begin{pmatrix} \cos\alpha & -\sin\alpha \\ \sin\alpha & \cos\alpha \end{pmatrix}, \qquad R(\beta) = \begin{pmatrix} \cos\beta & -\sin\beta \\ \sin\beta & \cos\beta \end{pmatrix}, \tag{3.3}$$

the mass eigenstates of Higgs- and would-be-Goldstone-boson fields are obtained by the following transformations

$$\begin{pmatrix} \rho_1 \\ \rho_2 \end{pmatrix} = R(\alpha) \begin{pmatrix} H_\mathrm{h} \\ H_\mathrm{l} \end{pmatrix}, \qquad \begin{pmatrix} \phi_1^\pm \\ \phi_2^\pm \end{pmatrix} = R(\beta) \begin{pmatrix} G^\pm \\ H^\pm \end{pmatrix}, \qquad \begin{pmatrix} \eta_1 \\ \eta_2 \end{pmatrix} = R(\beta) \begin{pmatrix} G_0 \\ H_\mathrm{a} \end{pmatrix}, \tag{3.4}$$

for a suitable choice of α and β.

The Higgs sector is coupled to the gauge sector by means of covariant derivatives. Identifying the mass eigenstates of the vector bosons, one obtains the well-known tree-level relations in the 2HDM

$$M_\mathrm{W} = \frac{1}{2} g v, \qquad M_\mathrm{Z} = \frac{1}{2}\sqrt{g^2 + g'^2}\, v, \qquad v = \sqrt{v_1^2 + v_2^2}, \tag{3.5}$$

JHEP09(2016)115

where g and g' denote the weak isospin and hypercharge gauge couplings, and M_{W} and M_{Z} the W- and Z-boson masses, respectively. The mixing angle β is related to the ratio of vevs according to $t_\beta \equiv \tan\beta = v_2/v_1$. The angle α is chosen such that it diagonalizes the symmetric mass-squared matrix defined by

$$M_{ij} := \left.\frac{\partial^2 V}{\partial\rho_i \partial\rho_j}\right|_{\varphi=0}, \tag{3.6}$$

where V is the potential in eq. (3.2). The solution reads [3]

$$\sin 2\alpha = \frac{2M_{12}}{\sqrt{(M_{11}-M_{22})^2 + 4M_{12}^2}}. \tag{3.7}$$

The parameters of the Higgs potential can then be substituted for physical parameters after SSB and after diagonalizing the neutral Higgs sector. The minimum conditions for the scalar potential, $\langle\rho_i\rangle = 0$, read

$$\begin{aligned} m_1^2 &= M_{\mathrm{sb}}^2 \sin^2\beta - \frac{2M_{\mathrm{W}}^2}{g^2}\Big[\lambda_1 \cos^2\beta + (\lambda_3+\lambda_4+\lambda_5)\sin^2\beta\Big], \\ m_2^2 &= M_{\mathrm{sb}}^2 \cos^2\beta - \frac{2M_{\mathrm{W}}^2}{g^2}\Big[\lambda_2 \sin^2\beta + (\lambda_3+\lambda_4+\lambda_5)\cos^2\beta\Big], \end{aligned} \tag{3.8}$$

where we have defined the soft-breaking scale M_{sb} as

$$M_{\mathrm{sb}}^2 = \frac{m_{12}^2}{\cos\beta\sin\beta}. \tag{3.9}$$

The quartic coupling parameters λ_i are expressed by the masses of the physical particles, i.e. the Higgs-boson masses $M_{H_{\mathrm{l}}}$, $M_{H_{\mathrm{h}}}$, $M_{H_{\mathrm{a}}}$, $M_{H^\pm}$ and the gauge-boson masses $M_{\mathrm{W}}, M_{\mathrm{Z}}$, the soft-breaking scale M_{sb}, and the mixing angles α and β as

$$\begin{aligned} \lambda_1 &= \frac{g^2}{4M_{\mathrm{W}}^2\cos^2\beta}\left[\cos^2\alpha M_{H_{\mathrm{h}}}^2 + \sin^2\alpha M_{H_{\mathrm{l}}}^2 - \sin^2\beta M_{\mathrm{sb}}^2\right], \\ \lambda_2 &= \frac{g^2}{4M_{\mathrm{W}}^2\sin^2\beta}\left[\sin^2\alpha M_{H_{\mathrm{h}}}^2 + \cos^2\alpha M_{H_{\mathrm{l}}}^2 - \cos^2\beta M_{\mathrm{sb}}^2\right], \\ \lambda_3 &= \frac{g^2}{4M_{\mathrm{W}}^2}\left[\frac{\cos\alpha\sin\alpha}{\cos\beta\sin\beta}\left(M_{H_{\mathrm{h}}}^2 - M_{H_{\mathrm{l}}}^2\right) + 2M_{H^\pm}^2 - M_{\mathrm{sb}}^2\right], \\ \lambda_4 &= \frac{g^2}{4M_{\mathrm{W}}^2}\left(M_{H_{\mathrm{a}}}^2 - 2M_{H^\pm}^2 + M_{\mathrm{sb}}^2\right), \\ \lambda_5 &= \frac{g^2}{4M_{\mathrm{W}}^2}\left(M_{\mathrm{sb}}^2 - M_{H_{\mathrm{a}}}^2\right), \end{aligned} \tag{3.10}$$

where the vev v has been substituted using eq. (3.5).

3.3 Yukawa Lagrangian for the type-II 2HDM

In the type-II 2HDM, the up-type quarks couple to Φ_2, while the down-type quarks and leptons couple to Φ_1. This corresponds to the Higgs sector in the MSSM, but here, it is

JHEP09(2016)115

realized by the discrete Z_2 symmetry $\Phi_1 \to -\Phi_1$, $d_\mathrm{R} \to -d_\mathrm{R}$, $l_\mathrm{R} \to -l_\mathrm{R}$ and all other fields unchanged. The corresponding Yukawa Lagrangian reads

$$\mathcal{L}_Y = -\Gamma_\mathrm{d}\overline{Q}_\mathrm{L}\Phi_1 d_\mathrm{R} - \Gamma_\mathrm{u}\overline{Q}_\mathrm{L}\tilde{\Phi}_2 u_\mathrm{R} - \Gamma_\mathrm{l}\overline{L}_\mathrm{L}\Phi_1 l_\mathrm{R} + \mathrm{h.c.}, \tag{3.11}$$

where $\tilde{\Phi}_2$ is the charge-conjugated Higgs doublet of Φ_2. Neglecting flavour mixing, the coefficients are expressed by the fermion masses m_d, m_u and m_l, and the mixing angle β,

$$\Gamma_\mathrm{d} = \frac{g\, m_\mathrm{d}}{\sqrt{2} M_\mathrm{W} \cos\beta}, \qquad \Gamma_\mathrm{u} = \frac{g\, m_\mathrm{u}}{\sqrt{2} M_\mathrm{W} \sin\beta}, \qquad \Gamma_\mathrm{l} = \frac{g\, m_\mathrm{l}}{\sqrt{2} M_\mathrm{W} \cos\beta}. \tag{3.12}$$

Again, the vev v has been substituted using eq. (3.5).

3.4 Physical parameters

In the mass eigenbasis the physical parameters resulting from the Higgs sector are identified with the Higgs-boson masses, M_{H_l} (light Higgs boson), M_{H_h} (heavy Higgs boson), M_{H_a} (pseudoscalar Higgs boson), $M_{H^\pm}$ (charged Higgs boson), the two mixing angles α and β, the soft-Z_2-breaking scale M_sb, and the vacuum expectation value v. The mass of the light Higgs boson is commonly identified with the mass of the observed Higgs boson, and v also keeps its SM value being directly related to the W-boson mass M_W. This leaves a total of six new parameters compared to the SM. This identification allows to translate the parameters in the symmetric basis to the mass eigenbasis

$$\lambda_1, \lambda_2, \lambda_3, \lambda_4, \lambda_5, m_1, m_2, m_{12} \;\to\; M_{H_\mathrm{l}}, M_{H_\mathrm{h}}, M_{H_\mathrm{a}}, M_{H^\pm}, M_\mathrm{sb}, \alpha, \beta, M_\mathrm{W}/g. \tag{3.13}$$

Note that the vevs v_1 and v_2 are no independent physical parameters. In the following, we choose a more natural representation for the angles in view of the alignment limit [3]

$$\alpha,\ \beta \quad \to \quad c_{\alpha\beta} := \cos(\alpha-\beta),\ t_\beta := \tan\beta, \tag{3.14}$$

which can be achieved by using simple trigonometric identities.[5] We have chosen the sign convention for the angles in such a way that the alignment limit is reached by

$$s_{\alpha\beta} \to -1, \qquad c_{\alpha\beta} \to 0. \tag{3.15}$$

4 Renormalization conditions in the 2HDM

As argued in section 2, the 2HDM is an example of a theory with new parameters, namely the mixing angles α and β and the soft-Z_2-breaking scale M_sb, whose on-shell renormalization through vertex functions would introduce a process dependence or would be plagued by IR singularities. This has been discussed for the decays of heavy scalar and charged Higgs bosons in ref. [11] and for the renormalization of the mixing angle β in the context of the MSSM in ref. [6]. Therefore, an $\overline{\mathrm{MS}}$ renormalization is advantageous. It requires, however, care in the treatment of tadpoles to assure the gauge independence of the bare physical

[5] $\cos\beta = \frac{1}{\sqrt{1+t_\beta^2}}$, $\sin\beta = \frac{t_\beta}{\sqrt{1+t_\beta^2}}$, $\cos\alpha = \frac{c_{\alpha\beta}-s_{\alpha\beta}t_\beta}{\sqrt{1+t_\beta^2}}$, $\sin\alpha = \frac{s_{\alpha\beta}+c_{\alpha\beta}t_\beta}{\sqrt{1+t_\beta^2}}$.

JHEP09(2016)115

parameters of the theory and thereby of the S-matrix. This is guaranteed by the *FJ Tadpole Scheme* presented in section 2. In this section, this scheme is applied to the 2HDM. The corresponding renormalization conditions are listed in sections 4.3–4.5, including the tadpole counterterms which are essential for the gauge independence of the expressions.

The bare parameters split into the finite, renormalized parameters and counterterms,

$$\begin{aligned}
e_{\mathrm{B}} &= e + \delta e, \\
M^2_{\mathrm{W,B}} &= M^2_{\mathrm{W}} + \delta M^2_{\mathrm{W}}, & M^2_{\mathrm{Z,B}} &= M^2_{\mathrm{Z}} + \delta M^2_{\mathrm{Z}}, \\
M^2_{H_{\mathrm{l}},\mathrm{B}} &= M^2_{H_{\mathrm{l}}} + \delta M^2_{H_{\mathrm{l}}}, & M^2_{H_{\mathrm{h}},\mathrm{B}} &= M^2_{H_{\mathrm{h}}} + \delta M^2_{H_{\mathrm{h}}}, \\
M^2_{H_{\mathrm{a}},\mathrm{B}} &= M^2_{H_{\mathrm{a}}} + \delta M^2_{H_{\mathrm{a}}}, & M^2_{H^\pm,\mathrm{B}} &= M^2_{H^\pm} + \delta M^2_{H^\pm}, \\
\alpha_{\mathrm{B}} &= \alpha + \delta\alpha, & \beta_{\mathrm{B}} &= \beta + \delta\beta, \\
M^2_{\mathrm{sb,B}} &= M^2_{\mathrm{sb}} + \delta M^2_{\mathrm{sb}}, \\
m_{f,\mathrm{B}} &= m_f + \delta m_f,
\end{aligned} \tag{4.1}$$

where f stands for any fermion. In the SM, only the Z-boson field Z and the photon field A mix and require the introduction of renormalization matrices. In the 2HDM, we introduce additional renormalization matrices for the mixing of the two neutral scalars H_{l} and H_{h}, the pseudo scalars G_0 and H_{a}, and the charged scalars $G^\pm$ and $H^\pm$. The complete field renormalization is given by

$$\begin{aligned}
W^\pm_{\mathrm{B}} &= \left(1 + \frac{1}{2}\delta Z_{WW}\right) W^\pm, \\
\begin{pmatrix} Z_{\mathrm{B}} \\ A_{\mathrm{B}} \end{pmatrix} &= \begin{pmatrix} 1 + \frac{1}{2}\delta Z_{ZZ} & \frac{1}{2}\delta Z_{ZA} \\ \frac{1}{2}\delta Z_{AZ} & 1 + \frac{1}{2}\delta Z_{AA} \end{pmatrix} \begin{pmatrix} Z \\ A \end{pmatrix}, \\
\begin{pmatrix} S_{\mathrm{B}} \\ S'_{\mathrm{B}} \end{pmatrix} &= \begin{pmatrix} 1 + \frac{1}{2}\delta Z_{SS} & \frac{1}{2}\delta Z_{SS'} \\ \frac{1}{2}\delta Z_{S'S} & 1 + \frac{1}{2}\delta Z_{S'S'} \end{pmatrix} \begin{pmatrix} S \\ S' \end{pmatrix},
\end{aligned} \tag{4.2}$$

where $SS' = \{G_0 H_{\mathrm{a}}, G^\pm H^\pm, H_{\mathrm{h}} H_{\mathrm{l}}\}$. The fermion field renormalization is defined as

$$\begin{aligned}
f^{\mathrm{L}}_{\mathrm{B}} &= \left(1 + \frac{1}{2}\delta Z_{f,\mathrm{L}}\right) f^{\mathrm{L}}, \\
f^{\mathrm{R}}_{\mathrm{B}} &= \left(1 + \frac{1}{2}\delta Z_{f,\mathrm{R}}\right) f^{\mathrm{R}},
\end{aligned} \tag{4.3}$$

for left-handed (L) and right-handed (R) fermions, where we neglect fermion mixing.

4.1 The FJ Tadpole Scheme applied to the 2HDM

The 2HDM as presented in the previous section contains two Higgs doublets with the corresponding two vevs, such that eq. (2.2) becomes

$$\mathcal{L}_{\mathrm{H,B}}\left(\rho_{1,\mathrm{B}} + v_{1,\mathrm{B}} + \Delta v_1, \rho_{2,\mathrm{B}} + v_{2,\mathrm{B}} + \Delta v_2; \ldots\right). \tag{4.4}$$

JHEP09(2016)115

As in the SM, we use eq. (2.5) to obtain Δv_1 and Δv_2 expressed by the L-loop tadpole counterterms, but instead of calculating the tadpoles in the generic basis, we define the vevs in terms of the tadpole counterterms associated to the physical Higgs fields H_l and H_h. Of course, the result does not depend on the choice of parametrization. In the 2HDM, the tadpole counterterms are defined as

$$\begin{aligned} t_{H_\mathrm{l}} &= \Delta\mathcal{L}_{H_\mathrm{l}}\left(\rho_{1,\mathrm{B}} + v_{1,\mathrm{B}} + \Delta v_1, \rho_{2,\mathrm{B}} + v_{2,\mathrm{B}} + \Delta v_2; \ldots\right), \\ t_{H_\mathrm{h}} &= \Delta\mathcal{L}_{H_\mathrm{h}}\left(\rho_{1,\mathrm{B}} + v_{1,\mathrm{B}} + \Delta v_1, \rho_{2,\mathrm{B}} + v_{2,\mathrm{B}} + \Delta v_2; \ldots\right). \end{aligned} \tag{4.5}$$

At tree level, the tadpole counterterms t_{H_l} and t_{H_h} vanish, such that $\Delta v_1 = \Delta v_2 = 0$. This provides the conditions (3.8) for the potential minimum at tree level, and the relations between the generic and the physical Higgs basis (3.10) for bare quantities. Thus, the bare parameters in the symmetric basis are expressed by the bare parameters in the physical basis. Linearizing eq. (4.5) by using the expansion (2.14), we can solve for $\Delta v_1^{(1)}$ and $\Delta v_2^{(1)}$. The results for $\Delta v_1^{(1)}$and $\Delta v_2^{(1)}$simplify after using the potential minimum conditions at lowest order and the relation between the parameters in the generic and physical basis.

Evaluating the linearized versions of eq. (4.5) for bare physical parameters, we obtain the one-loop expressions

$$\begin{aligned} \Delta v_1^{(1)} &= \frac{t_{H_\mathrm{l}}^{(1)} \sin\alpha}{M_{H_\mathrm{l}}^2} - \frac{t_{H_\mathrm{h}}^{(1)} \cos\alpha}{M_{H_\mathrm{h}}^2}, \\ \Delta v_2^{(1)} &= -\frac{t_{H_\mathrm{l}}^{(1)} \cos\alpha}{M_{H_\mathrm{l}}^2} - \frac{t_{H_\mathrm{h}}^{(1)} \sin\alpha}{M_{H_\mathrm{h}}^2}. \end{aligned} \tag{4.6}$$

Just as in the SM, tadpole counterterms arise from all terms in the Lagrangian that depend on the vevs. This results in tadpole counterterms to two- and three-point functions involving scalars and vector bosons as well as to fermionic two-point functions.

In the following, we assume that the tadpole counterterms are fixed according to eq. (2.13). Explicit results for the tadpoles T_{H_l} and T_{H_h} in the 2HDM in the R_ξ-gauge are listed in appendix A.

4.2 Renormalized two-point functions

Using eq. (2.9) and the condition $\hat{T}_i = 0$, the renormalized self-energies $\hat{\Sigma}(q^2)$ for vector bosons are given by

$$\hat{\Sigma}^\mathrm{T}_{VV}(q^2) = \Sigma^{\mathrm{1PI,T}}_{VV}(q^2) + (q^2 - M_V^2)\delta Z_{VV} - \delta M_V^2 - t_{VV} \quad \text{with} \quad t^{\mu\nu}_{VV} =: g^{\mu\nu} t_{VV}, \tag{4.7}$$

for $V = \{W, Z, A\}$, with the 1PI contributions $\Sigma^{\mathrm{1PI,T}}_{VV}$, and

$$\hat{\Sigma}^\mathrm{T}_{AZ}(q^2) = \Sigma^{\mathrm{1PI,T}}_{AZ}(q^2) + \frac{1}{2}(q^2 - M_Z^2)\delta Z_{ZA} + \frac{1}{2} q^2 \delta Z_{AZ} \tag{4.8}$$

for the mixing of photons and Z bosons. The scalar sector works similarly, with

$$\hat{\Sigma}_{SS}(q^2) = \Sigma^{\mathrm{1PI}}_{SS}(q^2) + (q^2 - M_S^2)\delta Z_{SS} - \delta M_S^2 + t_{SS} \tag{4.9}$$

JHEP09(2016)115

for $S = \{G_0, G^\pm, H_a, H^\pm, H_l, H_h\}$ and

$$\hat{\Sigma}_{SS'}(q^2) = \Sigma^{\text{1PI}}_{SS'}(q^2) + \frac{1}{2}(q^2 - M_S^2)\delta Z_{SS'} + \frac{1}{2}(q^2 - M_{S'}^2)\delta Z_{S'S} + t_{SS'} \tag{4.10}$$

for the mixing of the scalar fields, where $SS' = \{G_0 H_\text{a}, G^\pm H^\pm, H_\text{h} H_\text{l}\}$. The renormalized scalar-vector-boson mixing energy reads

$$\hat{\Sigma}^\mu_{VS}(q) = t^\mu_{VS} + \Sigma^{\text{1PI},\mu}_{VS}(q), \tag{4.11}$$

where $VS = \{W^\pm G^\mp, W^\pm H^\mp, Z G_0, Z H_\text{a}\}$. Defining the helicity projectors

$$P_\text{L} = \frac{1-\gamma_5}{2}, \qquad P_\text{R} = \frac{1+\gamma_5}{2}, \tag{4.12}$$

the renormalized fermionic self-energies can be decomposed into covariants

$$\hat{\Sigma}_{ff}(q) = \not{q} P_\text{L} \hat{\Sigma}^\text{L}_{ff}(q^2) + \not{q} P_\text{R} \hat{\Sigma}^\text{R}_{ff}(q^2) + \hat{\Sigma}^\text{S}_{ff}(q^2), \tag{4.13}$$

which are given by

$$\begin{aligned}
\hat{\Sigma}^\text{L}_{ff}(q^2) &= \Sigma^{\text{1PI,L}}_{ff}(q^2) + \delta Z_{f,\text{L}}, \\
\hat{\Sigma}^\text{R}_{ff}(q^2) &= \Sigma^{\text{1PI,R}}_{ff}(q^2) + \delta Z_{f,\text{R}}, \\
\hat{\Sigma}^\text{S}_{ff}(q^2) &= \Sigma^{\text{1PI,S}}_{ff}(q^2) - \frac{1}{2} m_f (\delta Z_{f,\text{L}} + \delta Z_{f,\text{R}}) - \delta m_f + t_{ff}.
\end{aligned} \tag{4.14}$$

We omit the renormalization of Faddeev-Popov ghosts which are not needed for the discussion of the processes under consideration (see section 6) and in general not at one-loop order. As a result of using the *FJ Tadpole Scheme*, all self-energies involving massive particles receive tadpole contributions. These tadpole contributions assure the gauge independence of the on-shell self-energies. Results for the tadpole contributions entering the renormalized self-energies in terms of the tadpole counterterms t_{H_l} and t_{H_h} are provided in the 't Hooft-Feynman gauge in appendix B.

4.3 Mass and field renormalization conditions

In the complex-mass scheme[6] [24–26], the scalar and vector-boson mass and field renormalization constants are derived from the conditions

$$\begin{aligned}
\hat{\Sigma}^\text{T}_{VV}(M_V^2) = 0, \qquad & \left.\frac{\partial \hat{\Sigma}^\text{T}_{VV}(q^2)}{\partial q^2}\right|_{q^2=M_V^2} = 0, \\
\hat{\Sigma}_{SS}(M_S^2) = 0, \qquad & \left.\frac{\partial \hat{\Sigma}_{SS}(q^2)}{\partial q^2}\right|_{q^2=M_S^2} = 0.
\end{aligned} \tag{4.15}$$

[6] In the usual on-shell scheme, the real part should be taken in all renormalization conditions (4.15), (4.16), (4.17), and (4.20).

JHEP09(2016)115

The off-diagonal elements of the field renormalization matrices of scalars and vector bosons are obtained from requiring

$$\begin{aligned} \hat{\Sigma}^{\mathrm{T}}_{AZ}(0) &= 0, \qquad & \hat{\Sigma}^{\mathrm{T}}_{AZ}(M_Z^2) &= 0, \\ \hat{\Sigma}_{SS'}(M_S^2) &= 0, \qquad & \hat{\Sigma}_{SS'}(M_{S'}^2) &= 0. \end{aligned} \tag{4.16}$$

For fermions, the renormalization conditions are given by

$$\begin{aligned} & m_f \hat{\Sigma}^{\mathrm{L}}_{ff}(m_f^2) + \hat{\Sigma}^{\mathrm{S}}_{ff}(m_f^2) = 0, \\ & m_f \hat{\Sigma}^{\mathrm{R}}_{ff}(m_f^2) + \hat{\Sigma}^{\mathrm{S}}_{ff}(m_f^2) = 0, \\ & \hat{\Sigma}^{\mathrm{R}}_{ff}(m_f^2) + \hat{\Sigma}^{\mathrm{L}}_{ff}(m_f^2) \\ & + 2\frac{\partial}{\partial q^2}\left[m_f^2 \left(\hat{\Sigma}^{\mathrm{R}}_{ff}(q^2) + \hat{\Sigma}^{\mathrm{L}}_{ff}(q^2) \right) + 2 m_f \hat{\Sigma}^{\mathrm{S}}_{ff}(q^2) \right] \Bigg|_{q^2 = m_f^2} = 0. \end{aligned} \tag{4.17}$$

Inserting the expressions (4.7)–(4.14) into the renormalization conditions (4.15)–(4.17), we obtain the mass and field renormalization constants in terms of the 1PI self-energy and tadpole contributions.

4.4 Renormalization of the electroweak coupling

The electromagnetic coupling e as well as the weak coupling g can be related to the fine-structure constant α (not to be confused with the mixing angle of the neutral, scalar Higgs bosons)

$$e = g s_{\mathrm{w}} = \sqrt{4\pi\alpha}, \tag{4.18}$$

where we define the weak mixing angle in the on-shell scheme as

$$c_{\mathrm{w}} = \cos\theta_{\mathrm{w}} = \frac{M_{\mathrm{W}}}{M_{\mathrm{Z}}}, \qquad s_{\mathrm{w}} = \sqrt{1 - c_{\mathrm{w}}^2}. \tag{4.19}$$

Renormalizing the electromagnetic coupling in the Thomson limit and using a Ward identity leads to [22, 27]

$$\frac{\delta e}{e} = \frac{1}{2} \frac{\partial \Sigma^{\mathrm{1PI,T}}_{AA}(q^2)}{\partial q^2}\bigg|_{q^2=0} - \frac{s_{\mathrm{w}}}{c_{\mathrm{w}}} \frac{\Sigma^{\mathrm{1PI,T}}_{AZ}(0)}{M_{\mathrm{Z}}^2}. \tag{4.20}$$

Since the counterterm δe does not receive any tadpole contributions, the 1PI self-energies can be replaced by the full self-energies in eq. (4.20).

In the G_{F} scheme, the fine-structure constant is expressed by the Fermi coupling constant G_{F}, using the well-known relation

$$M_{\mathrm{W}}^2 \left(1 - \frac{M_{\mathrm{W}}^2}{M_{\mathrm{Z}}^2} \right) = \frac{\pi\alpha}{\sqrt{2} G_{\mathrm{F}}} \left(1 + \Delta r \right), \tag{4.21}$$

where Δr contains the EW corrections to muon decay. The correction term Δr depends on the on-shell photon self-energy $\Sigma^{\mathrm{1PI,T}}_{AA}(0)$, the on-shell Z-boson self-energy $\Sigma^{\mathrm{1PI,T}}_{ZZ}(M_{\mathrm{Z}}^2)$, the W-boson self-energy $\Sigma^{\mathrm{1PI,T}}_{WW}$ at $q^2 = 0$ and $q^2 = M_{\mathrm{W}}^2$, the photon-Z-boson mixing energy

JHEP09(2016)115

$\Sigma^{1PI,T}_{AZ}(0)$, and explicit vertex and box contributions to the muon decay [28–30]. Since the tadpole terms cancel within Δr, this quantity takes the same form in terms of the full self-energies or their 1PI parts. Under the assumption that the couplings of the Higgs bosons to electrons and muons are negligible, only the self-energies are modified in the 2HDM, while the vertex and box contributions to the muon decay remain the same as in the SM.

In the G_F scheme, the renormalization constant for the electromagnetic coupling reads

$$\frac{\delta e}{e} = \frac{1}{2}\frac{\partial \Sigma^{1PI,T}_{AA}(q^2)}{\partial q^2}\bigg|_{q^2=0} - \frac{s_w}{c_w}\frac{\Sigma^{1PI,T}_{AZ}(0)}{M_Z^2} - \frac{1}{2}\Delta r, \tag{4.22}$$

using the conventions of ref. [22].

4.5 Renormalization of the parameters α, β, and M_{sb}

4.5.1 Mixing angle β

The angle β is renormalized using $\overline{\text{MS}}$ subtraction for the process $H_a \to \tau^-\tau^+$,

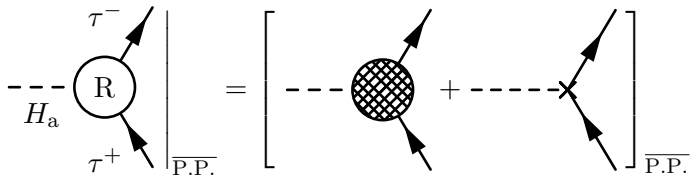

$$\overset{!}{=} 0, \tag{4.23}$$

where $\overline{\text{P.P.}}$ denotes the projection onto the pole part including the generic finite parts that are subtracted within the $\overline{\text{MS}}$ scheme, i.e. the terms proportional to

$$\frac{2}{4-D} - \gamma_E + \log(4\pi) \tag{4.24}$$

with the space-time dimension D. The corresponding counterterm explicitly reads

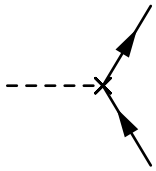

$$= \frac{e m_\tau t_\beta}{2 M_W s_w}\left[\frac{\delta m_\tau}{m_\tau} + \frac{\delta e}{e} + \frac{c_w^2 - s_w^2}{2 s_w^2}\frac{\delta M_W^2}{M_W^2} - \frac{c_w^2}{2 s_w^2}\frac{\delta M_Z^2}{M_Z^2} + \frac{1+t_\beta^2}{t_\beta}\delta\beta - \frac{1}{t_\beta}\frac{\delta Z_{G_0 H_a}}{2}\right]. \tag{4.25}$$

Since there are no explicit tadpoles for this vertex, it follows that there are no tadpole counterterms in the *FJ Tadpole Scheme*. The renormalization condition (4.23) determines $\delta\beta^{\overline{\text{MS}}}$.

It has been remarked before (e.g. refs. [11, 13]) that the relation

$$\delta\beta^{\overline{\text{MS}}} = \frac{\delta Z^{\overline{\text{MS}}}_{G_0 H_a} - \delta Z^{\overline{\text{MS}}}_{H_a G_0}}{4}, \tag{4.26}$$

holds at one-loop order, and we have explicitly verified this in the general R_ξ-gauge. This relation has also been used as a renormalization condition [11, 13]. It is particularly useful because it is valid in any of the schemes which we consider in section 5. We verified by explicit calculation in the R_ξ-gauge that $\delta\beta^{\overline{\text{MS}}}$ is gauge independent in the *FJ Tadpole Scheme*. The gauge dependence of $\delta\beta^{\overline{\text{MS}}}$ in Schemes 1 and 2 is discussed in appendix D.

JHEP09(2016)115

4.5.2 Mixing angle α

The angle α is renormalized using $\overline{\text{MS}}$ subtraction in the process $H_\text{l} \to \tau^-\tau^+$,

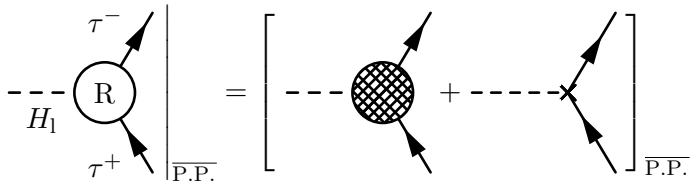

$$\overset{!}{=} 0. \tag{4.27}$$

The corresponding counterterm is given by

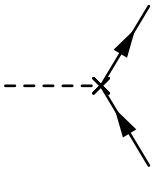

$$= \frac{\mathrm{i}e m_\tau}{2M_\text{W} s_\text{w}} \Bigg[(s_{\alpha\beta} + c_{\alpha\beta} t_\beta) \left(\frac{\delta m_\tau}{m_\tau} + \frac{\delta e}{e} + \frac{c_\text{w}^2 - s_\text{w}^2}{2 s_\text{w}^2} \frac{\delta M_\text{W}^2}{M_\text{W}^2} - \frac{c_\text{w}^2}{2 s_\text{w}^2} \frac{\delta M_\text{Z}^2}{M_\text{Z}^2} + t_\beta \delta\beta \right)$$

$$+ (c_{\alpha\beta} - s_{\alpha\beta} t_\beta) \left(\delta\alpha - \frac{\delta Z_{H_\text{h} H_\text{l}}}{2} \right) \Bigg]. \tag{4.28}$$

Again, there is no tadpole dependence, and the renormalization condition (4.27) determines $\delta\alpha^{\overline{\text{MS}}}$. Similarly to eq. (4.26) the relation

$$\delta\alpha^{\overline{\text{MS}}} = \frac{\delta Z_{H_\text{h} H_\text{l}}^{\overline{\text{MS}}} - \delta Z_{H_\text{l} H_\text{h}}^{\overline{\text{MS}}}}{4}, \tag{4.29}$$

is valid at one-loop order, which we have explicitly verified in the R_ξ-gauge. Moreover, we have checked by explicit calculation in the R_ξ-gauge that $\delta\alpha^{\overline{\text{MS}}}$ is gauge independent in the *FJ Tadpole Scheme* but gauge dependent in Schemes 1 and 2. In addition, we have verified that the renormalized vertex $H_\text{l}\tau^-\tau^+$ is gauge independent in the *FJ Tadpole Scheme*, while it is gauge dependent in Schemes 1 and 2.

4.5.3 Soft-breaking scale M_sb

The parameter M_sb is renormalized using the $\overline{\text{MS}}$ subtraction of the process $H_\text{h} \to H_\text{l} H_\text{l}$,

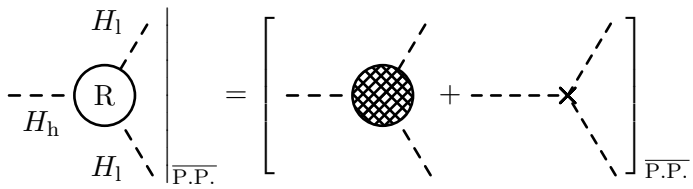

$$\overset{!}{=} 0. \tag{4.30}$$

The dependence of this vertex on δM_sb and the tadpole counterterm $t_{H_\text{h} H_\text{l} H_\text{l}}$ reads

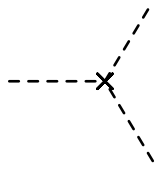

$$= \frac{e}{M_\text{W} s_\text{w}} \left[(\ldots) + \left(-2c_{\alpha\beta} + 3c_{\alpha\beta}^3 + \frac{3}{2} s_{\alpha\beta} c_{\alpha\beta}^2 \left(\frac{1}{t_\beta} - t_\beta \right) \right) \delta M_\text{sb}^2 \right] + t_{H_\text{h} H_\text{l} H_\text{l}},$$

where $(\ldots)$ stands for other counterterms.

JHEP09(2016)115

5 Discussion of gauge dependence

In this section, we discuss the gauge dependence of S-matrix elements assuming that the renormalization conditions listed in section 4 are employed. We show that tadpole renormalization schemes that are commonly used in literature in combination with $\overline{\text{MS}}$ renormalization lead to gauge-dependent predictions, while the use of the *FJ Tadpole Scheme* ensures gauge independence.

5.1 Gauge-fixing Lagrangian

To verify gauge independence of S-matrix elements and counterterms of physical parameters in the *FJ Tadpole Scheme*, we use a general R_ξ-gauge. The corresponding gauge-fixing Lagrangian is given by

$$\mathcal{L}_{\text{GF}} = -\frac{1}{\xi_W} C^+ C^- - \frac{1}{2\xi_Z}(C^Z)^2 - \frac{1}{2\xi_A}(C^A)^2 \tag{5.1}$$

with

$$C^A = \partial^\mu A_\mu, \qquad C^Z = \partial^\mu Z_\mu - \xi_Z M_{\text{Z}} G_0, \qquad C^+ = \partial^\mu W_\mu^\pm \mp \text{i}\xi_W M_{\text{W}} G^\pm. \tag{5.2}$$

We do not renormalize the gauge-fixing Lagrangian, i.e. we write it directly in terms of renormalized fields, which is sufficient to assure that all S-matrix elements are finite [31, 32]. To compensate the unphysical components in $\mathcal{L}_{\text{GF}}$, Faddeev-Popov ghosts are introduced as usual.

5.2 Characterizing different schemes

In the literature different tadpole renormalization schemes are employed. In order to efficiently generate the tadpole counterterms we follow the recipe presented at the end of section 2.3 for the SM. We start from the tree-level Lagrangian (2.2) in the symmetric basis in terms of the theory-defining parameters $m^2_{i,\text{B}}$, $i = 1, 2$, $m^2_{12,\text{B}}$, $\lambda^2_{j,\text{B}}$, $j = 1, \ldots, 5$, where the fields have been shifted by independent parameters $v_{i,\text{B}}$. Then we perform the shifts of the parameters as defined below. Thereafter, the vevs $v_{i,\text{B}}$ are determined at leading order, and the bare physical basis is introduced by using the tree-level relations (3.8)–(3.10), i.e. for $t_{H_\text{l}} = 0 = t_{H_\text{h}}$. Finally, the bare parameters are renormalized according to eq. (4.1).

The tadpole renormalization in the different schemes can be generated by shifting the corresponding bare parameters as follows:

Scheme 1.

A commonly used renormalization scheme for the SM was proposed in ref. [22]. There, the bare physical masses are defined as the coefficients of the quadratic terms in the fields, and the tadpoles are the coefficients of the terms linear in the fields. Applying this definition to the 2HDM, we can construct the corresponding Lagrangian by a

JHEP09(2016)115

shift in the bare parameters as

$$\begin{aligned}
\lambda_{1,\mathrm{B}} &\to \lambda_{1,\mathrm{B}} - \frac{1}{v_1^3}\left(t_{H_\mathrm{l}}\sin\alpha - t_{H_\mathrm{h}}\cos\alpha\right), \\
\lambda_{2,\mathrm{B}} &\to \lambda_{2,\mathrm{B}} + \frac{1}{v_2^3}\left(t_{H_\mathrm{l}}\cos\alpha + t_{H_\mathrm{h}}\sin\alpha\right), \\
\lambda_{3,\mathrm{B}} &\to \lambda_{3,\mathrm{B}} - \frac{2v_2^2}{v_1 v^4}\left(t_{H_\mathrm{l}}\sin\alpha - t_{H_\mathrm{h}}\cos\alpha\right) + \frac{2v_1^2}{v_2 v^4}\left(t_{H_\mathrm{l}}\cos\alpha + t_{H_\mathrm{h}}\sin\alpha\right), \\
\lambda_{4,\mathrm{B}} &\to \lambda_{4,\mathrm{B}} + \frac{v_2^2}{v_1 v^4}\left(t_{H_\mathrm{l}}\sin\alpha - t_{H_\mathrm{h}}\cos\alpha\right) - \frac{v_1^2}{v_2 v^4}\left(t_{H_\mathrm{l}}\cos\alpha + t_{H_\mathrm{h}}\sin\alpha\right), \\
\lambda_{5,\mathrm{B}} &\to \lambda_{5,\mathrm{B}} + \frac{v_2^2}{v_1 v^4}\left(t_{H_\mathrm{l}}\sin\alpha - t_{H_\mathrm{h}}\cos\alpha\right) - \frac{v_1^2}{v_2 v^4}\left(t_{H_\mathrm{l}}\cos\alpha + t_{H_\mathrm{h}}\sin\alpha\right), \\
m_{1,\mathrm{B}}^2 &\to m_{1,\mathrm{B}}^2 + \frac{3}{2v_1}\left(t_{H_\mathrm{l}}\sin\alpha - t_{H_\mathrm{h}}\cos\alpha\right), \\
m_{2,\mathrm{B}}^2 &\to m_{2,\mathrm{B}}^2 - \frac{3}{2v_2}\left(t_{H_\mathrm{l}}\cos\alpha + t_{H_\mathrm{h}}\sin\alpha\right).
\end{aligned} \tag{5.3}$$

One can verify that the prescription (5.3) leads to the tadpole equations (4.5) in the 2HDM. Note that in the alignment limit, the SM tadpoles (see appendix A in ref. [22]) are reproduced.

Scheme 2.

In the β_h scheme of ref. [20], the mass parameters in the Higgs potential are eliminated in favour of explicit tadpoles, while the quartic Higgs couplings λ_i are kept fixed. Thus, no tadpole counterterm contributions appear in the triple and quartic vertices between scalars, but the mass parameters of the Higgs potential and thus the two-point functions are shifted by tadpole counterterms,

$$\begin{aligned}
\lambda_{i,\mathrm{B}} &\to \lambda_{i,\mathrm{B}}, \\
m_{1,\mathrm{B}}^2 &\to m_{1,\mathrm{B}}^2 + \frac{\left(t_{H_\mathrm{l}}\sin\alpha - t_{H_\mathrm{h}}\cos\alpha\right)}{v_1}, \\
m_{2,\mathrm{B}}^2 &\to m_{2,\mathrm{B}}^2 - \frac{\left(t_{H_\mathrm{l}}\cos\alpha + t_{H_\mathrm{h}}\sin\alpha\right)}{v_2}.
\end{aligned} \tag{5.4}$$

For explicit computations, Scheme 2 is very simple because tadpole counterterms appear only in two-point functions. This scheme is widely used, e.g. in the 2HDM [8–10, 13, 33] and in the MSSM [5–7]. In contrast, in Scheme 1 two-point functions do not receive tadpole counterterms due to the definition of the bare masses in that scheme.

Scheme 3.

As described in detail in section 2.1, in the *FJ Tadpole Scheme*, the vevs are replaced by $(v_{1,\mathrm{B}} + \Delta v_1)$ and $(v_{2,\mathrm{B}} + \Delta v_2)$, which corresponds to the following shift

$$\begin{aligned}
v_{1,\mathrm{B}} &\to v_{1,\mathrm{B}} + \frac{t_{H_\mathrm{l}}\sin\alpha}{M_{H_\mathrm{l}}^2} - \frac{t_{H_\mathrm{h}}\cos\alpha}{M_{H_\mathrm{h}}^2}, \\
v_{2,\mathrm{B}} &\to v_{2,\mathrm{B}} - \frac{t_{H_\mathrm{l}}\cos\alpha}{M_{H_\mathrm{l}}^2} - \frac{t_{H_\mathrm{h}}\sin\alpha}{M_{H_\mathrm{h}}^2}.
\end{aligned} \tag{5.5}$$

JHEP09(2016)115

This prescription has to be applied to the full Lagrangian and is not restricted to the Higgs potential.

We stress again, as we have shown in section 2.2, that the bare parameters of the theory are shifted by (gauge-dependent) tadpole contributions in Schemes 1 and 2, as opposed to the prescription of the *FJ Tadpole Scheme* (5.5), where only the unphysical vevs receive a shift.

5.3 Differences of counterterms in different renormalization schemes

Employing different schemes leads to different expressions for the counterterms. Since we are mainly interested in the changes of amplitudes between different tadpole renormalization schemes, we compare counterterms in the different schemes. We name the schemes as in the previous section, i.e. Scheme 1 for the scheme employed in ref. [22] and Scheme 2 for the β_h scheme of ref. [20]. The *FJ Tadpole Scheme* is referred to as Scheme 3. We generically label the difference in the schemes for a counterterm δc_i by

$$\Delta_i \delta c = \delta c_i - \delta c_3, \quad i = 1, 2, \tag{5.6}$$

where the Δ_i describe the difference of Scheme i with respect to the Scheme 3.

In the following, we list the results for the counterterm parameters. Thereby, we make use of results for tadpoles listed in appendices A and B. As a first result, we note that the counterterms of couplings in the SM are not affected by the choice of the tadpole renormalization scheme, i.e.

$$\Delta_i \delta e = \Delta_i \delta c_{\mathrm{w}} = 0, \quad i = 1, 2. \tag{5.7}$$

However, the masses of all fermions and gauge bosons change equally for $i = 1, 2$ as

$$\begin{aligned}
\Delta_i \delta M_V^2 &= \frac{g}{M_{\mathrm{W}}} M_V^2 \left(\frac{t_{H_{\mathrm{l}}}}{M_{H_{\mathrm{l}}}^2} s_{\alpha\beta} - \frac{t_{H_{\mathrm{h}}}}{M_{H_{\mathrm{h}}}^2} c_{\alpha\beta} \right), \\
\Delta_i \delta m_f^{\mathrm{d}} &= \frac{g}{2M_{\mathrm{W}}} m_f^{\mathrm{d}} \left(\frac{t_{H_{\mathrm{l}}}}{M_{H_{\mathrm{l}}}^2} (c_{\alpha\beta} t_\beta + s_{\alpha\beta}) + \frac{t_{H_{\mathrm{h}}}}{M_{H_{\mathrm{h}}}^2} (s_{\alpha\beta} t_\beta - c_{\alpha\beta}) \right), \\
\Delta_i \delta m_f^{\mathrm{u}} &= \frac{g}{2M_{\mathrm{W}} t_\beta} m_f^{\mathrm{u}} \left(\frac{t_{H_{\mathrm{l}}}}{M_{H_{\mathrm{l}}}^2} (s_{\alpha\beta} t_\beta - c_{\alpha\beta}) - \frac{t_{H_{\mathrm{h}}}}{M_{H_{\mathrm{h}}}^2} (c_{\alpha\beta} t_\beta + s_{\alpha\beta}) \right), \\
\Delta_i \delta m_f^{\mathrm{l}} &= \frac{g}{2M_{\mathrm{W}}} m_f^{\mathrm{l}} \left(\frac{t_{H_{\mathrm{l}}}}{M_{H_{\mathrm{l}}}^2} (c_{\alpha\beta} t_\beta + s_{\alpha\beta}) + \frac{t_{H_{\mathrm{h}}}}{M_{H_{\mathrm{h}}}^2} (s_{\alpha\beta} t_\beta - c_{\alpha\beta}) \right),
\end{aligned} \tag{5.8}$$

which is easily derived because neither in Scheme 1 nor in Scheme 2 there are tadpole contributions to two-point functions of fermions and gauge bosons. Therefore, the difference is the full tadpole dependence of these two-point functions in the *FJ Tadpole Scheme* obtained from eq. (5.5). The results for the scalar fields are more complicated but not needed in the following. For Scheme 1, the difference is again given by the full tadpole dependence in the *FJ Tadpole Scheme*, which can be found in appendix A.

In the *FJ Tadpole Scheme*, the mass counterterms are gauge independent by definition, which we have verified in a general R_ξ-gauge. Consequently, the mass counterterms in

JHEP09(2016)115

Schemes 1 and 2 are gauge dependent, and their gauge dependence is given by the gauge dependence of the corresponding tadpole counterterms.

Next, we give the results for the new parameters in the 2HDM. Since those parameters are renormalized in the $\overline{\text{MS}}$ scheme, we only need to study the UV-divergent parts of vertex functions and can use the eqs. (4.26) and (4.29), which hold in any of the presented schemes. For β, we obtain

$$\Delta_i \delta\beta^{\overline{\text{MS}}} = \Delta_i \frac{\delta Z^{\overline{\text{MS}}}_{G_0 H_\text{a}} - \delta Z^{\overline{\text{MS}}}_{H_\text{a} G_0}}{4} = -\frac{\Delta_i t^{\overline{\text{MS}}}_{G_0 H_\text{a}}}{M^2_{H_\text{a}}}, \quad i = 1, 2, \tag{5.9}$$

where "$\overline{\text{MS}}$" denotes the UV-divergent part of the corresponding expression together with the finite terms in the $\overline{\text{MS}}$-scheme according to (4.24). In the first step, we use eq. (4.26). The second step can be derived by solving the renormalization conditions for the relevant mixing energies

$$\left(p^2 - M^2_{H_\text{a}}\right) \frac{\delta Z_{H_\text{a} G_0}}{2} + p^2 \frac{\delta Z_{G_0 H_\text{a}}}{2} + t_{G_0 H_\text{a}} + \text{self-energy diagrams} \stackrel{!}{=} \text{finite}, \tag{5.10}$$

where we omitted any explicit tadpoles because of $\hat{T}_i = 0$. Since the self-energy diagrams do not depend on the scheme, the scheme-dependent divergence of the tadpole counterterms has to cancel against the scheme-dependent divergence of the non-diagonal field renormalization constants, and for $i = 1, 2$ we obtain

$$\Delta_i \left(\left(p^2 - M^2_{H_\text{a}}\right) \delta Z^{\overline{\text{MS}}}_{H_\text{a} G_0} + p^2 \delta Z^{\overline{\text{MS}}}_{G_0 H_\text{a}} + 2 t^{\overline{\text{MS}}}_{G_0 H_\text{a}} \right) \stackrel{!}{=} 0, \tag{5.11}$$

which implies

$$\Delta_i \delta Z^{\overline{\text{MS}}}_{H_\text{a} G_0} = 2 \frac{\Delta_i t^{\overline{\text{MS}}}_{G_0 H_\text{a}}}{M^2_{H_\text{a}}}, \qquad \Delta_i \delta Z^{\overline{\text{MS}}}_{G_0 H_\text{a}} = -2 \frac{\Delta_i t^{\overline{\text{MS}}}_{G_0 H_\text{a}}}{M^2_{H_\text{a}}}. \tag{5.12}$$

Therefore, the scheme dependence of $\delta\beta^{\overline{\text{MS}}}$ is given by the one of the tadpole contribution $t_{G_0 H_\text{a}}$ of eq. (5.9). The explicit results for $t_{G_0 H_\text{a}}$ in the *FJ Tadpole Scheme* are listed in appendix B, and those for Schemes 1 and 2 are given by

$$t_{G_0 H_\text{a},1} = t_{G_0 H_\text{a},2} = \frac{g}{2 M_\text{W}} \left(t_{H_\text{l}} c_{\alpha\beta} + t_{H_\text{h}} s_{\alpha\beta} \right), \tag{5.13}$$

and hence

$$\frac{\Delta_i t_{G_0 H_\text{a}}}{M^2_{H_\text{a}}} = \frac{g}{2 M_\text{W}} \left(c_{\alpha\beta} \frac{t_{H_\text{l}}}{M^2_{H_\text{l}}} + s_{\alpha\beta} \frac{t_{H_\text{h}}}{M^2_{H_\text{h}}} \right), \quad i = 1, 2. \tag{5.14}$$

While the change in $\delta\beta^{\overline{\text{MS}}}$ at one-loop order is independent of the gauge parameters in the usual R_ξ-gauge and in their generalizations to non-linear gauges, we show in appendix A that it is nevertheless already gauge dependent at the one-loop level in the 2HDM. We expect that this applies as well to the MSSM, where it is known that $\delta\beta^{\overline{\text{MS}}}$ becomes gauge dependent at two loops [34].

For the difference in the counterterms to the mixing angle α, we obtain

$$\Delta_1 \delta\alpha^{\overline{\text{MS}}} = -\frac{\Delta_1 \delta Z^{\overline{\text{MS}}}_{H_\text{l} H_\text{h}}}{2} = \frac{\Delta_1 t^{\overline{\text{MS}}}_{H_\text{h} H_\text{l}}}{M^2_{H_\text{h}} - M^2_{H_\text{l}}} = -\frac{t^{\overline{\text{MS}}}_{H_\text{h} H_\text{l}}}{M^2_{H_\text{h}} - M^2_{H_\text{l}}} \tag{5.15}$$

JHEP09(2016)115

and

$$\Delta_2\delta\alpha^{\overline{\rm MS}} = -\frac{\Delta_2\delta Z^{\overline{\rm MS}}_{H_{\rm l}H_{\rm h}}}{2} = \frac{\Delta_2 t^{\overline{\rm MS}}_{H_{\rm h}H_{\rm l}}}{M^2_{H_{\rm h}} - M^2_{H_{\rm l}}} = -\frac{t^{\overline{\rm MS}}_{H_{\rm h}H_{\rm l}} - t^{\overline{\rm MS}}_{H_{\rm h}H_{\rm l},2}}{M^2_{H_{\rm h}} - M^2_{H_{\rm l}}}, \tag{5.16}$$

with $t_{H_{\rm h}H_{\rm l}}$ defined in appendix B and

$$t_{H_{\rm h}H_{\rm l},2} = -\frac{g}{2M_{\rm W}t_\beta}\left(t_{H_{\rm l}}c_{\alpha\beta} + t_{H_{\rm h}}s_{\alpha\beta}\right). \tag{5.17}$$

Here we used eq. (4.29) and the antisymmetry of $\Delta_1\delta Z^{\overline{\rm MS}}_{H_{\rm l}H_{\rm h}}$, which can be derived similarly as the one of $\Delta_{1,2}\delta Z^{\overline{\rm MS}}_{H_{\rm a}G_0}$ above. The result for $\Delta_1\delta\alpha^{\overline{\rm MS}}$ can be expressed by the tadpole counterterm in the *FJ Tadpole Scheme* only, because Scheme 1 [see eq. (5.3)] does not induce tadpole counterterms for two-point functions that do not involve external would-be Goldstone bosons.

The differences $\Delta_1\delta\alpha^{\overline{\rm MS}}$ and $\Delta_2\delta\alpha^{\overline{\rm MS}}$ are both gauge dependent at one-loop order, which can be seen by inserting the explicit expressions for the tadpoles from appendix A in the R_ξ-gauge. This result is used in the next section to demonstrate the gauge dependence of S-matrix elements in Schemes 1 and 2.

5.4 The $H_{\rm l}\tau^+\tau^-$ vertex

We study the renormalized $H_{\rm l}\tau^+\tau^-$ vertex for the different tadpole renormalization schemes defined above. In this section, we assume that the renormalized tadpole terms vanish, $\hat{T}^{(1)}_{H_{\rm l}} = 0$ and $\hat{T}^{(1)}_{H_{\rm h}} = 0$. Then, the shifts in the bare parameters that originate from tadpole counterterms $t^{(1)}_{H_{\rm l}}$ and $t^{(1)}_{H_{\rm h}}$ can be expressed in terms of the one-loop tadpole contributions $T^{(1)}_{H_{\rm l}}$ and $T^{(1)}_{H_{\rm h}}$.

As the tadpole renormalization schemes do not modify the bare Lagrangian, the bare loop amplitudes are not altered. However, the finite parts of the counterterms are affected, and thus receive gauge dependencies, as we demonstrate in the following. In particular, we show that the change in the renormalized vertex function is gauge dependent in the R_ξ-gauge, i.e.

$\partial_\xi\Delta_i$ 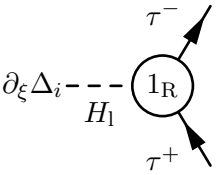

$\neq 0,$ (5.18)

which has been verified by direct computation.

The relevant Feynman rules read

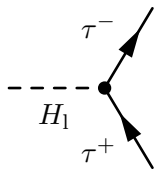

$= \dfrac{{\rm i}em_\tau}{2M_{\rm W}s_{\rm w}}\left(c_{\alpha\beta}t_\beta + s_{\alpha\beta}\right),$
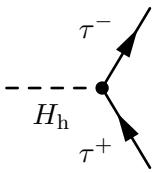

$= -\dfrac{{\rm i}em_\tau}{2M_{\rm W}s_{\rm w}}\left(c_{\alpha\beta} - s_{\alpha\beta}t_\beta\right).$ (5.19)

Computing the difference of the renormalized vertex function in different tadpole schemes yields

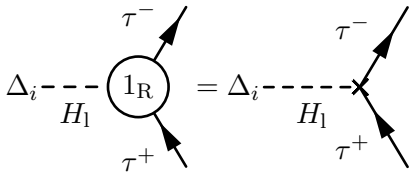

$$= \frac{\mathrm{i}em_\tau}{M_\mathrm{W} s_\mathrm{w}} \Bigg[(c_{\alpha\beta} t_\beta + s_{\alpha\beta}) \left(\Delta_i \delta\beta^{\overline{\mathrm{MS}}} + \frac{\Delta_i \delta m_\tau}{m_\tau} - \frac{\Delta_i \delta M_\mathrm{W}}{M_\mathrm{W}} \right) - (c_{\alpha\beta} - s_{\alpha\beta} t_\beta) \left(\Delta_i \frac{\delta Z_{H_\mathrm{h} H_\mathrm{l}}}{2} - \Delta_i \delta\alpha^{\overline{\mathrm{MS}}} \right) \Bigg]. \tag{5.20}$$

The terms can be split into two parts which are separately UV finite, thus allowing for a simple interpretation

$$\begin{aligned} \Delta_i \delta\beta^{\overline{\mathrm{MS}}} + \frac{\Delta_i \delta m_\tau}{m_\tau} - \frac{\Delta_i \delta M_\mathrm{W}}{M_\mathrm{W}} &= \Delta_i \frac{\delta Z^{\mathrm{fin}}_{H_\mathrm{a} G_0}}{2}, \\ \Delta_i \frac{\delta Z_{H_\mathrm{h} H_\mathrm{l}}}{2} - \Delta_i \delta\alpha^{\overline{\mathrm{MS}}} &= -\Delta_i \frac{\delta Z^{\mathrm{fin}}_{H_\mathrm{l} H_\mathrm{h}}}{2}, \end{aligned} \tag{5.21}$$

where we used eqs. (5.8), (5.9), (5.15), and (5.16) and "fin" denotes the UV-finite part, i.e. the remnant after $\overline{\mathrm{MS}}$ subtraction. The final result reads

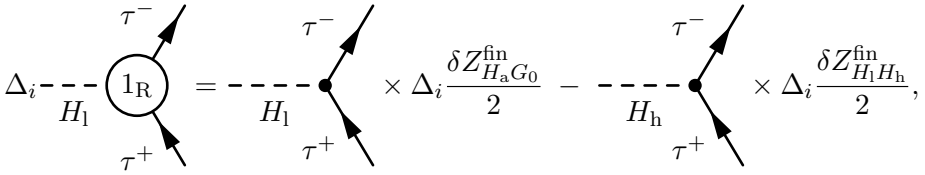

(5.22)

with

$$\begin{aligned} \Delta_{1,2} \delta Z^{\mathrm{fin}}_{H_\mathrm{a} G_0} &= -2 \frac{t^{\mathrm{fin}}_{G_0 H_\mathrm{a}}}{M^2_{H_\mathrm{a}}}, \\ \Delta_1 \delta Z^{\mathrm{fin}}_{H_\mathrm{l} H_\mathrm{h}} &= 2 \frac{t^{\mathrm{fin}}_{H_\mathrm{h} H_\mathrm{l}}}{M^2_{H_\mathrm{h}} - M^2_{H_\mathrm{l}}}, \qquad \Delta_2 \delta Z^{\mathrm{fin}}_{H_\mathrm{l} H_\mathrm{h}} = 2 \frac{t^{\mathrm{fin}}_{H_\mathrm{h} H_\mathrm{l}} - t^{\mathrm{fin}}_{H_\mathrm{h} H_\mathrm{l}, 2}}{M^2_{H_\mathrm{h}} - M^2_{H_\mathrm{l}}}, \end{aligned} \tag{5.23}$$

where $t_{G_0 H_\mathrm{a}}$ and $t_{H_\mathrm{h} H_\mathrm{l}}$ are defined in appendix B, and $t_{H_\mathrm{h} H_\mathrm{l}, 2}$ in eq. (5.17). The first contribution in eq. (5.22) appears owing to the differences in the definition of β, the second one is a consequence of the definition of α. Both are gauge dependent at one-loop order as discussed in section 5.3.

The *FJ Tadpole Scheme* yields gauge-independent predictions for the decay rate $H_\mathrm{l} \to \tau^+\tau^-$, whereas in Schemes 1 and 2 the prediction is gauge dependent. This has been confirmed via explicit calculation of the S-matrix element in the R$_\xi$-gauge.

At one-loop order, the results for the *FJ Tadpole Scheme* can be obtained from Schemes 1 and 2 via the mapping

$$\left(\delta\beta^{\overline{\mathrm{MS}}}\right)_i \to \left(\delta\beta^{\overline{\mathrm{MS}}}\right)_i - \Delta_i \frac{\delta Z^{\mathrm{fin}}_{H_\mathrm{a} G_0}}{2}, \quad \left(\delta\alpha^{\overline{\mathrm{MS}}}\right)_i \to \left(\delta\alpha^{\overline{\mathrm{MS}}}\right)_i - \Delta_i \frac{\delta Z^{\mathrm{fin}}_{H_\mathrm{l} H_\mathrm{h}}}{2}, \quad i = 1, 2. \tag{5.24}$$

JHEP09(2016)115

It is interesting to mention that the "Tadpole scheme" introduced in ref. [6] for the renormalization of t_β in the MSSM is equivalent to the *FJ Tadpole Scheme* applied to the MSSM combined with $\overline{\text{MS}}$ subtraction for t_β. Indeed for the MSSM the finite shift $\delta t_\beta^{\text{fin}}$ defined in eq. (43) of ref. [6] corresponds exactly to the shift of $\left(\delta\beta^{\overline{\text{MS}}}\right)_2$ in eq. (5.24), which translates the popular Scheme 2 to the *FJ Tadpole Scheme*. While in the *FJ Tadpole Scheme* the $\overline{\text{MS}}$ subtracted t_β is directly gauge independent, an additional finite renormalization is required in Scheme 2 to restore the gauge independence after $\overline{\text{MS}}$ subtraction.

5.5 The ZZH_h vertex

In this section, we present the finite correction of the ZZH_h vertex due to the tadpole scheme. We obtain formally analogous results as in the previous section. The following Feynman rules were used

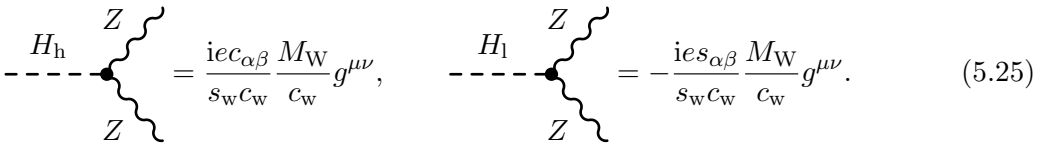

(5.25)

The calculation proceeds as in section 5.4 except that one has to take into account a tadpole contribution which is given by

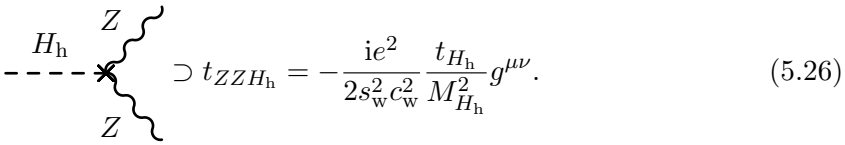

(5.26)

With the same line of arguments as in the previous section we obtain the difference of the renormalized vertex in different tadpole schemes as

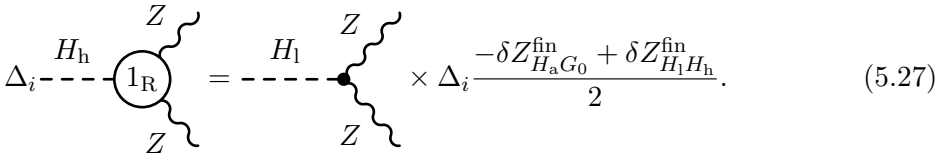

(5.27)

The gauge independence of the renormalized ZZH_h vertex has been verified in the *FJ Tadpole Scheme* by explicit computation in the R_ξ-gauge. In this way it has also been confirmed that this vertex is gauge dependent in Scheme 1. Schemes 1 and 2 can be mapped to the *FJ Tadpole Scheme* by a redefinition of α and β via eq. (5.24). It is expected that the same is true for other vertices which are sensitive to the renormalization of α, β, and SM parameters, but not to M_sb. Since the mapping (5.24) is gauge dependent, the renormalized ZZH_h vertex becomes gauge dependent in Schemes 1 and 2.

6 Electroweak NLO corrections to Higgs-boson production processes in the 2HDM

In this section, we analyze the EW NLO corrections for two Higgs-boson production channels in the 2HDM. First, in section 6.1, we discuss results for the production of a light

JHEP09(2016)115

	M_{H_h}	M_{H_a}	$M_{H^\pm}$	m_{12}	t_β	M_{sb}
BP21A	200 GeV	500 GeV	200 GeV	135 GeV	1.5	198.7 GeV
BP21B	200 GeV	500 GeV	500 GeV	135 GeV	1.5	198.7 GeV
BP21C	400 GeV	225 GeV	225 GeV	0 GeV	1.5	0 GeV
BP21D	400 GeV	100 GeV	400 GeV	0 GeV	1.5	0 GeV
BP3A1	180 GeV	420 GeV	420 GeV	70.71 GeV	3	129.1 GeV

Table 1. 2HDM benchmark points in the alignment limit, i.e. $s_{\alpha\beta} \to -1$, $c_{\alpha\beta} \to 0$, taken from ref. [35]. The parameter M_{sb} depends on the other parameters and is given for convenience.

SM-like Higgs boson produced through gluon fusion for scenarios in the alignment limit. A more detailed description of the implementation of this process and results for the production of a light or a heavy neutral Higgs boson for the case of non-alignment will be presented elsewhere. In section 6.2, we provide results for the production of a light SM-like Higgs boson in vector-boson fusion at NLO. Also here, a more detailed study including the description of the implementation of the process will be published separately.

In both processes all external particles are SM particles such that the new Higgs bosons only appear as virtual particles in the loops. In both cases, we apply the renormalization scheme defined in section 4[7] and discuss the size of the EW corrections. We study the dependence on the renormalization scale that appears owing to the $\overline{\text{MS}}$ renormalization of the mixing angles α and β and analyze the decoupling of the new (heavy) Higgs particles. Besides investigating scenarios close to the decoupling limit, we provide results for selected benchmark points from refs. [35, 36]. The benchmark points BP21A–D, BP22A, and BP43–5 were originally designed for the study of exotic Higgs-boson decays, the points BP3A1 and BP3B1–2 for a successful EW baryogenesis and the points a-1 and b-1 for Higgs-boson pair production. All benchmark points fulfil theoretical constraints from vacuum stability and perturbativity as well as experimental constraints in flavour physics, EW precision measurements, and direct searches. In table 1 we list the benchmark points in the alignment limit, which we study in gluon fusion and Higgs strahlung. In table 2 we provide benchmark scenarios that are not in the alignment limit and which we study in Higgs strahlung only.

For the numerical evaluation of the two Higgs-boson production processes we use the following values for the SM input parameters [37]:

$$\begin{aligned} G_F &= 1.16638 \cdot 10^{-5}\,\text{GeV}^{-2}, & m_t &= 173.21\,\text{GeV}, & M_h &= 125.09\,\text{GeV} = M_{H_l}, \\ M_W &= 80.385\,\text{GeV}, & \Gamma_W &= 2.0850\,\text{GeV}, & M_Z &= 91.1876\,\text{GeV}, & \Gamma_Z &= 2.4952\,\text{GeV}. \end{aligned} \quad (6.1)$$

The numerical results presented in the following have been obtained in the 't Hooft-Feynman gauge.

[7] Since both considered processes do not depend on the soft-breaking scale M_{sb} at LO, this parameter does not require renormalization.

JHEP09(2016)115

	M_{H_h}	M_{H_a}	$M_{H^\pm}$	m_{12}	t_β	$c_{\alpha\beta}$	M_{sb}
a-1	700 GeV	700 GeV	670 GeV	424.3 GeV	1.5	−0.0910	624.5 GeV
b-1	200 GeV	383 GeV	383 GeV	100 GeV	2.52	−0.0346	204.2 GeV
BP22A	500 GeV	500 GeV	500 GeV	187.08 GeV	7	0.28	500 GeV
BP3B1	200 GeV	420 GeV	420 GeV	77.78 GeV	3	0.3	142.0 GeV
BP3B2	200 GeV	420 GeV	420 GeV	77.78 GeV	3	0.5	142.0 GeV
BP43	263.7 GeV	6.3 GeV	308.3 GeV	52.32 GeV	1.9	0.14107	81.5 GeV
BP44	227.1 GeV	24.7 GeV	226.8 GeV	58.37 GeV	1.8	0.14107	89.6 GeV
BP45	210.2 GeV	63.06 GeV	333.5 GeV	69.2 GeV	2.4	0.71414	116.2 GeV

Table 2. 2HDM benchmark points outside the alignment limit taken from ref. [36] (a-1, b-1) and ref. [35]. The parameter M_{sb} depends on the other parameters and is given for convenience.

6.1 Higgs-boson production in gluon fusion

Higgs-boson production through gluon fusion is a loop-induced process, i.e. its LO contribution appears at the one-loop level. Despite its loop suppression, it is the dominant Higgs-boson production mechanism in the SM at the LHC. Since the Yukawa couplings of the Higgs boson to fermions are proportional to the fermion mass, the dominant contribution arises from top-quark loops. Treating all other fermions as massless, the LO partonic cross section $\hat{\sigma}$ for SM Higgs-boson production is generated only via a top-quark loop.

In the SM, the QCD corrections to Higgs-boson production in gluon fusion are known up to N^{3}LO and are large [38–42]. The complete NLO EW corrections have been calculated in refs. [43, 44] and are also sizable. EW radiative corrections may significantly change a process, if BSM particles propagate in the loop. In refs. [45, 46], for example, the influence of a fourth generation of heavy fermions on the EW corrections to Higgs-boson production in gluon fusion has been discussed, and the EW corrections turned out to be large. In the following, we present the behaviour of the NLO EW corrections to this Higgs-boson production channel in the alignment limit of the 2HDM of type II, where the light, neutral Higgs boson H_l becomes SM-like. All results are calculated in the *FJ Tadpole Scheme* with the renormalization conditions given in section 4 with the exception of the top-quark mass which has been renormalized in the on-shell scheme for gluon fusion.

The coupling of the light neutral Higgs boson to top quarks in the 2HDM of type II is given by the $H_l t\bar{t}$ vertex:

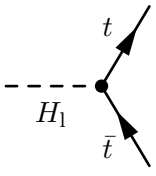

$$= -\frac{\mathrm{i}e m_t}{2 M_W s_w}\left(\frac{c_{\alpha\beta}}{t_\beta} - s_{\alpha\beta}\right). \tag{6.2}$$

In the alignment limit ($c_{\alpha\beta} = 0, s_{\alpha\beta} = -1$) the coupling of the light neutral Higgs boson to up-type fermions equals the one in the SM. Therefore, the LO production cross section

JHEP09(2016)115

of the light neutral Higgs boson through gluon fusion in the 2HDM is the same as in the SM, and the QCD corrections do not change. For small t_β the alignment limit is reached slower and one speaks of a delayed decoupling [3]. Without alignment, the LO cross section changes only by the factor $(c_{\alpha\beta}/t_\beta - s_{\alpha\beta})^2$, such that the relative QCD corrections stay the same. In the alignment limit, the t_β dependence of the process disappears at LO, but survives in the NLO EW corrections. The derivation of the counterterms for the NLO calculation requires special care. The fact that the alignment limit implies $c_{\alpha\beta} = 0$ (and consequently $s_{\alpha\beta} = -1$), but does not affect t_β, leads to an explicit dependence of the $H_1 t\bar{t}$ counterterm on t_β, $\delta\alpha$, and $\delta\beta$:

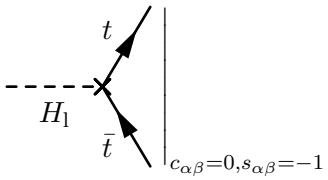

$$\supset -\frac{\mathrm{i}em_t}{2M_\mathrm{W}s_\mathrm{w}}\frac{\delta\alpha - \delta\beta}{t_\beta}. \tag{6.3}$$

As a result, the NLO corrections to this process are still scale dependent despite of the alignment limit. The scale dependence originates from the renormalization of α and β in the $\overline{\mathrm{MS}}$ scheme.

The calculation of the NLO EW corrections proceeds in several steps. First, the 2HDM Feynman rules are derived using `FeynRules` [47]. These are used in the code `QGS` in order to construct the amplitudes based on Feynman diagrams generated with `QGRAF` [48]. The program `QGS` is an extension of `GraphShot` [49], which has been used to accomplish the corresponding SM calculation and performs the algebraic manipulations of the amplitudes with `Form` [50]. The reducible scalar products are removed, the symmetries are taken into account in order to reduce the number of loop integrals, the UV renormalization as well as the cancellation of collinear logarithms is performed analytically, and finally the remaining finite integrals are mapped onto form factors. The latter are evaluated numerically with Fortran routines. In the alignment limit of the 2HDM the same types of Feynman integrals arise as in the SM calculation of refs. [43, 44] such that we can employ the same Fortran library for their numerical evaluation. For the numerical evaluation of the two-loop massive diagrams the library uses the methods of refs. [51, 52] for self-energies and of refs. [44, 53–55] for vertex functions.

The NLO EW corrections to the partonic cross section are expressed as percentage correction $\delta_\mathrm{EW}^\mathrm{NLO}$ relative to the LO result,

$$\hat{\sigma} = \hat{\sigma}^\mathrm{LO} + \hat{\sigma}^\mathrm{NLO} = \hat{\sigma}^\mathrm{LO}(1 + \delta_\mathrm{EW}^\mathrm{NLO}). \tag{6.4}$$

In order to study the scale dependence we consider the following scenario: we choose $\tan\beta = 2$ and $M^* = 700\,\mathrm{GeV}$ as a typical mass scale for the new degrees of freedom. The soft-breaking scale M_sb and the masses of all heavy Higgs bosons, except for the heavy, neutral one, are set equal to M^*. By allowing for a different mass value for the heavy, neutral Higgs boson, we find enhanced scale-dependent logarithms in the alignment limit. This can be seen from the analytical expression for the scale-dependent part of the relative

JHEP09(2016)115

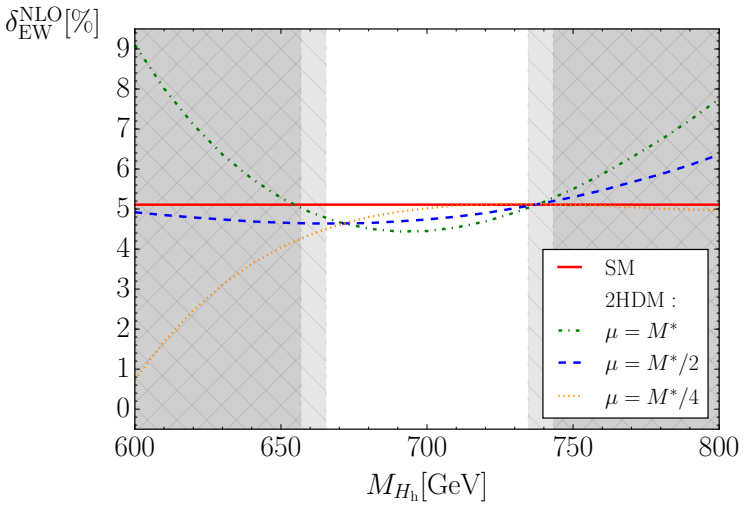

Figure 1. EW NLO corrections to Higgs-boson production in gluon fusion. The solid line indicates the SM result. The dashed-dotted, dashed and dotted lines are the percentage corrections in the 2HDM as a function of the heavy, neutral Higgs-boson mass $M_{H_{\rm h}}$ for different values of the renormalization scale $\mu = M^*, M^*/2, M^*/4$. The heavy Higgs-boson masses $M_{H_{\rm a}} = M_{H^\pm} = M_{\rm sb} = M^* = 700\,\text{GeV}$ are kept constant and $t_\beta = 2$.

correction to the LO matrix-element squared

$$\begin{aligned}\delta_{\rm EW}^{\rm NLO,\mu-dep.} = {} & \frac{G_{\rm F}\sqrt{2}}{8\pi^2 t_\beta^2 M_{H_{\rm h}}^2 (M_{H_{\rm h}}^2 - M_{H_{\rm l}}^2)} \ln\frac{\mu^2}{M_{H_{\rm l}}^2} \\ & \times \Big[(1-t_\beta^2)(M_{H_{\rm h}}^2 - M_{\rm sb}^2)\Big[3M_{H_{\rm h}}^2 M_{H_{\rm l}}^2 + M_{\rm sb}^2(M_{H_{\rm a}}^2 + 2M_{H^\pm}^2 - 3M_{H_{\rm h}}^2)\Big] \\ & + 6m_{\rm t}^2(M_{H_{\rm h}}^2 M_{H_{\rm l}}^2 - 4M_{\rm sb}^2 m_{\rm t}^2)\Big]. \end{aligned} \tag{6.5}$$

This expression is proportional to $(\delta\alpha - \delta\beta)/t_\beta$ in the $\overline{\rm MS}$ scheme as expected from eq. (6.3). If the mass of the heavy, neutral Higgs boson differs from the soft-breaking scale and the masses of the other heavy Higgs bosons, the terms in the second line dominate the scale dependence. If also the heavy, neutral Higgs-boson mass is chosen to be equal to the typical mass scale M^* only the top-mass-dependent terms in the last line contribute. In order to see the effect of the enhanced logarithms, we thus vary the mass of the heavy, neutral Higgs boson. The variation of the renormalization scale μ can be used in order to estimate the uncertainty due to unknown higher-order corrections. To this end, we evaluate the NLO corrections for different values of the renormalization scale $\mu = M^*, M^*/2, M^*/4$.

In figure 1 we show the percentage correction $\delta_{\rm EW}^{\rm NLO}$ as a function of the heavy, neutral Higgs-boson mass $M_{H_{\rm h}}$ for the three different values of the renormalization scale μ and compare the EW corrections of the 2HDM to those in the SM. For a small mass splitting, i.e. for a heavy, neutral Higgs-boson mass $M_{H_{\rm h}}$ in the vicinity of $M^* = 700\,\text{GeV}$, the size of the corrections is comparable to the one in the SM, and the scale dependence is small, i.e. perturbation theory is well-behaved and higher-order EW corrections can be expected

JHEP09(2016)115

to be small. For large mass splittings, e.g. for a heavy, neutral Higgs-boson mass M_{H_h} that deviates significantly from the mass values of the other heavy Higgs bosons and thus from $M^* = 700\,\mathrm{GeV}$, the scale dependence becomes large. This indicates large uncertainties owing to unknown higher-order corrections, which signals the breakdown of the perturbative expansion and the onset of a non-perturbative regime. This behaviour is expected, since the mass splitting of the heavy Higgs bosons is restricted by perturbativity. The parameters λ_i in eq. (3.2) have to fulfil the condition $|\lambda_i| \lesssim \mathcal{O}(1)$ in order to ensure that the Higgs-boson sector does not become strongly coupled [3]. This is important to maintain tree-level unitarity [56]. The requirement $|\lambda_i| \lesssim \mathcal{O}(1)$ leads to a bound on the mass splitting [3] of

$$|M_{H_\mathrm{h}} - M^*|, \;\; |M_{H_\mathrm{a}} - M^*|, \;\; |M_{H^\pm} - M^*| \;\; \lesssim \mathcal{O}\left(\frac{v^2}{M^*}\right), \tag{6.6}$$

where $v \approx 246\,\mathrm{GeV}$ is the SM vev. Using this information as well as the knowledge of the NLO EW corrections, we study the region of M_{H_h} in figure 1 for which perturbativity or non-perturbativity can be expected. For this purpose, we constrain the allowed region of M_{H_h} around the typical mass scale M^* via

$$M^* - f\frac{v^2}{M^*} < M_{H_\mathrm{h}} < M^* + f\frac{v^2}{M^*}. \tag{6.7}$$

Perturbativity should be realized if the parameter f is sufficiently smaller than one. In figure 1 the M_{H_h} region corresponding to $f > 0.4$ is marked in light grey, and the region $f > 0.5$ in dark grey. The scale dependence can be used to estimate uncertainties from unknown higher-order corrections and provides useful means to determine the onset of the non-perturbative regime. This is supported by figure 1, where the scale dependence becomes stronger when f becomes large. We conclude that the scale dependence introduced by the $\overline{\mathrm{MS}}$ renormalization of the mixing angles α and β is less than a percent, as long as perturbativity is not violated, i.e. $f < 0.5$. Thus, the $\overline{\mathrm{MS}}$ renormalization of α and β provides stable results for sound scenarios in the perturbative regime.

In figure 2, we analyze the decoupling of the heavy Higgs-boson sector for different values of f. We vary the mass scale M^* and choose the masses of the heavy Higgs bosons as

$$M_{H_\mathrm{h}} = M^* - f\frac{v^2}{M^*}, \qquad M_{H_\mathrm{a}} = M_{\mathrm{sb}} = M^*, \qquad M_{H^\pm} = M^* + f\frac{v^2}{M^*}. \tag{6.8}$$

For the rather large value $f = 0.4$, the NLO corrections in the 2HDM approach the SM value of 5.1% only slowly; at a typical mass scale $M^* = 1200\,\mathrm{GeV}$ the decoupling limit is almost reached. For smaller values of f decoupling is approached considerably faster. For $f = 0.1$ the decoupling of the heavy Higgs-boson sector already occurs at about 400 GeV.

Finally, in table 3 we present the relative NLO corrections for the benchmark points of table 1 which fulfil perturbativity in the sense that $|\lambda_i| < 4\pi$ [35]. For all scenarios, we observe large NLO EW corrections on top of the SM value of 5.1%. Owing to the large corrections, it should be possible to exclude these scenarios at the LHC, as soon as computations for the relevant decay channels like $H_\mathrm{l} \to \gamma\gamma$ are available at the same order in the weak coupling.

JHEP09(2016)115

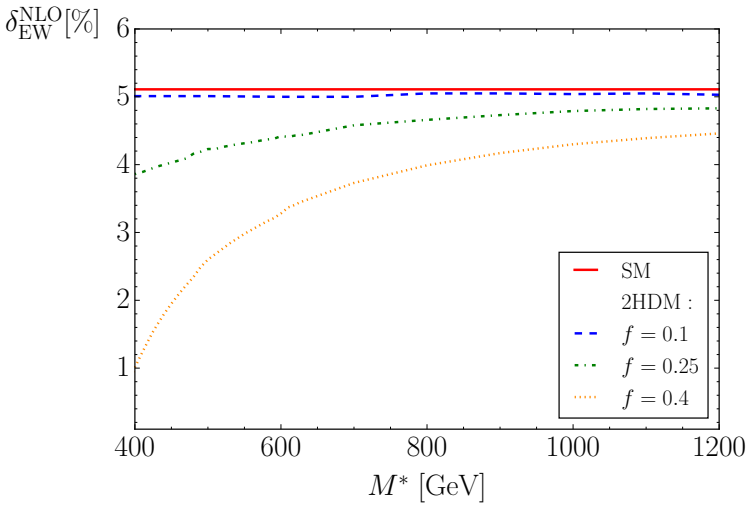

Figure 2. EW NLO corrections to Higgs-boson production in gluon fusion as a function of the scale M^*. The values of M_{H_h}, M_{H_a}, $M_{H^\pm}$ and $M_{\rm sb}$ are chosen according to eq. (6.8). The solid line represents the SM. The dashed, dashed-dotted, and dotted lines correspond to $f = 0.1$, $f = 0.25$ and $f = 0.4$.

μ	M_{H_l}	$2M_{H_l}$	$4M_{H_l}$
BP21A	8.5%	−1.3%	−11.2%
BP21B	7.3%	−2.7%	−12.7%
BP21C	13.2%	12.6%	12.0%
BP21D	15.1%	14.6%	14.0%
BP3A1	21.3%	13.2%	5.1%

Table 3. Relative NLO corrections $\delta_{\rm EW}^{\rm NLO}$ to Higgs-boson production in gluon fusion for the benchmark points of table 1. The scale μ is varied as a function of M_{H_l}.

The scale uncertainty turns out to be at the level of ±10% for the benchmark points BP21A, BP21B and BP3A1, but small for BP21C and BP21D. The large scale dependencies are due to rather large values of the λ_i in these benchmark scenarios, the largest values for $|\lambda_i|$ ranging between 3.7 and 7.7. The results from table 3 can be understood from the analytic expression for the scale dependence in eq. (6.5). For BP21A and BP21B, $M_{H_h} \approx M_{\rm sb}$ and, thus, basically only the m_t-dependent terms in the last line of eq. (6.5) contribute. The scale dependence is enhanced by the factor $(M_{H_l}^2 - 4m_t^2)/(M_{H_h}^2 - M_{H_l}^2)$. For BP21C and BP21D all terms involving $M_{\rm sb}$ vanish, and the scale dependence is suppressed by the ratio $M_{H_l}^2/M_{H_h}^2 \sim 0.1$. For BP3A1, the m_t-independent terms dominate the scale dependences, the leading term being proportional to $M_{H^\pm}^2/M_{H_h}^2 \sim 5.4$.

JHEP09(2016)115

6.2 Higgs production in association with a weak boson

Besides the gluon-fusion channel and the vector-boson fusion channel, the associated Higgs production with a vector boson, also called Higgs strahlung, is used to study the properties of the Higgs boson. In this section, we focus on this process which allows in particular to measure the decay mode $\mathrm{H} \to \mathrm{b\bar{b}}$ and to study BSM physics in the VVH vertex.

There has been enormous progress in higher-order calculations to Higgs strahlung in the SM. The QCD corrections are known up to NNLO for the inclusive cross section [57–59] as well as for differential cross sections [60, 61]. The NLO EW corrections were first computed in ref. [62] for stable vector bosons. Meanwhile public codes are available including the vector-boson decays, e.g. V2HV [63], MCFM [64], HAWK2.0 [65] and vh@nnlo [66], allowing to study any final state in this process class at NLO QCD and EW and also partially at NNLO QCD. Higgs strahlung has also been investigated in the 2HDM [67], where the ratio of inclusive WH and ZH production for light and heavy Higgs bosons has been studied and the impact of type-I and type-II Yukawa couplings to the SM Higgs production has been analyzed including all available and numerically relevant contributions.

The following analysis is restricted to the case of two charged leptons in the final state, $\mathrm{pp} \to \mathrm{H}l^+l^- + X$. For massless leptons one has to be careful with final-state collinear radiation, which requires special treatment (see e.g. ref. [68]). We do not recombine collinear photons and leptons and assume that the leptons can be perfectly isolated, which is justified for a pair of muons in the final state. We employ the cuts used in the analysis of ref. [69], i.e. we require the muons to

- have transverse momentum $p_{\mathrm{T}}^l > 20\,\mathrm{GeV}$ for $l = \mu^+, \mu^-$,
- be central with rapidity $|\eta_l| < 2.4$ for $l = \mu^+, \mu^-$,
- have a pair invariant mass m_{ll} of $75\,\mathrm{GeV} < m_{ll} < 105\,\mathrm{GeV}$.

In addition, we demand a boosted Z boson with

- transverse momentum $p_{\mathrm{T}}^{\mathrm{Z}} > 160\,\mathrm{GeV}$.

All predictions are for the hadronic cross section at the center-of-mass energy of 13 TeV using the NLO PDF set NNPDF2.3 with QED corrections [70].

The numerical results were produced using an extended version of RECOLA [71] and HAWK 2.0 [65]. RECOLA has been used to calculate all needed one-loop S-matrix elements in the 2HDM, and HAWK 2.0 served as integrator for Higgs strahlung.

As in the case of gluon fusion, we discuss the scale dependence in the decoupling limit. In the alignment limit the 2HDM leaves its marks in Higgs strahlung only at NLO, but, in contrast to gluon fusion, Higgs strahlung is scale independent in the alignment limit because the tree-level vertices VVH do not depend on t_β but only on $c_{\alpha\beta}$ and $s_{\alpha\beta}$ (see discussion in section 6.1). For this reason the analysis has been extended to the decoupling limit with only approximate alignment compatible with perturbative unitarity, i.e. the requirement $|\lambda_i| \lesssim \mathcal{O}(1)$ is extended [3] by

$$|c_{\alpha\beta}| \lesssim \mathcal{O}\left(\frac{v^2}{M^{*2}}\right). \tag{6.9}$$

JHEP09(2016)115

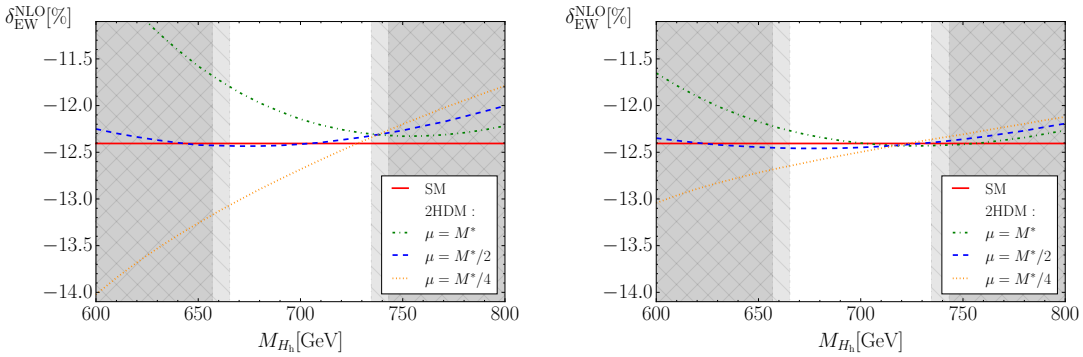

(a) $k = 0.4$. **(b)** $k = 0.25$.

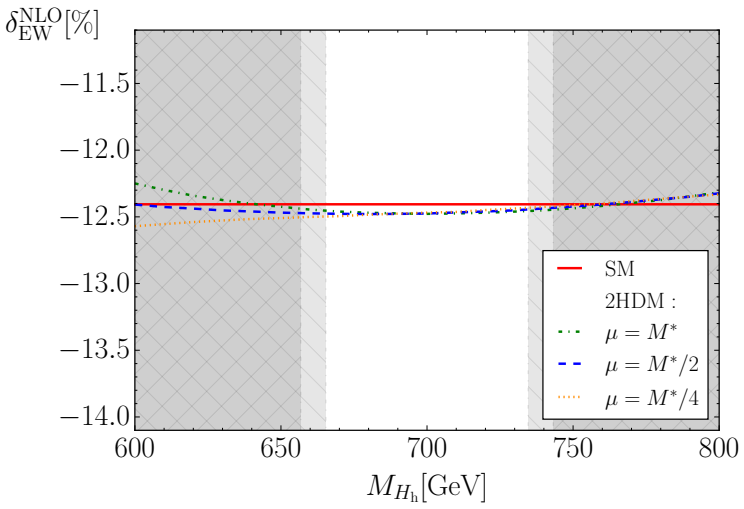

(c) $k = 0.1$.

Figure 3. NLO percentage EW corrections to the integrated cross section of $pp \to Hl^+l^- + X$ as a function of the heavy Higgs-boson mass $M_{H_{\rm h}}$ for three different scenarios, which differ by the value of $c_{\alpha\beta}$ parametrized according to eq. (6.10). The solid line indicates the SM result. The dashed-dotted, dashed, and dotted lines show the percentage correction in the 2HDM (normalized to the 2HDM Born) for different values of the renormalization scale $\mu = M^*, M^*/2, M^*/4$. The heavy masses $M_{H_{\rm a}} = M_{H^\pm} = M_{\rm sb} = M^* = 700\,\text{GeV}$ and $t_\beta = 2$ are kept constant. The bright grey band represents the region $0.4 \leq f \leq 0.5$ [see eq. (6.7)] and the dark grey band the region $f > 0.5$.

We perform an analysis for Higgs strahlung similar to the one for gluon fusion in figure 1. In figure 3 we present the percentage EW correction $\delta_{\rm EW}^{\rm NLO}$ as a function of the heavy, neutral Higgs-boson mass $M_{H_{\rm h}}$ for three different scales μ centered around $M^*/2$. All other parameters are kept fixed, the masses are set to the decoupling scale $M^* = 700\,\text{GeV}$, and we choose $t_\beta = 2$. The results are presented for three different scenarios where we investigate the decoupling in terms of $c_{\alpha\beta}$, parametrizing

$$c_{\alpha\beta} = k\frac{v^2}{M^{*2}} \tag{6.10}$$

JHEP09(2016)115

μ	M_{H_h}	$2M_{H_h}$	$4M_{H_h}$
BP21A	-11.8 %	-11.8 %	-11.8 %
BP21B	-13.1 %	-13.1 %	-13.1 %
BP21C	-13.2 %	-13.2 %	-13.2 %
BP21D	-13.6 %	-13.6 %	-13.6 %
BP3A1	-13.3 %	-13.3 %	-13.3 %

Table 4. Relative NLO correction $\delta_{\rm EW}^{\rm NLO}$ to the integrated cross section of $pp \to Hl^+l^- + X$ for the benchmark points in the alignment limit of table 1. The SM correction is -12.4%.

a-1	-7.6 %	-10.5 %	-13.3 %
b-1	-12.5 %	-12.5 %	-12.4 %
BP22A	-239 %	-54.8 %	130 %
BP3B1	-23.2 %	-20.0 %	-16.9 %
BP3B2	-56.0 %	-39.5 %	-23.0 %
BP43	-11.9 %	-10.6 %	-9.3%
BP44	-11.1 %	-11.2 %	-11.3 %
BP45	-50.6 %	-14.3 %	21.9%

Table 5. Relative NLO correction $\delta_{\rm EW}^{\rm NLO}$ to the integrated cross section of $pp \to Hl^+l^- + X$ for the benchmark points outside the alignment limit of table 2. The SM correction is -12.4%

with $k = 0.1, 0.25, 0.4$. The expected non-perturbative region is shown in dark grey for $f > 0.5$ and the transition region in bright grey defined by $0.4 \leq f \leq 0.5$. The first plot in figure 3 shows the case $k = 0.4$, which is at the border of perturbative unitarity independently of f because $c_{\alpha\beta}$ is close to its upper limit [see eq. (6.9)]. This scenario exhibits moderate scale uncertainties of the order of one percent in the perturbative regime. Decreasing k to 0.25 reduces the scale dependence to below one percent in the perturbative region $f \leq 0.4$, and for $k = 0.1$ almost no scale dependence is left. While the considered scenario is not in the decoupling limit, the resulting corrections are nevertheless comparable to those in the SM. The decoupling limit is reached by setting $c_{\alpha\beta} = 0$, where the corrections coincide with those in the SM.

In tables 4 and 5 we present the results for the benchmark points of tables 1 and 2. For scenarios in the alignment limit compiled in table 4 there is no scale dependence, and the differences between EW corrections in the 2HDM and in the SM, where they amount to -12.4%, are typically at the level of one percent.

The scenarios outside the alignment limit shown in table 5 are more interesting. In the scenarios a-1, b-1, BP43, and BP44, which are close to the alignment limit, the scale variations are small of the order of 0.5%. The corrections are comparable to those in the SM, differing typically at the level of one percent. The scenarios BP3B1, BP3B2, BP45

JHEP09(2016)115

significantly deviate from the alignment limit with a mass splitting of more than 200 GeV and exhibit scale uncertainties up to 35%. For all these scenarios we find absolute values of λ of the order of $|\lambda_i|/(4\pi) \approx 0.3$. The scenario BP22A is in the decoupling limit, but does not fulfil condition (6.9). We observe large scale uncertainties of the order of 180% which raises the question of perturbativity of this scenario. In fact, we find $\lambda_2/(4\pi) \approx 1.1$ and $\lambda_3/(4\pi) \approx 0.7$ for BP22A. Thus, large scale uncertainties signal a breakdown of the perturbative expansion.

In conclusion, as in gluon fusion, violation of perturbative unitarity and large scale dependence are connected. We observe small scale uncertainties of the EW corrections in the 2HDM both in the decoupling limit and for benchmark points that are close to the alignment limit or involve small mass splittings, while respecting perturbative unitarity.

7 Conclusion

The precise study of theories with extended Higgs sectors is of utmost importance for the investigation of the Higgs sector at the LHC. To this end, NLO corrections of QCD and electroweak origin have to be calculated.

We have proposed a consistent gauge-independent renormalization scheme for the CP-conserving 2HDM of type II. While masses are renormalized in the on-shell scheme, the mixing angles of the Higgs sector and the soft-Z_2-symmetry-breaking scale are renormalized in the $\overline{\text{MS}}$ scheme. To render this approach gauge independent, a consistent treatment of tadpoles is crucial. This is provided by the method proposed by Fleischer and Jegerlehner many years ago for the Standard Model.

We have generalized this method specifically to the 2-Higgs-Doublet Model of type II. We have investigated the difference to popular renormalization schemes used in the literature and clarified their range of applicability. We showed in particular that an $\overline{\text{MS}}$ renormalization of the mixing angles in the extended Higgs sector within popular schemes leads to gauge-dependent predictions in the 2-Higgs-Doublet Model of type II. We expect that this is also the case in the Minimal Supersymmetric Standard Model.

The proposed extension of the Fleischer-Jegerlehner tadpole scheme can be straightforwardly applied to more general theories. This opens the way for consistent renormalization prescriptions of theories with more complicated extended Higgs sectors.

We have applied the renormalization scheme to the calculation of NLO EW corrections for Higgs production in gluon fusion and Higgs strahlung and have, in particular, investigated the scale dependence of the corrections and the decoupling of the heavy Higgs bosons within this scheme.

Acknowledgments

We thank S. Uccirati for valuable discussions and providing an early version of the code QGS. A.D. and J.-N.L. acknowledge support from the German Research Foundation (DFG) via grants DE 623/2-1 and DE 623/4-1. The work of L.J. and C.S. was supported by the

JHEP09(2016)115

DFG under contract STU 615/1-1 and the work of J.-N.L. by the Studienstiftung des Deutschen Volkes.

A Results for tadpoles in the 2HDM

We give the results for the tadpoles t_{H_l} and t_{H_h} corresponding to the Higgs bosons H_l and H_h in the 2HDM in the R$_\xi$-gauge defined in section 5.1,

$$
\begin{aligned}
t_{H_\mathrm{l}} = -T_{H_\mathrm{l}} = \; & \frac{s_{\alpha\beta}\, g}{8\pi^2 M_\mathrm{W}} \Bigg\{ - 3m_\mathrm{t}^2 A_0\left(m_\mathrm{t}\right) \\
& + \frac{M_{H_\mathrm{l}}^2}{8}\left(A_0\left(\sqrt{\xi_Z} M_\mathrm{Z}\right) + 2A_0\left(\sqrt{\xi_W} M_\mathrm{W}\right)\right) + \frac{(D-1)}{4}\left(M_\mathrm{Z}^2 A_0\left(M_\mathrm{Z}\right) + 2M_\mathrm{W}^2 A_0\left(M_\mathrm{W}\right)\right) \\
& + \frac{3}{8}\left(M_{H_\mathrm{l}}^2\left(1+2c_{\alpha\beta}^2\right) - 2c_{\alpha\beta}^2 M_\mathrm{sb}^2\right) A_0\left(M_{H_\mathrm{l}}\right) \\
& + \frac{1}{8}\Bigg(\left(1-2c_{\alpha\beta}^2\right)\left(M_{H_\mathrm{l}}^2 + 2M_{H_\mathrm{h}}^2\right) - 2M_\mathrm{sb}^2\left(1-3c_{\alpha\beta}^2\right)\Bigg) A_0\left(M_{H_\mathrm{h}}\right) \\
& + \frac{1}{8}\left(2M_{H_\mathrm{a}}^2 + M_{H_\mathrm{l}}^2 - 2M_\mathrm{sb}^2\right) A_0\left(M_{H_\mathrm{a}}\right) + \frac{1}{4}\left(2M_{H^\pm}^2 + M_{H_\mathrm{l}}^2 - 2M_\mathrm{sb}^2\right) A_0\left(M_{H^\pm}\right) \Bigg\} \\
& + \frac{c_{\alpha\beta}\, g}{8\pi^2 M_\mathrm{W} t_\beta} \Bigg\{ 3m_\mathrm{t}^2 A_0\left(m_\mathrm{t}\right) \\
& + \frac{t_\beta^2 - 1}{8}\Bigg(3c_{\alpha\beta}^2\left(M_{H_\mathrm{l}}^2 - M_\mathrm{sb}^2\right) A_0\left(M_{H_\mathrm{l}}\right) + s_{\alpha\beta}^2\left(2M_{H_\mathrm{h}}^2 + M_{H_\mathrm{l}}^2 - 3M_\mathrm{sb}^2\right) A_0\left(M_{H_\mathrm{h}}\right) \\
& + \left(M_{H_\mathrm{l}}^2 - M_\mathrm{sb}^2\right) A_0\left(M_{H_\mathrm{a}}\right) + 2\left(M_{H_\mathrm{l}}^2 - M_\mathrm{sb}^2\right) A_0\left(M_{H^\pm}\right)\Bigg)\Bigg\},
\end{aligned}
\tag{A.1}
$$

$$
\begin{aligned}
t_{H_\mathrm{h}} = -T_{H_\mathrm{h}} = \; & \frac{c_{\alpha\beta}\, g}{8\pi^2 M_\mathrm{W}} \Bigg\{ 3m_\mathrm{t}^2 A_0\left(m_\mathrm{t}\right) \\
& - \frac{M_{H_\mathrm{h}}^2}{8}\left(A_0\left(\sqrt{\xi_Z} M_\mathrm{Z}\right) + 2A_0\left(\sqrt{\xi_W} M_\mathrm{W}\right)\right) - \frac{(D-1)}{4}\left(M_\mathrm{Z}^2 A_0\left(M_\mathrm{Z}\right) + 2M_\mathrm{W}^2 A_0\left(M_\mathrm{W}\right)\right) \\
& - \frac{3}{8}\left(M_{H_\mathrm{h}}^2\left(1+2s_{\alpha\beta}^2\right) - 2s_{\alpha\beta}^2 M_\mathrm{sb}^2\right) A_0\left(M_{H_\mathrm{h}}\right) \\
& - \frac{1}{8}\Bigg(\left(1-2s_{\alpha\beta}^2\right)\left(M_{H_\mathrm{h}}^2 + 2M_{H_\mathrm{l}}^2\right) - 2M_\mathrm{sb}^2\left(1-3s_{\alpha\beta}^2\right)\Bigg) A_0\left(M_{H_\mathrm{l}}\right) \\
& - \frac{1}{8}\left(2M_{H_\mathrm{a}}^2 + M_{H_\mathrm{h}}^2 - 2M_\mathrm{sb}^2\right) A_0\left(M_{H_\mathrm{a}}\right) - \frac{1}{4}\left(2M_{H^\pm}^2 + M_{H_\mathrm{h}}^2 - 2M_\mathrm{sb}^2\right) A_0\left(M_{H^\pm}\right) \Bigg\} \\
& + \frac{s_{\alpha\beta} g}{8\pi^2 M_\mathrm{W} t_\beta} \Bigg\{ 3m_\mathrm{t}^2 A_0\left(m_\mathrm{t}\right) \\
& + \frac{t_\beta^2 - 1}{8}\Bigg(3s_{\alpha\beta}^2\left(M_{H_\mathrm{h}}^2 - M_\mathrm{sb}^2\right) A_0\left(M_{H_\mathrm{h}}\right) + c_{\alpha\beta}^2\left(M_{H_\mathrm{h}}^2 + 2M_{H_\mathrm{l}}^2 - 3M_\mathrm{sb}^2\right) A_0\left(M_{H_\mathrm{l}}\right) \\
& + \left(M_{H_\mathrm{h}}^2 - M_\mathrm{sb}^2\right) A_0\left(M_{H_\mathrm{a}}\right) + 2\left(M_{H_\mathrm{h}}^2 - M_\mathrm{sb}^2\right) A_0\left(M_{H^\pm}\right)\Bigg)\Bigg\}.
\end{aligned}
\tag{A.2}
$$

The scalar integral A_0 is defined in D dimensions by

$$A_0(m) = \frac{(2\pi\mu)^{4-D}}{\mathrm{i}\pi^2} \int \mathrm{d}^D q \, \frac{1}{q^2 - m^2 + \mathrm{i}\epsilon}. \tag{A.3}$$

Note that by the transformation

$$s_{\alpha\beta} \to c_{\alpha\beta},\ c_{\alpha\beta} \to -s_{\alpha\beta},\ M_{H_\mathrm{l}} \leftrightarrow M_{H_\mathrm{h}} \tag{A.4}$$

the tadpoles turn into each other in the following way

$$t_{H_\mathrm{l}} \to -t_{H_\mathrm{h}},\ t_{H_\mathrm{h}} \to t_{H_\mathrm{l}}. \tag{A.5}$$

B Results for 2-point tadpole counterterms in the FJ Tadpole Scheme in the 2HDM

In this section, we list the tadpole counterterms for the two-point functions derived according to the definition (2.6). Using the abbreviations

$$t_s(a,b) = a\, t_\beta + b\left(1 - t_\beta^2\right), \tag{B.1}$$

$$t_{\alpha\beta} = \left(s_{\alpha\beta} + c_{\alpha\beta} t_\beta\right)\left(c_{\alpha\beta} - s_{\alpha\beta} t_\beta\right), \tag{B.2}$$

$$t_{f,1} = \frac{g}{2M_\mathrm{W}} \left[-\frac{t_{H_\mathrm{l}}}{M_{H_\mathrm{l}}^2}\left(s_{\alpha\beta} + t_\beta c_{\alpha\beta}\right) + \frac{t_{H_\mathrm{h}}}{M_{H_\mathrm{h}}^2}\left(c_{\alpha\beta} - s_{\alpha\beta} t_\beta\right) \right], \tag{B.3}$$

$$t_{f,2} = \frac{g}{2M_\mathrm{W} t_\beta} \left[\frac{t_{H_\mathrm{l}}}{M_{H_\mathrm{l}}^2}\left(c_{\alpha\beta} - s_{\alpha\beta} t_\beta\right) + \frac{t_{H_\mathrm{h}}}{M_{H_\mathrm{h}}^2}\left(s_{\alpha\beta} + c_{\alpha\beta} t_\beta\right) \right], \tag{B.4}$$

the expressions read:

$$\begin{aligned} t_{H_\mathrm{l}H_\mathrm{l}} = & -t_{H_\mathrm{l}} \frac{3g}{2M_\mathrm{W} t_\beta} \left[s_{\alpha\beta} t_{\alpha\beta} + t_s(2s_{\alpha\beta}, -c_{\alpha\beta}) \left(1 - \frac{M_\mathrm{sb}^2 c_{\alpha\beta}^2}{M_{H_\mathrm{l}}^2}\right) \right] \\ & - t_{H_\mathrm{h}} \frac{g\, c_{\alpha\beta}}{2M_\mathrm{W} t_\beta} \left[-\left(1 + \frac{2M_{H_\mathrm{l}}^2}{M_{H_\mathrm{h}}^2}\right) t_{\alpha\beta} + \frac{M_\mathrm{sb}^2}{M_{H_\mathrm{h}}^2} t_s(2(c_{\alpha\beta}^2 - 2s_{\alpha\beta}^2), 3s_{\alpha\beta} c_{\alpha\beta}) \right], \end{aligned} \tag{B.5}$$

$$\begin{aligned} t_{H_\mathrm{h}H_\mathrm{h}} = & -t_{H_\mathrm{h}} \frac{3g}{2M_\mathrm{W} t_\beta} \left[c_{\alpha\beta} t_{\alpha\beta} - t_s(2c_{\alpha\beta}, s_{\alpha\beta}) \left(1 - \frac{M_\mathrm{sb}^2}{M_{H_\mathrm{h}}^2} s_{\alpha\beta}^2\right) \right] \\ & - t_{H_\mathrm{l}} \frac{g s_{\alpha\beta}}{2M_\mathrm{W} t_\beta} \left[-\left(1 + \frac{2M_{H_\mathrm{l}}^2}{M_{H_\mathrm{h}}^2}\right) t_{\alpha\beta} - \frac{M_\mathrm{sb}^2}{M_{H_\mathrm{l}}^2} t_s(2(s_{\alpha\beta}^2 - 2c_{\alpha\beta}^2), -3s_{\alpha\beta} c_{\alpha\beta}) \right], \end{aligned} \tag{B.6}$$

$$\begin{aligned} t_{H_\mathrm{h}H_\mathrm{l}} = t_{H_\mathrm{l}H_\mathrm{h}} = & \frac{g}{2M_\mathrm{W} t_\beta} t_{H_\mathrm{l}} c_{\alpha\beta} \left[\left(2 + \frac{M_{H_\mathrm{h}}^2}{M_{H_\mathrm{l}}^2}\right) t_{\alpha\beta} + \frac{M_\mathrm{sb}^2}{M_{H_\mathrm{l}}^2} t_s(2(2s_{\alpha\beta}^2 - c_{\alpha\beta}^2), -3s_{\alpha\beta} c_{\alpha\beta}) \right] \\ & + \frac{g}{2M_\mathrm{W} t_\beta} t_{H_\mathrm{h}} s_{\alpha\beta} \left[\left(2 + \frac{M_{H_\mathrm{l}}^2}{M_{H_\mathrm{h}}^2}\right) t_{\alpha\beta} - \frac{M_\mathrm{sb}^2}{M_{H_\mathrm{h}}^2} t_s(2(2c_{\alpha\beta}^2 - s_{\alpha\beta}^2), 3s_{\alpha\beta} c_{\alpha\beta}) \right], \end{aligned} \tag{B.7}$$

$$\begin{aligned} t_{H_\mathrm{a}H_\mathrm{a}} = & t_{H_\mathrm{l}} \frac{g}{2M_\mathrm{W} t_\beta} \left[\frac{M_\mathrm{sb}^2}{M_{H_\mathrm{l}}^2} t_s(2s_{\alpha\beta}, -c_{\alpha\beta}) - \frac{M_{H_\mathrm{a}}^2}{M_{H_\mathrm{l}}^2} 2s_{\alpha\beta} t_\beta - t_s(s_{\alpha\beta}, -c_{\alpha\beta}) \right] \\ & + t_{H_\mathrm{h}} \frac{g}{2M_\mathrm{W} t_\beta} \left[-\frac{M_\mathrm{sb}^2}{M_{H_\mathrm{h}}^2} t_s(2c_{\alpha\beta}, s_{\alpha\beta}) + \frac{M_{H_\mathrm{a}}^2}{M_{H_\mathrm{h}}^2} 2c_{\alpha\beta} t_\beta + t_s(c_{\alpha\beta}, s_{\alpha\beta}) \right], \end{aligned} \tag{B.8}$$

JHEP09(2016)115

$$t_{H^\pm H^\mp} = t_{H_\mathrm{a} H_\mathrm{a}}\left(M_{H_\mathrm{a}} \to M_{H^\pm}\right), \tag{B.9}$$

$$t_{G_0 G_0} = t_{G^\pm G^\mp} = \frac{g}{2M_\mathrm{W}}\left(-t_{H_\mathrm{l}} s_{\alpha\beta} + t_{H_\mathrm{h}} c_{\alpha\beta}\right), \tag{B.10}$$

$$t_{G_0 H_\mathrm{a}} = t_{H_\mathrm{a} G_0} = t_{H_\mathrm{l}} \frac{g\, c_{\alpha\beta}}{2M_\mathrm{W}}\left(1 - \frac{M_{H_\mathrm{a}}^2}{M_{H_\mathrm{l}}^2}\right) + t_{H_\mathrm{h}} \frac{g\, s_{\alpha\beta}}{2M_\mathrm{W}}\left(1 - \frac{M_{H_\mathrm{a}}^2}{M_{H_\mathrm{h}}^2}\right), \tag{B.11}$$

$$t_{G^\pm H^\mp} = t_{H^\pm G^\mp} = t_{G_0 H_\mathrm{a}}\left(M_{H_\mathrm{a}} \to M_{H^\pm}\right), \tag{B.12}$$

$$t^{\mu\nu}_{W^\pm W^\mp} = g^{\mu\nu} g M_\mathrm{W}\left(\frac{t_{H_\mathrm{l}}}{M_{H_\mathrm{l}}^2} s_{\alpha\beta} - \frac{t_{H_\mathrm{h}}}{M_{H_\mathrm{h}}^2} c_{\alpha\beta}\right), \tag{B.13}$$

$$t^{\mu\nu}_{ZZ} = \frac{t^{\mu\nu}_{W^\pm W^\mp}}{c_\mathrm{w}}, \tag{B.14}$$

$$t^{\mu}_{W^\pm H^\mp} = \mathrm{i} q^\mu \frac{g}{2}\left(\frac{t_{H_\mathrm{l}}}{M_{H_\mathrm{l}}^2} c_{\alpha\beta} + \frac{t_{H_\mathrm{h}}}{M_{H_\mathrm{h}}^2} s_{\alpha\beta}\right), \tag{B.15}$$

$$t^{\mu}_{W^\pm G^\mp} = \pm\, q^\mu \frac{g}{2}\left(\frac{t_{H_\mathrm{l}}}{M_{H_\mathrm{l}}^2} s_{\alpha\beta} - \frac{t_{H_\mathrm{h}}}{M_{H_\mathrm{h}}^2} c_{\alpha\beta}\right), \tag{B.16}$$

$$t^{\mu}_{Z H_\mathrm{a}} = -\,\mathrm{i}\frac{t^{\mu}_{W^\pm H^\mp}}{c_\mathrm{w}}, \tag{B.17}$$

$$t^{\mu}_{Z G_0} = -\,\mathrm{i}\frac{t^{\mu}_{W^- G^+}}{c_\mathrm{w}}, \tag{B.18}$$

$$t_{ff} = \begin{cases} m_f t_{f,1} \text{ if } f \text{ couples to } \Phi_1 \text{ in eq. (3.11)} \\ \\ m_f t_{f,2} \text{ if } f \text{ couples to } \Phi_2 \text{ in eq. (3.11)} \end{cases}, \tag{B.19}$$

with q^μ being the incoming momentum of the corresponding vector boson. The Feynman rules for the tadpole counterterms are obtained by multiplying the tadpole expression with the imaginary unit i.

C Tadpoles in the two-loop Higgs-boson self-energy in the FJ Tadpole Scheme

In this appendix, we relate the renormalized two-loop self-energy of the Higgs boson in the SM in the two schemes based on $\hat{T}_h = 0$ and $\Delta v = 0$. Analogously to eq. (2.26) at one loop, we show that the two-loop tadpole contributions to the self-energy, which are generated by Δv in the scheme with $\hat{T}_h = 0$, reproduce the self-energy in the scheme with $\Delta v = 0$, where unrenormalized tadpoles are explicitly taken into account. The latter situation is given in eq. (2.11) if the renormalized tadpoles are replaced by unrenormalized ones.

To start with, we note that the 1PI two-loop self-energy and tadpole contributions depend on the tadpole renormalization scheme, more precisely, they differ by Δv-dependent terms. Having performed the renormalization at one-loop, the 1PI two-loop self-energy diagrams in both schemes are related via

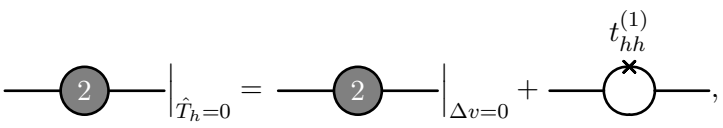

(C.1)

JHEP09(2016)115

where the second diagram on the right-hand side schematically denotes all one-loop self-energy diagrams with an additional insertion of the one-loop two-point tadpole counterterm $t_{hh}^{(1)}$. Using the one-loop result (2.26) which relates $t_{hh}^{(1)}$ with the bare one-loop tadpole $t_h^{(1)}$, this can be written as

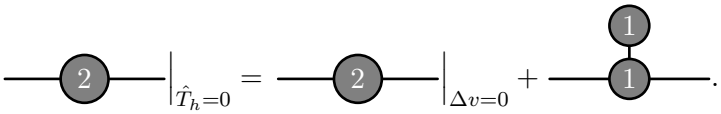

(C.2)

Next, we consider the two-loop 1PI tadpole which fixes $t_h^{(2)}$ in the scheme where $\hat{T}_h = 0$,

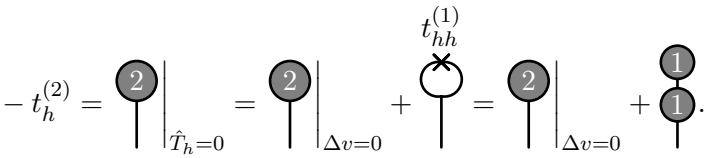

(C.3)

The first equality is the renormalization condition. In the second equality we separate the Δv-dependent terms, where the second diagram schematically represents all tadpole one-loop diagrams with an additional insertion of $t_{hh}^{(1)}$. In the third equality we use again the one-loop result (2.26). In the scheme where the tadpoles are renormalized according to $\hat{T}_h = 0$ the renormalized two-loop self-energy can be expressed exclusively by 1PI contributions and is given by

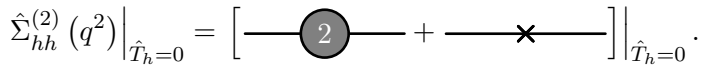

(C.4)

The *FJ Tadpole Scheme* for $\hat{T}_h = 0$ includes tadpoles via the Δv-dependent counterterms. In addition to the $\Delta v^{(1)}$-dependent one-loop counterterms appearing in eqs. (C.1) and (C.3), the two-loop counterterm induces a further dependence on $\Delta v^{(1)}$ and $\Delta v^{(2)}$. In the SM the additional two-loop tadpole counterterms are derived from eq. (2.37), which can be written as

$$t_{hh} h_{\rm B}^2 = \left(\lambda_{hhh,{\rm B}} \Delta v + \frac{\lambda_{hhhh,{\rm B}}}{2} (\Delta v)^2\right) h_{\rm B}^2 \tag{C.5}$$

upon identifying $\lambda_{hhh,{\rm B}}$ and $\lambda_{hhhh,{\rm B}}$ as the bare triple and quartic Higgs-boson couplings. The dependence on the two-loop tadpole counterterm $t_h^{(2)}$ originates from the term proportional to $\lambda_{hhh,{\rm B}} \Delta v^{(2)}$. Using eqs. (2.35) and (C.3) the contribution of $t_h^{(2)}$ can be written as

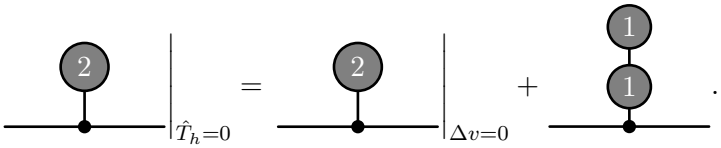

(C.6)

Next, we consider the quadratic 1PI one-loop tadpole contributions which are included in $\Delta v^{(2)}$ and $\left(\Delta v^{(1)}\right)^2$ being proportional to λ_{hhh} and λ_{hhhh}, respectively. We identify the two contributions with

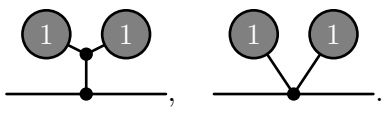

(C.7)

JHEP09(2016)115

The last two-loop tadpole counterterms result from products of the one-loop tadpole $t_h^{(1)}$ with the counterterms to λ_{hhh}, the Higgs-boson mass [entering via eq. (2.34)], and the Higgs-boson field-renormalization constant and can be represented as follows:

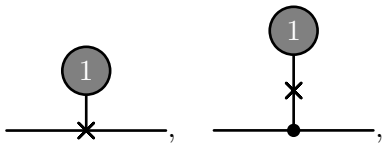

(C.8)

where in the counterterms $\Delta v = 0$ is understood. Finally, we separate the Δv dependence from the renormalized two-loop self-energy (C.4). For the bare 1PI two-loop self-energy we use the result (C.2). The two-loop Δv-dependent counterterms are given by the sum of the diagrams in eqs. (C.6), (C.7), and (C.8). The result reads

$\hat{\Sigma}^{(2)}_{hh}\left(q^2\right)\Big|_{\hat{T}_h=0}$ =

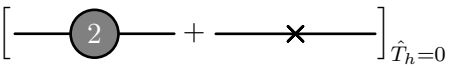

=

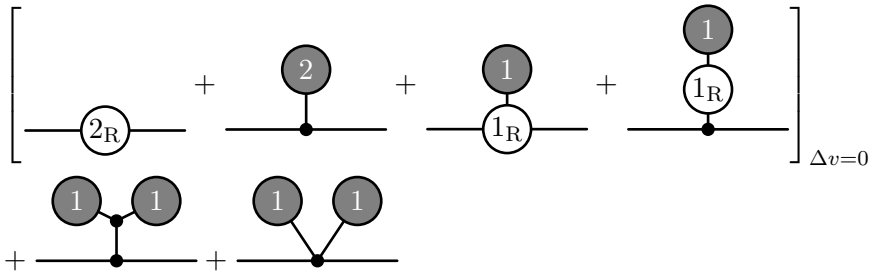

$= \hat{\Sigma}^{(2)}_{hh}\left(q^2\right)\Big|_{\Delta v=0}$. (C.9)

In the second equation we combine counterterms, evaluated for $\Delta v = 0$, and bare-loop topologies to renormalized objects. The result matches the renormalized two-loop self-energy in eq. (2.11) when tadpoles are not renormalized, i.e. for $\Delta v = 0$.

D Gauge dependence of β in popular tadpole schemes

In the MSSM, $\delta\beta^{\overline{\text{MS}}}$ as obtained in Scheme 2 is gauge dependent at two loops [34], while it does not dependent on the gauge parameters in the R_ξ-gauge at one-loop order. The latter result translates to the 2HDM of type II.

In the 2HDM the apparent gauge independence of $\delta\beta^{\overline{\text{MS}}}$ in the R_ξ-gauge at the one-loop level can be understood as follows: consider the linear combination of Φ_1 and Φ_2 that does not have a vev. Using the explicit rotations in eq. (3.4), this Higgs doublet is identified as

$$\cos\beta\Phi_2 - \sin\beta\Phi_1 = \begin{pmatrix} H^\pm \\ \frac{1}{\sqrt{2}}\left(\cos\beta v_2 - \sin\beta v_1 + H_\text{l} c_{\alpha\beta} + H_\text{h} s_{\alpha\beta} + \text{i}H_\text{a}\right) \end{pmatrix}, \tag{D.1}$$

with $\cos\beta v_2 - \sin\beta v_1 = 0$. Performing the shift in the vevs according to eq. (4.5) and using eq. (4.6), we obtain the tadpole corresponding to the neutral Higgs field $\widetilde{H} = H_\text{l} c_{\alpha\beta} + H_\text{h} s_{\alpha\beta}$,

$$\sin\beta\Delta v_1 - \cos\beta\Delta v_2 = c_{\alpha\beta}\frac{t_{H_\text{l}}}{M^2_{H_\text{l}}} + s_{\alpha\beta}\frac{t_{H_\text{h}}}{M^2_{H_\text{h}}}, \tag{D.2}$$

JHEP09(2016)115

which enters the shift of $\Delta_i\beta^{\overline{\rm MS}}$ between the *FJ Tadpole Scheme* and the popular Schemes 1 and 2 found in eqs. (5.9) and (5.14). The Higgs field $\widetilde{H}$ does neither couple to two gauge bosons nor to two would-be Goldstone bosons, and, moreover, it does not enter the gauge fixing in the R_ξ-gauge and thus does not couple to Faddeev-Popov ghost fields. Consequently, there are no gauge-dependent Feynman diagrams for the $\widetilde{H}$ tadpole at one-loop order and thus $\Delta_i\delta\beta^{\overline{\rm MS}}$ does not depend on the gauge-parameter in the R_ξ-gauge. Since $\delta\beta^{\overline{\rm MS}}$ is gauge independent in the *FJ Tadpole Scheme*, this translates to Schemes 1 and 2. This argument can be generalized to non-linear R_ξ-gauges at one-loop order.[8]

Nevertheless, it is possible to demonstrate the gauge dependence of $\delta\beta^{\overline{\rm MS}}$ in Schemes 1 and 2 at one-loop order in a suitably chosen gauge. Since $\widetilde{H}$ couples to one gauge boson or would-be Goldstone boson and $H_{\rm a}$, we can generate a gauge-dependent contribution to its tadpole by allowing for mixing propagators induced by the gauge fixing. Here, we provide an appropriate gauge-fixing function and prove the gauge dependence of $\delta\beta^{\overline{\rm MS}}$ via two different approaches. In addition, we show that also in this class of gauges the gauge independence of $\delta\beta^{\overline{\rm MS}}$ is preserved in the *FJ Tadpole Scheme*.

The appropriate choice of the gauge-fixing function can be motivated as follows. From the point of view of the *FJ Tadpole Scheme* the gauge dependence appears in the Schemes 1 [eq. (5.3)] or 2 [eq. (5.4)] if it is possible to generate a gauge-dependent tadpole contribution of the form of eq. (D.2). For a gauge-fixing function C linear in the gauge fields the infinitesimal variation of Green's functions under a change in the gauge-fixing function, ΔC, with respect to some parameter can be derived (see e.g. section 2.5.4.4 of ref. [27], section 12.4 of ref. [72], or ref. [32]). For the one-point function of a field φ this reads

$$\delta_{\Delta C}\,\langle T\varphi(x)\rangle := \delta_{\Delta C}$$

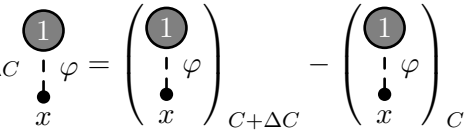

$$= \mathrm{i}\langle T(s\varphi(x))\int \mathrm{d}^4y\,\bar{u}(y)\Delta C(y)\rangle$$

$$= \mathrm{i}\int \mathrm{d}^4y$$

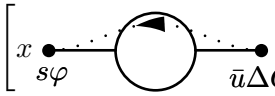

(D.3)

where $s\varphi$ represents the BRST transformation of the field φ at the space-time point x and $\bar{u}$ is the anti-ghost field associated to the gauge-fixing function C, both at the space-time point y. For

$$\varphi = \widetilde{H} = c_{\alpha\beta}H_{\rm l} + s_{\alpha\beta}H_{\rm h}, \tag{D.4}$$

the required BRST transformation in eq. (D.3) reads

$$s\widetilde{H} = \frac{e}{2s_{\rm w}c_{\rm w}}u^{\rm Z}H_{\rm a} + \frac{\mathrm{i}e}{2s_{\rm w}}\left(u^-H^+ - u^+H^-\right). \tag{D.5}$$

We note that $s\widetilde{H}$ does neither induce would-be Goldstone bosons nor vevs. Hence, one can easily read off the condition for a gauge dependence of eq. (D.2). We modify the gauge-fixing function in eq. (5.2) by setting $\xi_W = \xi_A = \xi_Z = 1$ and adding a term proportional

[8] Specifically, we verified the independence of $\delta\beta^{\overline{\rm MS}}$ of the gauge parameters for a non-linear gauge-fixing function $C^Z = \partial_\mu Z_\mu - \xi_{G_0}M_{\rm Z}G_0\,(1+\xi_{H_{\rm h}}H_{\rm h})$ for general ξ_{G_0} and $\xi_{H_{\rm h}}$.

JHEP09(2016)115

to H_a to C^Z,

$$C^Z = \partial^\mu Z_\mu - M_\mathrm{Z} G_0 - \xi_\beta M_{H_\mathrm{a}} H_\mathrm{a}, \tag{D.6}$$

which is required to obtain non-vanishing contributions to eq. (D.3). The resulting gauge-fixing function (D.6) in the ξ_β-gauge looks simple, but gives rise to a non-diagonal propagator matrix (see appendix E for the Feynman rules). An infinitesimal change in the gauge-fixing function is obtained by performing an expansion for small ξ_β, i.e. we identify ΔC with $-\xi_\beta M_{H_\mathrm{a}} H_\mathrm{a}$, defining

$$\delta_{\xi_\beta} X := \frac{\partial}{\partial \xi_\beta} X \bigg|_{\xi_\beta = 0} \xi_\beta. \tag{D.7}$$

While we work only to leading order in ξ_β, an exact calculation is possible and straightforward in the gauge of eq. (D.6). At one-loop order we find after Fourier transformation to momentum space

$$\text{F.T.} \int \mathrm{d}^4 y \left[x \; \overset{u_Z}{\bullet\!\!\cdots\!\!\bullet} \; y \right]_{H_\mathrm{a}} = \int \frac{\mathrm{d}^4 q}{(2\pi)^4} \frac{\mathrm{i}}{q^2 - M_\mathrm{Z}^2} \frac{\mathrm{i}}{q^2 - M_{H_\mathrm{a}}^2}, \tag{D.8}$$

and hence using eq. (D.3)

$$\left\langle \widetilde{H} \right\rangle_{\xi_\beta} := \text{F.T.}\, \delta_{\xi_\beta} \left\langle T \widetilde{H}(x) \right\rangle = \text{F.T.} \left[c_{\alpha\beta}\, \delta_{\xi_\beta} \; \overset{1}{\bullet}\!\!\!\!\underset{x}{\vdots} H_\mathrm{l} + s_{\alpha\beta}\, \delta_{\xi_\beta} \; \overset{1}{\bullet}\!\!\!\!\underset{x}{\vdots} H_\mathrm{h} \right] \tag{D.9}$$

$$= -\frac{\mathrm{i} e \xi_\beta M_{H_\mathrm{a}}}{2 s_\mathrm{w} c_\mathrm{w}} \int \frac{\mathrm{d}^4 q}{(2\pi)^4} \frac{\mathrm{i}}{q^2 - M_\mathrm{Z}^2} \frac{\mathrm{i}}{q^2 - M_{H_\mathrm{a}}^2}. \tag{D.10}$$

Consequently, there is a non-zero gauge-dependent and UV-divergent contribution to the tadpole in eq. (D.2), which proves the gauge dependence in the popular schemes, where tadpole contributions are absorbed in bare parameters. Note that this argument can be carried over to the supersymmetric case, where $\left\langle \widetilde{H} \right\rangle_{\xi_\beta}$ does not change if the same gauge is used. This result is used below to derive the ξ_β dependence of $\delta\beta^{\overline{\mathrm{MS}}}$ in Schemes 1 and 2 [see eq. (D.27)].

We validate eq. (D.10) in the 2HDM using an explicit Feynman-diagrammatic calculation of the tadpole $\langle \widetilde{H} \rangle$. Inspecting the Feynman rules listed in appendix E, we find three sources that can induce a linear ξ_β dependence of the tadpole $\langle \widetilde{H} \rangle$. These are provided by the mixing propagators ZH_a and $G_0 H_\mathrm{a}$ and the coupling of the neutral Higgs bosons H_l and H_h to Faddeev-Popov ghosts $\bar{u}^Z$ and u^Z. For the ξ_β-dependent tadpole contributions corresponding to eq. (D.9) in momentum space we obtain

$$\delta_{\xi_\beta} \; \overset{1}{\bullet}\!\!\!\!\underset{\varphi}{\vdots} = Z \; \underset{\varphi}{\circlearrowleft\!\!\vdots} H_\mathrm{a} + G_0 \; \underset{\varphi}{\circlearrowleft\!\!\vdots} H_\mathrm{a} + \; \underset{\varphi}{\circlearrowleft\!\!\vdots} u_Z \quad \text{for} \quad \varphi = H_\mathrm{l}, H_\mathrm{h}, \tag{D.11}$$

JHEP09(2016)115

and the sum of the contributions yields

$$\delta_{\xi_\beta}\ \overset{1}{\bullet}\!\!-\!\!\!-\ H_\mathrm{l} = -\frac{\mathrm{i}e\xi_\beta M_{H_\mathrm{a}} c_{\alpha\beta}}{2 s_\mathrm{w} c_\mathrm{w}} \int \frac{\mathrm{d}^4 q}{(2\pi)^4}\, \frac{\mathrm{i}}{q^2 - M_\mathrm{Z}^2}\, \frac{\mathrm{i}}{q^2 - M_{H_\mathrm{a}}^2} = c_{\alpha\beta} \left\langle \widetilde{H} \right\rangle_{\xi_\beta},$$
$$\delta_{\xi_\beta}\ \overset{1}{\bullet}\!\!-\!\!\!-\ H_\mathrm{h} = -\frac{\mathrm{i}e\xi_\beta M_{H_\mathrm{a}} s_{\alpha\beta}}{2 s_\mathrm{w} c_\mathrm{w}} \int \frac{\mathrm{d}^4 q}{(2\pi)^4}\, \frac{\mathrm{i}}{q^2 - M_\mathrm{Z}^2}\, \frac{\mathrm{i}}{q^2 - M_{H_\mathrm{a}}^2} = s_{\alpha\beta} \left\langle \widetilde{H} \right\rangle_{\xi_\beta}. \tag{D.12}$$

Thus, we reproduce the result in eq. (D.10).

Finally, we show explicitly that $\delta\beta^{\overline{\mathrm{MS}}}$ remains gauge independent in the *FJ Tadpole Scheme* at one-loop order but depends explicitly on ξ_β in the gauge of eq. (D.6) in Schemes 1 and 2. We cannot make use of eq. (4.26) because it does not hold in the ξ_β-gauge for Schemes 1 and 2, but instead we derive the gauge dependence directly from the renormalized vertex function in eq. (4.23). We consider only the terms linear in ξ_β.

In the *FJ Tadpole Scheme* it is enough to verify that all counterterm parameters that enter the renormalization of β are gauge independent and that no gauge dependence is introduced by the bare vertex function in eq. (4.23). The renormalization constant δZ_e is independent of ξ_β since no Higgs-boson couplings enter this quantity. For δM_W^2 and δM_Z^2, the tadpole contributions to the WW and ZZ two-point functions are proportional to (see appendix B)

$$s_{\alpha\beta} \frac{t_{H_\mathrm{l}}}{M_{H_\mathrm{l}}^2} - c_{\alpha\beta} \frac{t_{H_\mathrm{h}}}{M_{H_\mathrm{h}}^2}, \tag{D.13}$$

which is not sensitive to our choice of gauge-fixing function. The W-boson self-energy receives no other contributions linear in ξ_β. The linear ξ_β-dependent contribution induced in the Z-boson self-energy contributes only to its longitudinal part and does not influence δM_Z^2. This implies the ξ_β independence of δM_W^2 and δM_Z^2 which we have also verified via explicit calculation in the ξ_β-gauge. For the vertex $H_\mathrm{a}\tau^+\tau^-$ there is no ξ_β-dependent and at the same time UV-divergent term. This is consistent with the fact that there is no tadpole contribution to the bare vertex function which could cancel a would-be gauge dependence. For $\delta Z_{G_0 H_\mathrm{a}}$ and δm_τ no such argument can be given, and a cancellation of ξ_β-dependent terms between self-energy diagrams and tadpoles takes place. We explicitly show this cancellation starting with $\delta Z_{G_0 H_\mathrm{a}}$.

The terms linear in ξ_β contributing to the $G_0 H_\mathrm{a}$ mixing energy are given by[9]

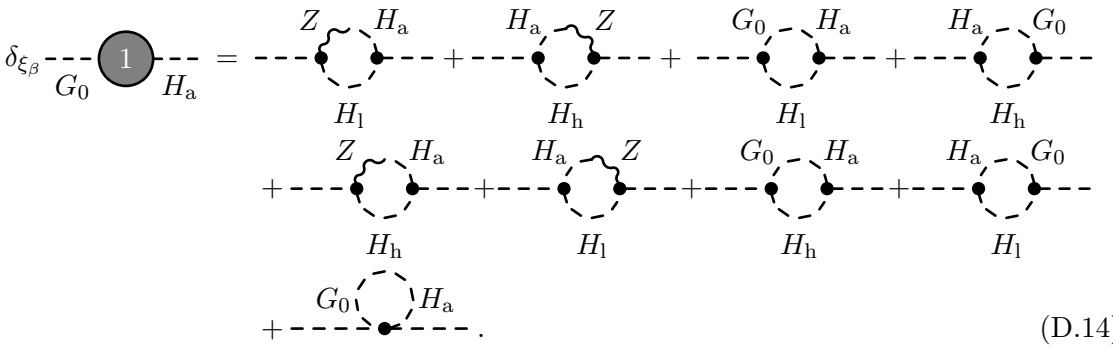

(D.14)

[9] In the alignment limit, the second line in eq. (D.14) vanishes.

JHEP09(2016)115

Note that each diagram contains one mixing propagator. The diagrams involving a neutral Higgs boson propagator and a mixing propagator of a pseudoscalar Higgs boson and a would-be Goldstone boson do not contribute to the $\overline{\text{MS}}$ renormalization of β because they are UV finite. The other self-energy diagrams are UV divergent, and we obtain for the combined contributions to the $G_0 H_\text{a}$ mixing energy

$$\sum_{\varphi=H_\text{l},H_\text{h}} \quad = -\frac{\mathrm{i}e}{2s_\text{w}M_\text{W}}\Big[s^2_{\alpha\beta}M^2_{H_\text{l}} + c^2_{\alpha\beta}M^2_{H_\text{h}} + 2M^2_{H_\text{a}} - 2M^2_{\text{sb}} + c_{\alpha\beta}s_{\alpha\beta}\frac{1-t^2_\beta}{t_\beta}\big(M^2_{H_\text{h}} - M^2_{H_\text{l}}\big)\Big]\Big\langle\widetilde{H}\Big\rangle_{\xi_\beta} + \text{UV-finite terms}, \tag{D.15}$$

$$\sum_{\varphi=H_\text{l},H_\text{h}} \quad = \frac{\mathrm{i}e}{2s_\text{w}M_\text{W}}\left[M^2_{H_\text{a}} - s^2_{\alpha\beta}M^2_{H_\text{h}} - c^2_{\alpha\beta}M^2_{H_\text{l}}\right]\Big\langle\widetilde{H}\Big\rangle_{\xi_\beta} + \text{UV-finite terms}, \tag{D.16}$$

$$\quad = \frac{\mathrm{i}e}{2s_\text{w}M_\text{W}}\Big[M^2_{H_\text{l}} + 2M^2_{H_\text{h}} - 2M^2_{\text{sb}} + c_{\alpha\beta}\left(-c_{\alpha\beta} + s_{\alpha\beta}\frac{1-t^2_\beta}{t_\beta}\right)\left(M^2_{H_\text{h}} - M^2_{H_\text{l}}\right)\Big]\Big\langle\widetilde{H}\Big\rangle_{\xi_\beta}, \tag{D.17}$$

where for arriving at the eqs. (D.15) and (D.16) the numerator structure has been cancelled against one of the neutral Higgs-boson propagators. Adding all contributions leads to

$$\delta_{\xi_\beta} \quad = -\frac{\mathrm{i}e}{2s_\text{w}M_\text{W}}\left[M^2_{H_\text{a}} - s^2_{\alpha\beta}M^2_{H_\text{h}} - c^2_{\alpha\beta}M^2_{H_\text{l}}\right]\Big\langle\widetilde{H}\Big\rangle_{\xi_\beta} + \text{UV-finite terms} \tag{D.18}$$

for the linear dependence of self-energy diagrams on ξ_β. The tadpole contributions to the $G_0 H_\text{a}$ mixing energy are derived using the results in eq. (D.12) leading to

$$\sum_{\varphi=H_\text{l},H_\text{h}} \quad = \frac{\mathrm{i}e}{2s_\text{w}M_\text{W}}\left[M^2_{H_\text{a}} - s^2_{\alpha\beta}M^2_{H_\text{h}} - c^2_{\alpha\beta}M^2_{H_\text{l}}\right]\Big\langle\widetilde{H}\Big\rangle_{\xi_\beta}, \tag{D.19}$$

which cancels against the ξ_β dependent terms in eq. (D.18) contributing to the renormalization of β. Thus, we have proven that

$$\Big(\delta_{\xi_\beta}\delta Z^{\overline{\text{MS}}}_{G_0 H_\text{a}}\Big)_3 = 0. \tag{D.20}$$

For the on-shell renormalization of δm_τ we pursue the same strategy. The ξ_β-dependent contributions to the τ self-energy are given by

$$\delta_{\xi_\beta} \quad = \quad + \quad + \quad + \quad . \tag{D.21}$$

JHEP09(2016)115

Projecting the τ self-energy onto a Dirac spinor, putting the momentum on shell, using the Dirac equation, and considering only the scalar and vector part that is relevant for the mass counterterm, we find

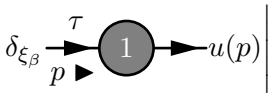

$$\Big|_{p^2=m_\tau^2} = \frac{\mathrm{i}e^2 t_\beta m_\tau \xi_\beta M_{H_\mathrm{a}}}{4 M_\mathrm{W} s_\mathrm{w}^2 c_\mathrm{w}} u(p) \tag{D.22}$$

$$\times \int \frac{\mathrm{d}^4 q}{(2\pi)^4} \frac{\mathrm{i}}{q^2 - M_\mathrm{Z}^2} \frac{\mathrm{i}}{q^2 - M_{H_\mathrm{a}}^2} \frac{\mathrm{i}}{(p+q)^2 - m_\tau^2} \left((p+q)^2 - m_\tau^2\right) \Big|_{p^2=m_\tau^2}$$

$$= -\frac{\mathrm{i}e m_\tau t_\beta}{2 s_\mathrm{w} M_\mathrm{W}} \left\langle \widetilde{H} \right\rangle_{\xi_\beta} u(p) \Big|_{p^2=m_\tau^2} . \tag{D.23}$$

The tadpole contribution to the τ self-energy is derived using the results in eq. (D.12) leading to

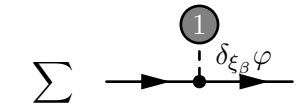

$$\sum_{\varphi=H_\mathrm{l},H_\mathrm{h}} = \frac{\mathrm{i}e m_\tau t_\beta}{2 s_\mathrm{w} M_\mathrm{W}} \left\langle \widetilde{H} \right\rangle_{\xi_\beta} . \tag{D.24}$$

The tadpole contribution in eq. (D.24) cancels against the self-energy contribution in eq. (D.23) and we conclude that δm_τ is independent of ξ_β in on-shell renormalization,

$$\left(\delta_{\xi_\beta} \delta m_\tau\right)_3 = 0. \tag{D.25}$$

Altogether, we have proven the gauge independence of $\delta\beta^{\overline{\mathrm{MS}}}$ in the ξ_β-gauge in the *FJ Tadpole Scheme*,

$$\left(\delta_{\xi_\beta} \delta\beta^{\overline{\mathrm{MS}}}\right)_3 = 0. \tag{D.26}$$

Finally, we can give the precise ξ_β dependence of $\delta\beta$ for Schemes 1 and 2 originating from the gauge dependence of the tadpoles in δm_τ and $\delta Z_{G_0 H_\mathrm{a}}$. Using eq. (4.25) for the counterterm, the full ξ_β dependence is obtained as

$$(\delta_{\xi_\beta} \delta\beta^{\overline{\mathrm{MS}}})_i = \frac{e}{2 s_\mathrm{w} M_\mathrm{W}} \left[1 - \frac{s_{\alpha\beta}^2 M_{H_\mathrm{h}}^2 + c_{\alpha\beta}^2 M_{H_\mathrm{l}}^2}{M_{H_\mathrm{a}}^2 \left(1 + t_\beta^2\right)}\right] \left\langle \widetilde{H} \right\rangle_{\xi_\beta} \Big|_{\overline{\mathrm{P.P.}}} , \quad i = 1, 2, \tag{D.27}$$

which is evidently nonzero.

E Feynman rules in the ξ_β-gauge

In this section, we list the Feynman rules used to derive the gauge dependence of $\delta\beta^{\overline{\mathrm{MS}}}$ in appendix D. The gauge-fixing function (D.6) gives rise to mixing of propagators, which is required to actually observe the gauge dependence at one-loop order. The gauge-fixing Lagrangian includes the following mixing terms

$$\mathcal{L}_\mathrm{GF} \supset \xi_\beta M_{H_\mathrm{a}} \left(\partial_\mu Z^\mu + M_\mathrm{Z} G_0\right) H_\mathrm{a}. \tag{E.1}$$

JHEP09(2016)115

The corresponding 2-point vertex function in the basis $(Z_\mu, G_0, H_\mathrm{a})$ reads

$$\Gamma = \begin{pmatrix} -\left(p^2 - M_\mathrm{Z}^2\right) g^{\mu\nu} & 0 & \mathrm{i}\xi_\beta M_{H_\mathrm{a}} p^\mu \\ 0 & p^2 - M_\mathrm{Z}^2 & \xi_\beta M_{H_\mathrm{a}} M_\mathrm{Z} \\ -\mathrm{i}\xi_\beta M_{H_\mathrm{a}} p^\mu & \xi_\beta M_{H_\mathrm{a}} M_\mathrm{Z} & p^2 - M_{H_\mathrm{a}}^2 \left(1 + \xi_\beta^2\right) \end{pmatrix}. \tag{E.2}$$

By inverting the vertex function to linear order in ξ_β we obtain the propagators as

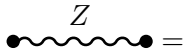

$$= \frac{-\mathrm{i}g^{\mu\nu}}{p^2 - M_\mathrm{Z}^2} + \mathcal{O}\left(\xi_\beta^2\right), \tag{E.3}$$

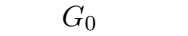

$$= \frac{\mathrm{i}}{p^2 - M_\mathrm{Z}^2} + \mathcal{O}\left(\xi_\beta^2\right), \tag{E.4}$$

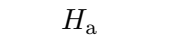

$$= \frac{\mathrm{i}}{p^2 - M_{H_\mathrm{a}}^2}, \tag{E.5}$$

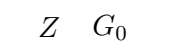

$$= \mathcal{O}\left(\xi_\beta^2\right), \tag{E.6}$$

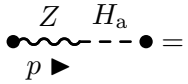

$$= -\xi_\beta M_{H_\mathrm{a}} p^\mu \frac{\mathrm{i}}{p^2 - M_\mathrm{Z}^2} \frac{\mathrm{i}}{p^2 - M_{H_\mathrm{a}}^2}, \tag{E.7}$$

$$= \mathrm{i}\xi_\beta M_{H_\mathrm{a}} M_\mathrm{Z} \frac{\mathrm{i}}{p^2 - M_\mathrm{Z}^2} \frac{\mathrm{i}}{p^2 - M_{H_\mathrm{a}}^2}, \tag{E.8}$$

where the momentum flows from left to right. We identify mixing propagators by two particle labels. The Faddeev-Popov-ghost Lagrangian is derived by the standard methods which requires for the ξ_β-gauge the BRST variation of H_a,

$$sH_\mathrm{a} = -\frac{e}{2 s_\mathrm{w} c_\mathrm{w}} u^Z \left(c_{\alpha\beta} H_\mathrm{l} + s_{\alpha\beta} H_\mathrm{h}\right) + \frac{e}{2 s_\mathrm{w}} \left(u^+ H^- + u^- H^+\right). \tag{E.9}$$

The additional contribution to the ghost Lagrangian involving ξ_β is then given by

$$\mathcal{L}_\mathrm{gh} \supset \xi_\beta M_{H_\mathrm{a}} \frac{e}{2 s_\mathrm{w} c_\mathrm{w}} \bar{u}^Z u^Z \left(c_{\alpha\beta} H_\mathrm{l} + s_{\alpha\beta} H_\mathrm{h}\right), \tag{E.10}$$

yielding the following gauge-dependent Feynman rules

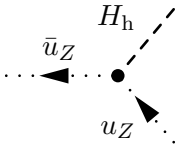

$$= \frac{\mathrm{i}e s_{\alpha\beta}}{2 s_\mathrm{w} c_\mathrm{w}} \xi_\beta M_{H_\mathrm{a}},$$

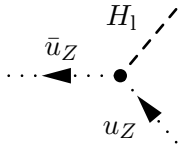

$$= \frac{\mathrm{i}e c_{\alpha\beta}}{2 s_\mathrm{w} c_\mathrm{w}} \xi_\beta M_{H_\mathrm{a}}. \tag{E.11}$$

Finally, we list all other vertices needed in the calculation of appendix D with the convention that all particles and momenta are incoming:

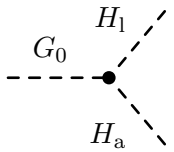

$$= \frac{\mathrm{i}c_{\alpha\beta} e}{2 M_\mathrm{W} s_\mathrm{w}} \left(M_{H_\mathrm{a}}^2 - M_{H_\mathrm{l}}^2\right),$$

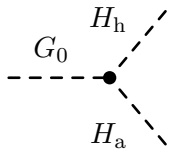

$$= \frac{\mathrm{i}s_{\alpha\beta} e}{2 M_\mathrm{W} s_\mathrm{w}} \left(M_{H_\mathrm{a}}^2 - M_{H_\mathrm{h}}^2\right), \tag{E.12}$$

JHEP09(2016)115

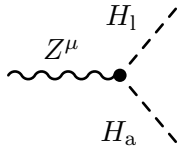

$$= \frac{c_{\alpha\beta} e}{2 s_{\rm w} c_{\rm w}} \left(p^\mu_{H_{\rm a}} - p^\mu_{H_{\rm l}} \right), \tag{E.13}$$

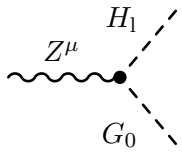

$$= -\frac{e s_{\alpha\beta}}{2 s_{\rm w} c_{\rm w}} \left(p^\mu_{G_0} - p^\mu_{H_{\rm l}} \right),$$

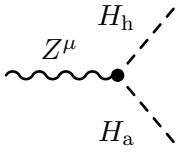

$$= \frac{s_{\alpha\beta} e}{2 s_{\rm w} c_{\rm w}} \left(p^\mu_{H_{\rm a}} - p^\mu_{H_{\rm h}} \right), \tag{E.14}$$

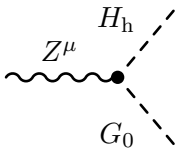

$$= \frac{e c_{\alpha\beta}}{2 s_{\rm w} c_{\rm w}} \left(p^\mu_{G_0} - p^\mu_{H_{\rm h}} \right),$$

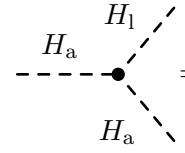

$$= \frac{\mathrm{i}e}{2 M_{\rm W} s_{\rm w}} \left(s_{\alpha\beta} \left(M^2_{H_{\rm l}} + 2 M^2_{H_{\rm a}} - 2 M^2_{\rm sb} \right) - c_{\alpha\beta} \frac{1 - t^2_\beta}{t_\beta} \left(M^2_{H_{\rm l}} - M^2_{\rm sb} \right) \right), \tag{E.15}$$

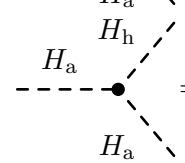

$$= \frac{\mathrm{i}e}{2 M_{\rm W} s_{\rm w}} \left(-c_{\alpha\beta} \left(M^2_{H_{\rm h}} + 2 M^2_{H_{\rm a}} - 2 M^2_{\rm sb} \right) - s_{\alpha\beta} \frac{1 - t^2_\beta}{t_\beta} \left(M^2_{H_{\rm h}} - M^2_{\rm sb} \right) \right), \tag{E.16}$$

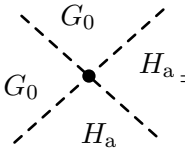

$$= -\frac{\mathrm{i}e^2}{2 M^2_{\rm W} s^2_{\rm w}} \left(\left(M^2_{H_{\rm l}} + 2 M^2_{H_{\rm h}} - 2 M^2_{\rm sb} \right) - c_{\alpha\beta} \left(c_{\alpha\beta} - s_{\alpha\beta} \frac{1 - t^2_\beta}{t_\beta} \right) \left(M^2_{H_{\rm h}} - M^2_{H_{\rm l}} \right) \right). \tag{E.17}$$

References

[1] CMS collaboration, *Observation of a new boson at a mass of* 125 *GeV with the CMS experiment at the LHC*, *Phys. Lett.* **B 716** (2012) 30 [arXiv:1207.7235] [INSPIRE].

[2] ATLAS collaboration, *Observation of a new particle in the search for the Standard Model Higgs boson with the ATLAS detector at the LHC*, *Phys. Lett.* **B 716** (2012) 1 [arXiv:1207.7214] [INSPIRE].

[3] J.F. Gunion and H.E. Haber, *The CP conserving two Higgs doublet model: the approach to the decoupling limit*, *Phys. Rev.* **D 67** (2003) 075019 [hep-ph/0207010] [INSPIRE].

[4] G.C. Branco, P.M. Ferreira, L. Lavoura, M.N. Rebelo, M. Sher and J.P. Silva, *Theory and phenomenology of two-Higgs-doublet models*, *Phys. Rept.* **516** (2012) 1 [arXiv:1106.0034] [INSPIRE].

[5] D. Pierce and A. Papadopoulos, *Radiative corrections to the Higgs boson decay rate* $\Gamma(H \to ZZ)$ *in the minimal supersymmetric model*, *Phys. Rev.* **D 47** (1993) 222 [hep-ph/9206257] [INSPIRE].

[6] A. Freitas and D. Stöckinger, *Gauge dependence and renormalization of* $\tan\beta$ *in the MSSM*, *Phys. Rev.* **D 66** (2002) 095014 [hep-ph/0205281] [INSPIRE].

JHEP09(2016)115

[7] N. Baro, F. Boudjema and A. Semenov, *Automatised full one-loop renormalisation of the MSSM. I. The Higgs sector, the issue of* $\tan\beta$ *and gauge invariance*, *Phys. Rev.* **D 78** (2008) 115003 [arXiv:0807.4668] [INSPIRE].

[8] R. Santos and A. Barroso, *On the renormalization of two Higgs doublet models*, *Phys. Rev.* **D 56** (1997) 5366 [hep-ph/9701257] [INSPIRE].

[9] S. Kanemura, Y. Okada, E. Senaha and C.P. Yuan, *Higgs coupling constants as a probe of new physics*, *Phys. Rev.* **D 70** (2004) 115002 [hep-ph/0408364] [INSPIRE].

[10] D. Lopez-Val and J. Solà, *Neutral Higgs-pair production at linear colliders within the general 2HDM: quantum effects and triple Higgs boson self-interactions*, *Phys. Rev.* **D 81** (2010) 033003 [arXiv:0908.2898] [INSPIRE].

[11] M. Krause, R. Lorenz, M. Mühlleitner, R. Santos and H. Ziesche, *Gauge-independent renormalization of the 2-Higgs-doublet model*, arXiv:1605.04853 [INSPIRE].

[12] A. Denner and T. Sack, *Renormalization of the quark mixing matrix*, *Nucl. Phys.* **B 347** (1990) 203 [INSPIRE].

[13] S. Kanemura, M. Kikuchi and K. Yagyu, *Fingerprinting the extended Higgs sector using one-loop corrected Higgs boson couplings and future precision measurements*, *Nucl. Phys.* **B 896** (2015) 80 [arXiv:1502.07716] [INSPIRE].

[14] P. Gambino, P.A. Grassi and F. Madricardo, *Fermion mixing renormalization and gauge invariance*, *Phys. Lett.* **B 454** (1999) 98 [hep-ph/9811470] [INSPIRE].

[15] Y. Yamada, *Gauge dependence of the on-shell renormalized mixing matrices*, *Phys. Rev.* **D 64** (2001) 036008 [hep-ph/0103046] [INSPIRE].

[16] J.M. Cornwall, *Dynamical mass generation in continuum QCD*, *Phys. Rev.* **D 26** (1982) 1453 [INSPIRE].

[17] J.M. Cornwall and J. Papavassiliou, *Gauge invariant three gluon vertex in QCD*, *Phys. Rev.* **D 40** (1989) 3474 [INSPIRE].

[18] J. Fleischer and F. Jegerlehner, *Radiative corrections to Higgs decays in the extended Weinberg-Salam model*, *Phys. Rev.* **D 23** (1981) 2001 [INSPIRE].

[19] P. Gambino and P.A. Grassi, *The Nielsen identities of the SM and the definition of mass*, *Phys. Rev.* **D 62** (2000) 076002 [hep-ph/9907254] [INSPIRE].

[20] S. Actis, A. Ferroglia, M. Passera and G. Passarino, *Two-loop renormalization in the Standard Model. Part I: prolegomena*, *Nucl. Phys.* **B 777** (2007) 1 [hep-ph/0612122] [INSPIRE].

[21] O. Piguet and K. Sibold, *Gauge independence in ordinary Yang-Mills theories*, *Nucl. Phys.* **B 253** (1985) 517 [INSPIRE].

[22] A. Denner, *Techniques for calculation of electroweak radiative corrections at the one loop level and results for W physics at LEP-200*, *Fortsch. Phys.* **41** (1993) 307 [arXiv:0709.1075] [INSPIRE].

[23] B.A. Kniehl, C.P. Palisoc and A. Sirlin, *Higgs boson production and decay close to thresholds*, *Nucl. Phys.* **B 591** (2000) 296 [hep-ph/0007002] [INSPIRE].

[24] A. Denner, S. Dittmaier, M. Roth and D. Wackeroth, *Predictions for all processes* $e^+e^- \to 4$ *fermions* $+\gamma$, *Nucl. Phys.* **B 560** (1999) 33 [hep-ph/9904472] [INSPIRE].

JHEP09(2016)115

[25] A. Denner, S. Dittmaier, M. Roth and L.H. Wieders, *Electroweak corrections to charged-current $e^+e^- \to 4$ fermion processes: technical details and further results*, *Nucl. Phys.* **B 724** (2005) 247 [*Erratum ibid.* **B 854** (2012) 504] [hep-ph/0505042] [INSPIRE].

[26] A. Denner and S. Dittmaier, *The complex-mass scheme for perturbative calculations with unstable particles*, *Nucl. Phys. Proc. Suppl.* **160** (2006) 22 [hep-ph/0605312] [INSPIRE].

[27] M. Böhm, A. Denner and H. Joos, *Gauge theories of the strong and electroweak interaction*, Teubner, Stuttgart Germany (2001).

[28] A. Sirlin, *Radiative corrections in the $\mathrm{SU}(2)_L \times \mathrm{U}(1)$ theory: a simple renormalization framework*, *Phys. Rev.* **D 22** (1980) 971 [INSPIRE].

[29] W.J. Marciano and A. Sirlin, *Radiative corrections to neutrino induced neutral current phenomena in the $\mathrm{SU}(2)_L \times \mathrm{U}(1)$ theory*, *Phys. Rev.* **D 22** (1980) 2695 [*Erratum ibid.* **D 31** (1985) 213] [INSPIRE].

[30] A. Sirlin and W.J. Marciano, *Radiative corrections to $\nu_\mu + N \to \mu^- + X$ and their effect on the determination of ρ^2 and $\sin^2\theta_W$*, *Nucl. Phys.* **B 189** (1981) 442 [INSPIRE].

[31] G. 't Hooft and M.J.G. Veltman, *Regularization and renormalization of gauge fields*, *Nucl. Phys.* **B 44** (1972) 189 [INSPIRE].

[32] B.W. Lee and J. Zinn-Justin, *Spontaneously broken gauge symmetries. 4. General gauge formulation*, *Phys. Rev.* **D 7** (1973) 1049 [INSPIRE].

[33] D. Lopez-Val and J. Solà, *Δr in the two-Higgs-doublet model at full one loop level — and beyond*, *Eur. Phys. J.* **C 73** (2013) 2393 [arXiv:1211.0311] [INSPIRE].

[34] Y. Yamada, *Two loop renormalization of $\tan\beta$ and its gauge dependence*, *Phys. Lett.* **B 530** (2002) 174 [hep-ph/0112251] [INSPIRE].

[35] LHC Higgs Cross section Working Group collaboration, I. Low et al., *Beyond the Standard Model predictions*, LHCHXSWG-DRAFT-INT-2016-009, CERN, Geneva Switzerland accessed June 29 2016.

[36] J. Baglio, O. Eberhardt, U. Nierste and M. Wiebusch, *Benchmarks for Higgs pair production and heavy Higgs boson searches in the two-Higgs-doublet model of type II*, *Phys. Rev.* **D 90** (2014) 015008 [arXiv:1403.1264] [INSPIRE].

[37] Particle Data Group collaboration, K.A. Olive et al., *Review of particle physics*, *Chin. Phys.* **C 38** (2014) 090001 [INSPIRE].

[38] C. Anastasiou et al., *Higgs boson gluon-fusion production at threshold in N^3LO QCD*, *Phys. Lett.* **B 737** (2014) 325 [arXiv:1403.4616] [INSPIRE].

[39] C. Anastasiou et al., *Higgs boson gluon-fusion production beyond threshold in N^3LO QCD*, *JHEP* **03** (2015) 091 [arXiv:1411.3584] [INSPIRE].

[40] C. Duhr, T. Gehrmann and M. Jaquier, *Two-loop splitting amplitudes and the single-real contribution to inclusive Higgs production at N^3LO*, *JHEP* **02** (2015) 077 [arXiv:1411.3587] [INSPIRE].

[41] C. Anastasiou, C. Duhr, F. Dulat, F. Herzog and B. Mistlberger, *Higgs boson gluon-fusion production in QCD at three loops*, *Phys. Rev. Lett.* **114** (2015) 212001 [arXiv:1503.06056] [INSPIRE].

[42] C. Anastasiou et al., *High precision determination of the gluon fusion Higgs boson cross-section at the LHC*, *JHEP* **05** (2016) 058 [arXiv:1602.00695] [INSPIRE].

JHEP09(2016)115

[43] S. Actis, G. Passarino, C. Sturm and S. Uccirati, *NLO electroweak corrections to Higgs boson production at hadron colliders*, *Phys. Lett.* **B 670** (2008) 12 [arXiv:0809.1301] [INSPIRE].

[44] S. Actis, G. Passarino, C. Sturm and S. Uccirati, *NNLO computational techniques: the cases $H \to \gamma\gamma$ and $H \to gg$*, *Nucl. Phys.* **B 811** (2009) 182 [arXiv:0809.3667] [INSPIRE].

[45] G. Passarino, C. Sturm and S. Uccirati, *Complete electroweak corrections to Higgs production in a Standard Model with four generations at the LHC*, *Phys. Lett.* **B 706** (2011) 195 [arXiv:1108.2025] [INSPIRE].

[46] A. Denner et al., *Higgs production and decay with a fourth Standard-Model-like fermion generation*, *Eur. Phys. J.* **C 72** (2012) 1992 [arXiv:1111.6395] [INSPIRE].

[47] A. Alloul, N.D. Christensen, C. Degrande, C. Duhr and B. Fuks, *FeynRules* 2.0 — *a complete toolbox for tree-level phenomenology*, *Comput. Phys. Commun.* **185** (2014) 2250 [arXiv:1310.1921] [INSPIRE].

[48] P. Nogueira, *Automatic Feynman graph generation*, *J. Comput. Phys.* **105** (1993) 279 [INSPIRE].

[49] S. Actis, A. Ferroglia, G. Passarino, M. Passera, Ch. Sturm and S. Uccirati, `GraphShot`, *a* `Form` *package for automatic generation and manipulation of one- and two-loop Feynman diagrams*, unpublished.

[50] J.A.M. Vermaseren, *New features of FORM*, math-ph/0010025 [INSPIRE].

[51] G. Passarino, *An approach toward the numerical evaluation of multiloop Feynman diagrams*, *Nucl. Phys.* **B 619** (2001) 257 [hep-ph/0108252] [INSPIRE].

[52] G. Passarino and S. Uccirati, *Algebraic numerical evaluation of Feynman diagrams: two loop self-energies*, *Nucl. Phys.* **B 629** (2002) 97 [hep-ph/0112004] [INSPIRE].

[53] A. Ferroglia, M. Passera, G. Passarino and S. Uccirati, *Two loop vertices in quantum field theory: infrared convergent scalar configurations*, *Nucl. Phys.* **B 680** (2004) 199 [hep-ph/0311186] [INSPIRE].

[54] G. Passarino and S. Uccirati, *Two-loop vertices in quantum field theory: infrared and collinear divergent configurations*, *Nucl. Phys.* **B 747** (2006) 113 [hep-ph/0603121] [INSPIRE].

[55] S. Actis, A. Ferroglia, G. Passarino, M. Passera and S. Uccirati, *Two-loop tensor integrals in quantum field theory*, *Nucl. Phys.* **B 703** (2004) 3 [hep-ph/0402132] [INSPIRE].

[56] A. Arhrib, *Unitarity constraints on scalar parameters of the standard and two Higgs doublets model*, in *Workshop on Noncommutative Geometry, Superstrings and Particle Physics*, Rabat Morocco June 16–17 2000 [hep-ph/0012353] [INSPIRE].

[57] R. Hamberg, W.L. van Neerven and T. Matsuura, *A complete calculation of the order α_s^2 correction to the Drell-Yan K factor*, *Nucl. Phys.* **B 359** (1991) 343 [*Erratum ibid.* **B 644** (2002) 403] [INSPIRE].

[58] O. Brein, A. Djouadi and R. Harlander, *NNLO QCD corrections to the Higgs-strahlung processes at hadron colliders*, *Phys. Lett.* **B 579** (2004) 149 [hep-ph/0307206] [INSPIRE].

[59] O. Brein, R. Harlander, M. Wiesemann and T. Zirke, *Top-quark mediated effects in hadronic Higgs-strahlung*, *Eur. Phys. J.* **C 72** (2012) 1868 [arXiv:1111.0761] [INSPIRE].

[60] G. Ferrera, M. Grazzini and F. Tramontano, *Associated WH production at hadron colliders: a fully exclusive QCD calculation at NNLO*, *Phys. Rev. Lett.* **107** (2011) 152003 [arXiv:1107.1164] [INSPIRE].

JHEP09(2016)115

[61] G. Ferrera, M. Grazzini and F. Tramontano, *Associated ZH production at hadron colliders: the fully differential NNLO QCD calculation*, *Phys. Lett.* **B 740** (2015) 51 [arXiv:1407.4747] [INSPIRE].

[62] M.L. Ciccolini, S. Dittmaier and M. Krämer, *Electroweak radiative corrections to associated WH and ZH production at hadron colliders*, *Phys. Rev.* **D 68** (2003) 073003 [hep-ph/0306234] [INSPIRE].

[63] M. Spira, *V2HV webpage*, http://tiger.web.psi.ch/proglist.html.

[64] J. Campbell, K. Ellis and C. Williams, *MCFM — Monte Carlo for FeMtobarn processes webpage*, http://mcfm.fnal.gov/.

[65] A. Denner, S. Dittmaier, S. Kallweit and A. Mück, *HAWK 2.0: a Monte Carlo program for Higgs production in vector-boson fusion and Higgs strahlung at hadron colliders*, *Comput. Phys. Commun.* **195** (2015) 161 [arXiv:1412.5390] [INSPIRE].

[66] O. Brein, R.V. Harlander and T.J.E. Zirke, *vh@nnlo — Higgs strahlung at hadron colliders*, *Comput. Phys. Commun.* **184** (2013) 998 [arXiv:1210.5347] [INSPIRE].

[67] R.V. Harlander, S. Liebler and T. Zirke, *Higgs strahlung at the Large Hadron Collider in the 2-Higgs-doublet model*, *JHEP* **02** (2014) 023 [arXiv:1307.8122] [INSPIRE].

[68] A. Denner, S. Dittmaier, S. Kallweit and A. Mück, *Electroweak corrections to Higgs-strahlung off W/Z bosons at the Tevatron and the LHC with HAWK*, *JHEP* **03** (2012) 075 [arXiv:1112.5142] [INSPIRE].

[69] CMS collaboration, *Search for the Standard Model Higgs boson produced in association with a W or a Z boson and decaying to bottom quarks*, *Phys. Rev.* **D 89** (2014) 012003 [arXiv:1310.3687] [INSPIRE].

[70] NNPDF collaboration, R.D. Ball et al., *Parton distributions with QED corrections*, *Nucl. Phys.* **B 877** (2013) 290 [arXiv:1308.0598] [INSPIRE].

[71] S. Actis, A. Denner, L. Hofer, J.-N. Lang, A. Scharf and S. Uccirati, *RECOLA: REcursive Computation of One-Loop Amplitudes*, arXiv:1605.01090 [INSPIRE].

[72] J.C. Collins, *Renormalization*, Cambridge Monographs on Mathematical Physics, Cambridge University Press, Cambridge U.K. (1986).

JHEP09(2016)115